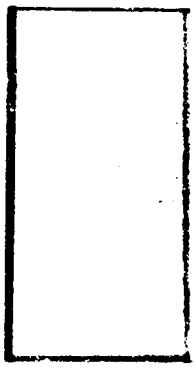

6, "A
tion
atory

THE UNIVERSITY OF KANSAS CENTER FOR RESEARCH, INC.
2291 Irving Hill Drive—Campus West
Lawrence, Kansas 66045

Progress Report for

A RESEARCH PROGRAM TO REDUCE INTERIOR NOISE
IN GENERAL AVIATION AIRPLANES

NASA Cooperative Agreement NCCI-6

STUDY OF NOISE REDUCTION CHARACTERISTICS OF MULTILAYERED PANELS AND DUAL PANE WINDOWS WITH HELMHOLTZ RESONATORS

KU-FRL-417-16

Prepared by: Ramasamy Navaneethan, Project Manager

Approved by: Jan Roskam, Principal Investigator

Flight Research Laboratory

University of Kansas

Lawrence, Kansas

May 1981

STUDY OF NOISE REDUCTION CHARACTERISTICS OF MULTILAYERED PANELS AND DUAL PANE WINDOWS WITH HELMHOLTZ RESONATORS

by

Ramasamy Navaneethan

Abstract of report submitted
to the University of Kansas in
partial fulfillment of the requirements
for the degree of Master of Science

May 1981

Studies have indicated that the airborne proprller noise transmitted through the aircraft sidewall is one of the important source path combinations of the sound transmission into an aircraft cabin. The typical sidewall is a multilayered panel. In this report the experimental noise attenuation characteristics of flat, general aviation type, multilayered panels are presented. Experimental results of stiffened panels, damping tape, honeycomb materials and sound absorption materials are presented. Single-degree-of-freedom theoretical models have been developed for sandwich type panels with both shear-resistant and non-shear-resistant core material. The experimental investigation, performed to test the concept of Helmholtz resonators used in conjunction with dual pane windows in increasing the noise reduction around a small range of frequency, is also described. It is concluded that the stiffening of the panels either by stiffeners or by sandwich construction increases the low frequency noise reduction. Application of damping materials while damping out the resonance peaks lowers the fundamental resonance frequency.

The theoretical models, within the constraints of the assumptions made in deriving them, predict the fundamental resonance frequency and the low frequency noise reduction fairly accurately. It is also concluded that the concept of Helmholtz resonators in conjunction with dual pane windows offers an attractive low cost solution to increase the noise attenuation of dual pane windows around a small range of frequency.

ACKNOWLEDGMENTS

The author wishes to express his sincere appreciation to Dr. Jan Roskam of the Advisory Committee for his enccuragement, advice, guidance and support throughout this study. Acknowledgments are due to Dr. Hillel Unz for his valuable comments and suggestions. The financial support of NASA Langley Research Center via David G. Stephens, Technical Monitor of Grant NCCI-6, is greatly appreciated. The author would like to express his appreciation to all the people who contributed in many ways to this study. Sincere thanks are due to Nancy Hanson for her patient typing, grammatical corrections, and help in making this report readable. Finally, thanks must go to Nirmala and Priya for their understanding and support.

TABLE OF CONTENTS

TABLE OF CONTENTS (continued)

LIST OF FIGURES

LIST OF FIGURES (continued)

LIST OF FIGURES (continued)

LIST OF TABLES

LIST OF SYMBOLS

Symbol	Definition	Dimension
A	Steady state sound pressure amplitude	$[N/m^2]$
A	Defined in Equation (2.3)	[Nm]
A	Area of single resonator tube	$[m^2]$
A_0	Total resonator tube area	$[m^2]$
a	Panel dimension	[m]
B	Defined in Equation (2.4)	[Nm]
B	Steady state sound pressure amplitude	$[N/m^2]$
b	Panel dimension	[m]
b	Propagation constant (= jk)	[-]
C	Steady state sound pressure amplitude	$[N/m^2]$
C	Defined in Equation (2.5)	[Nm]
c	Speed of sound in air	[m/s]
D	Steady state sound pressure amplitude	$[N/m^2]$
D	Flexural rigidity	[Nm]
D_x	Orthotropic elastic constant	[Nm]
D_y	Orthotropic elastic constant	[Nm]
D*	Transformed flexural rigidity	[Nm]
E	Steady state sound pressure amplitude	$[N/m^2]$
E	Young's modulus	$[N/m^2]$
f	Frequency	[Hz]
f_n	Natural frequency	[Hz]
f_d	First dilatational resonance frequency	[Hz]
f_0	Resonator resonance frequency	[Hz]

LIST OF SYMBOLS (continued)

Symbol	Definition	Dimension
f_1	Defined in Equation C.2	[-]
f_2	Defined in Equation C.3	[-]
H	Orthotropic elastic constant	[Nm]
h	Thickness of the layer	[m]
I	Moment of inertia of the stiffener cross section with respect to the middle surface of the sheet	[m^4]
j	$\sqrt{-1}$	[-]
K	Complex compressibility	[N/m^2]
k	Wave number	[rad/m]
l	Spacing between the panes	[m]
m	Mass per unit area	[kg/m^2]
m	Panel mode number (= 1, 2, 3 . . . ∞)	[-]
n	Panel mode number (= 1, 2, 3 . . . ∞)	[-]
n	Number of resonator tubes	[-]
P	Porosity	[-]
P	Time invariant sound pressure function	[N/m^2]
p	Lateral forcing function	[N/m^2]
q	Defined in Equation (2.43a)	[-]
R	Real part of complex impedance	[MKS Rayls]
R_s	Flow resistance in resonator tubes	[MKS Rayls]
R_1	Flow resistivity of a porous material	[MKS Rayls/m]
R_2	$= 1.2R_1$ (Defined in Appendix C)	[MKS Rayls/m]
S'	Spacing between the stiffeners	[m]

LIST OF SYMBOLS (continued)

Symbol	Definition	Dimension
S_1	Area of double window	[m^2]
s	Structures factor	[-]
t	Thickness of the plate	[m]
t	Resonator tube length	[m]
t'	Equivalent resonator tube length	[m]
u	Particle velocity	[m/s]
V	Volume of the resonator	[m^3]
W	Maximum amplitude of lateral deflection	[m]
w	Amplitude of lateral deflection	[m]
X	Imaginary part of complex impedance	[MKS Rayls]
x	X-coordinate	[m]
$\bar{Y}$	Y-coordinate of the neutral axis of the stiffener from its edges	[m]
y	Y-coordinate	[m]
Z	Impedance of the material	[MKS Rayls]
Z_0	Characteristic impedance of porous material	[MKS Rayls]
z	Z-coordinate	[m]
Greek Symbol		
α	Attenuation constant	[nepers/m]
α	Damping factor	[-]
α	Resonator resistance	[-]
β	Complex part of the propagation constant, b	[-]

LIST OF SYMBOLS (continued)

Symbol	Definition	Dimension
β	Resonator reactance	[-]
∂	Partial differential	[-]
ζ	Panel damping ratio	[-]
λ_n	Wavelength of acoustic wave in the material	[m]
ν	Poission's ratio	[-]
ρ	Density of the air	[kg/m^3]
ρ_m	Bulk density of the porous material	[kg/m^3]
ϕ	Phase difference between two faces of a sandwich panel	[deg]
θ	Phase angle of complex impedance	[deg]
ω	Angular frequency	[rad/s]
ω_n	Angular natural frequency of panel	[rad/s]
ω_{mn}	Angular natural frequency of panel	[rad/s]

Subscripts

c	Core
D	Damped
d	Dilatational
i	Integer (= 1 or 2)
i	Incident
k	Integer (= 1, 2, or 3)
m	Core material
m	modal number

LIST OF SYMBOLS (continued)

(Subscripts, cont'd.)	Definition
n	Resonance
n	Modal number
o	Characteristic
r	Reflected
t	Transmitted
1, 1	Fundamental resonance mode
I	Region defined in Figures 2.13 and 2.14
II	Region defined in Figures 2.13 and 2.14
III	Region defined in Figures 2.13 and 2.14

LIST OF ACRONYMS

Acronym	Definition
DB (dB)	Decibels
Hz	Hertz
KU-FRL	University of Kansas Flight Research Laboratory
NASA	National Aeronautics and Space Administration
P.V.C.	Polyvinyl chloride
SDOF	Single degree of freedom

CHAPTER 1

INTRODUCTION

The interior noise levels in general aviation aircraft are high and in many cases exceed acceptable comfort limits (References 1 through 3). The noise sources in a general aviation aircraft include engines, propellers, auxiliary equipment and airflow over the aircraft. The interior noise is low-frequency dominant, the propeller and engine being the major contributors (References 1 through 5). One of the important source-path combinations is the airborne propeller noise transmitted through the aircraft sidewall into the cabin. An improved sidewall noise attenuation will reduce the overall noise level inside the aircraft.

A normal aircraft sidewall is made of structural panels and windows. The noise control in the present-day aircraft is based on an after-the-fact approach. A significant NASA-sponsored research program to study the transmission of sound through aircraft panel type structures and windows is being conducted at the Flight Research Laboratory of the University of Kansas (KU-FRL). The research has accomplished documentation of experimental noise reduction characteristics of simple and treated panels (References 6 and 7). However, a typical actual aircraft sidewall is a multilayered panel. A review of the existing literature (References 8 through 11) indicates that the available information is limited to the high frequency region. It may, therefore, be inappropriate for general aviation aircraft, where the low frequency noise, especially around the blade passage frequency and its harmonics, is dominant. The current studies (References 12 and

13) indicate that stiffening of panels will increase noise reduction in the low frequency region. Sandwiching of panels is another way to increase the low frequency noise reduction through increased stiffness.

Past studies (References 4 and 5) have also demonstrated that sound transmission through windows is another important noise path. The normal sound proofing techniques cannot be applied to windows, since they will affect the optical properties of the windows. Use of double windows is one of the ways to increase noise reduction at higher frequencies. However, this introduces additional resonance at lower frequencies and an accompanying decrease in noise reduction. The concept of double windows with Helmholtz resonators, tuned to the resonance frequency of a double window, appeared promising in eliminating this additional resonance frequency.

The purposes of this study then are:

(a) to document the noise reduction characteristics of typical aircraft multilayered structures,

(b) to investigate the concept of using sandwich-type configurations for increased low frequency noise reduction and

(c) to investigate the concept of a double window with Helmholtz resonators.

The method used is to determine the noise reduction characteristics experimentally and to develop simple analytical models simultaneously. The analytical models are then used to explain the experimental results wherever possible.

The experimental investigation of noise reduction characteristics was carried out at the KU-FRL acoustic test facility. The maximum panel size that can be tested is 18 x 18 inch. References (14 and 15) give the details of the construction and the characteristics of this test facility. The salient features are excerpted in Appendix A.

The next chapter, Chapter 2, describes the experimental investigation carried out to find the noise reduction characteristics of multilayered panels. In the same chapter, analytical models are developed for simple multilayered panels. The noise reduction values calculated for some of the simpler structures are then compared with the experimental results. In Chapter 3, the noise reduction characteristics of a double window with Helmholz resonator are described. Conclusions and recommendations are presented in Chapter 4.

CHAPTER 2

NOISE REDUCTION CHARACTERISTICS OF MULTILAYERED PANELS

2.1 INTRODUCTION

Normally, the aircraft cabin sound proofing consists of a stiffened outer panel, a combination of fibrous blankets (sound absorbers), air gaps, impervious sheeting and trim panels. Theoretical studies have been made to determine the optimum positioning of the air gaps and the blankets (Reference 10); but in practical cases the installation is usually determined by other considerations such as stringer locations, frame depths and other structural details. Consequently, an actual aircraft sound proofing installation is not easily amenable to analytical treatments.

The problem was simplified by studying the effect of varying individual elements upon the noise reduction of a multilayered panel being investigated. In addition, the number of layers tested was gradually increased from one to four. The experimental investigation is described in Section 2.2. Analytical work to determine the noise reduction of typical sandwich panels is given in Section 2.3. In the same section, the applicability of the theoretical results to the simple experimental panels is discussed.

2.2 EXPERIMENTAL INVESTIGATION

During this investigation the effects of the following elements of the multiple layered panel were tested:

(a) Stiffened aluminum panel with damping material (Subsection 2.2.1)

(b) Rigid P.V.C.-based foam (Subsection 2.2.2)

(c) Sound absorption materials (Subsection 2.2.3)

(d) Rigid foam and sound absorption material (Subsection 2.2.4)

(e) Inner aluminum panel (Subsection 2.2.5)

(f) Air gaps (Subsection 2.2.6)

(g) Honeycomb panels (Subsection 2.2.7)

A schematic of a typical multilayered panel tested is shown in Figure 2.1. In each panel, neighboring layers were attached to each other with a strip method. Rigid spacers were used during testing of the sound absorption and soft core foam materials. These spacers were placed on the outer edge of the test panels, in between the outer and inner panels, to take any compressive loads. For the panel with an air gap, the airspace was maintained by placing on the outer edge an appropriate thickness of vinyl foam between the outer and inner panels, to seal the air gap. The stiffened aluminum panel was stiffened with three "L" stringers placed parallel to the edges at equal spacing. The stringers were 3/4 x 3/4 x 1/16 inch.

2.2.1 Effect of Stiffened Aluminum Panel with Damping Material

One stiffened aluminum panel was tested with and without Y370 damping material treatment (Figures 2.2 and 2.3). The entire panel was treated with damping material. The effect of damping material in the low frequency region is small and is negative. Due to the

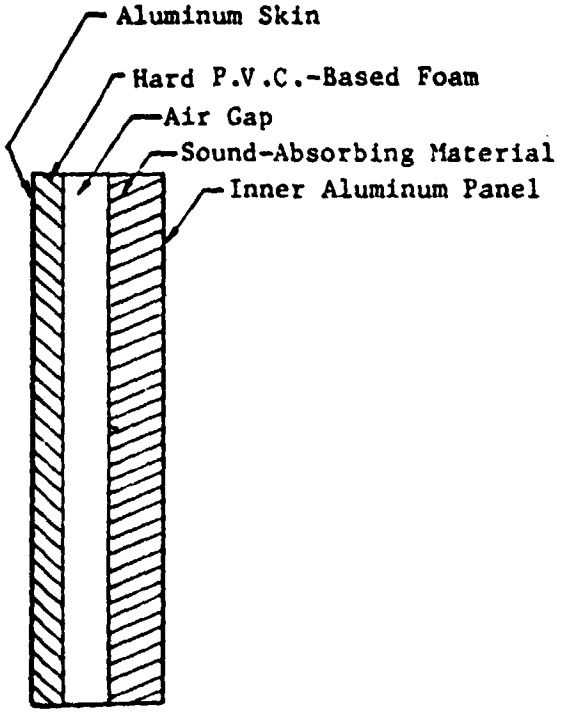

Figure 2.1 : A Typical Multilayered Panel Tested

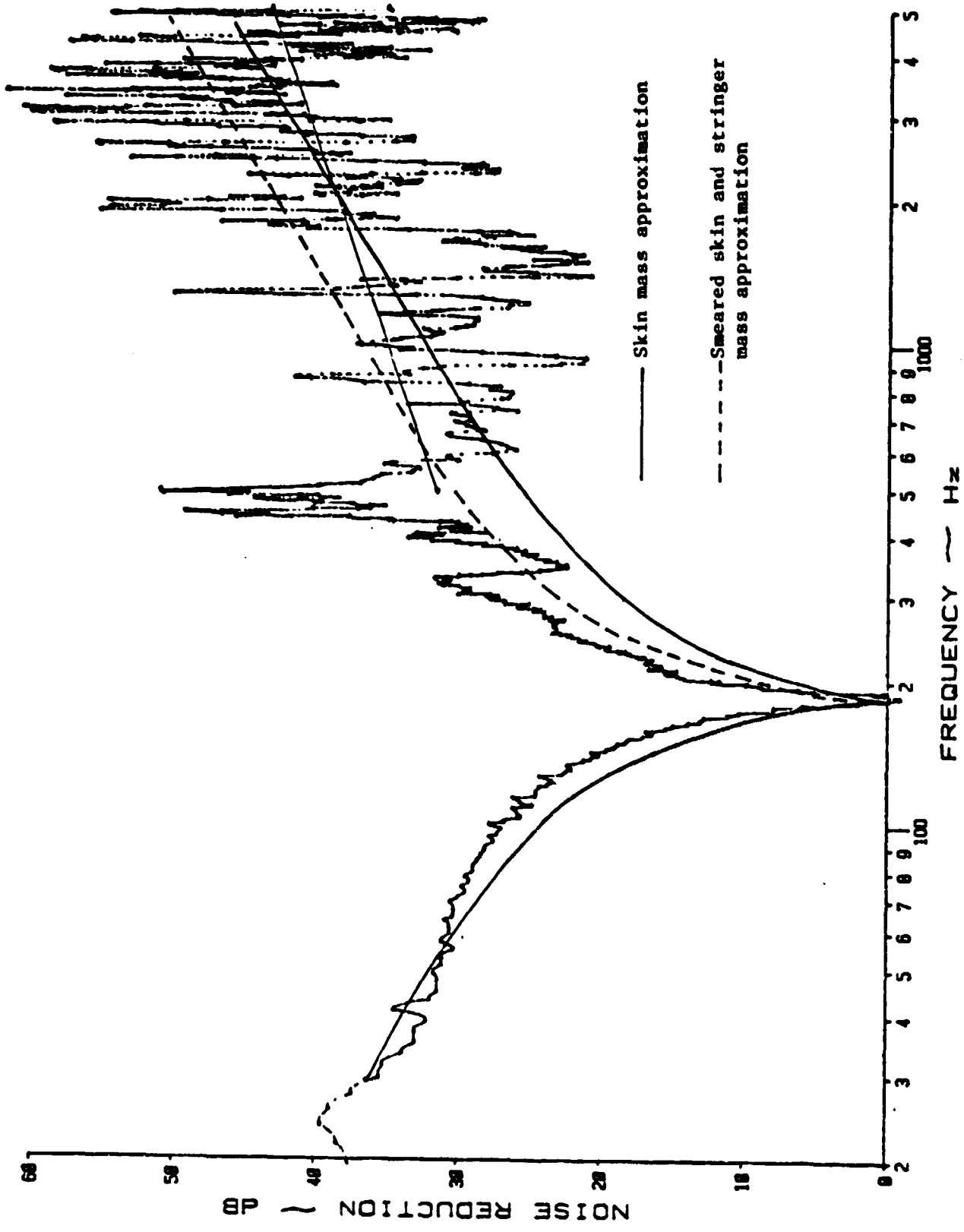

Figure 2.2: Noise Reduction Characteristics of Stiffened Aluminum Panel

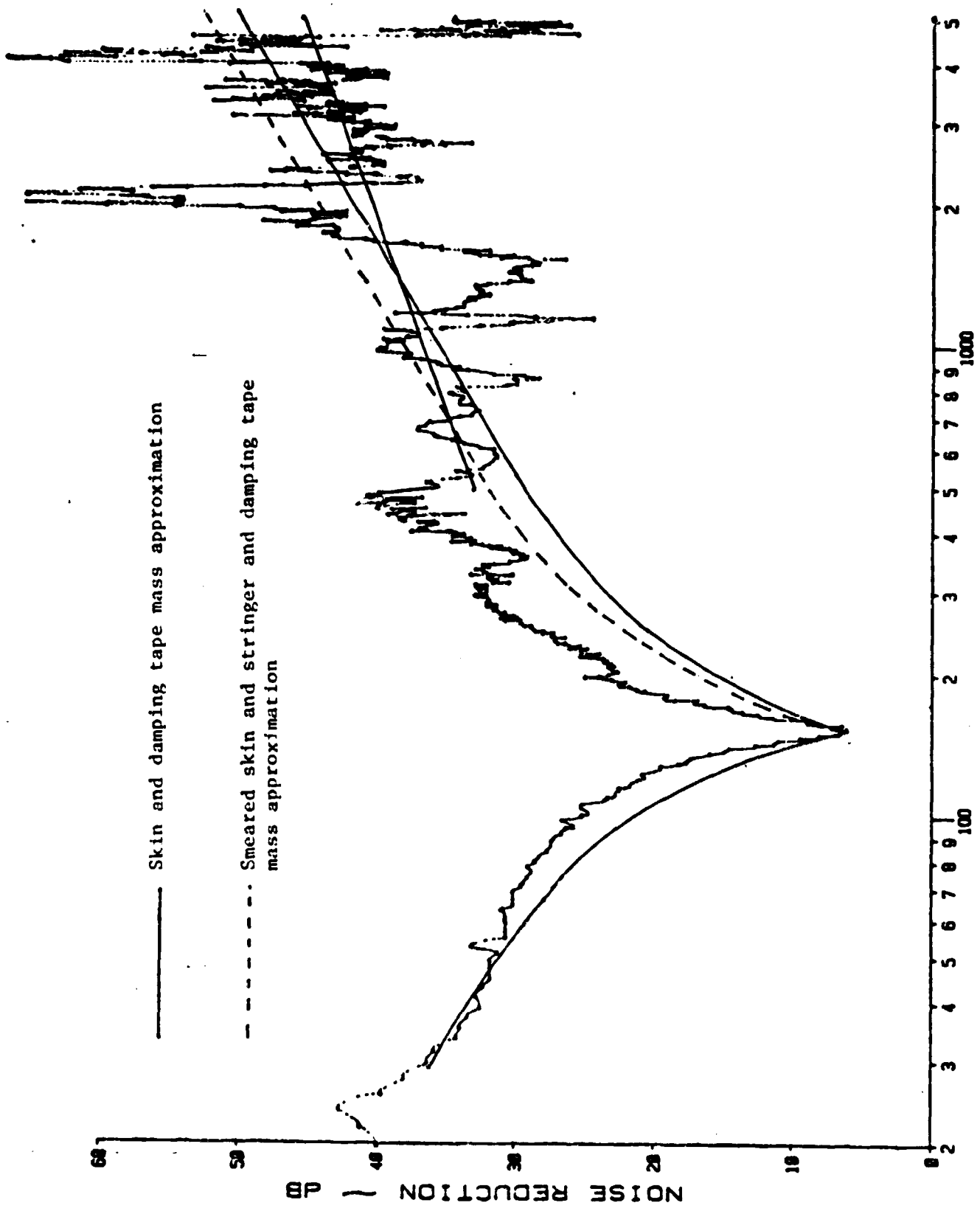

Figure 2.3: Noise Reduction Characteristics of Stiffened Aluminum Panel Treated with Y-370 Damping Material

low stiffness-to-mass ratio of the damping material, the stiffness-to-mass ratio of the treated panel decreases, causing a lowering of fundamental resonance frequency. A drop of as much as 25 Hz is noticed in the resonance frequency. In this case, the resonance frequency of the untreated panel is high (≈200 Hz), due to the stiffening effect of the stiffeners. The damping treatment increases the noise reduction at the resonance frequency from zero to 10 dB. Another contribution of the damping treatment is the absence of peaks and dips at higher panel modes.

2.2.2 Effect of Rigid P.V.C.-Based Foam

Rigid P.V.C.-based foam* was one of the four types of sound absorbing materials tested. It is discussed separately because of its ability to withstand loads. Three different densities (namely 0.107, 0.129 and 0.359 slugs/ft^3) of 1/4 inch thick foams were investigated. Two configurations were tested: (a) foam attached to a 0.025 inch aluminum panel, and (b) foam sandwiched between two 0.025 inch panels. The noise reduction curves obtained are shown in Appendix B (Figures B.1 through B.6). During the tests it was observed that the rigid foam would become loose from the panel at locations of maximum amplitude. When such a phenomenon occurs, both aluminum panel and rigid foam vibrate independently, reducing the noise reduction through the panels. In order to ensure proper bonding of adhesive on the rigid foam, a USP 735 Type A glass cloth was bonded between the P.V.C. foam and the aluminum. This layer

*manufactured by American Klegecell Corporation

has an additional advantage in that when an impervious layer is bonded to a sound absorbing material, an increase in noise reduction will occur in the low frequency region (Reference 16). Test results confirmed these observations. An increase in noise reduction of 5 dB is obtained at 30 Hz. (See Figure 2.4 for the effect or rigid foam density on the noise reduction values at 30 Hz and 3000 Hz.)

The effect of sandwiching rigid foam is to increase the noise reduction value by 10 dB over twin layered panels in the low frequency region. The increase in stiffness-to-mass ratio of the combined panel is due to the stiffness added by the additional aluminum panel. Increase in the mass of the panel increased the noise reduction at high frequencies (≈3000 Hz).

The fundamental resonance frequency obtained is also presented in Figure 2.4.

2.2.3 Effect of Sound Absorption Materials

Three other sound absorption materials investigated are (a) fibrous sound absorption material made by Conwed Corporation, (b) soft ployurethene foam, and (c) matte fiberglass.

2.2.3.1 Effect of Fibrous Sound Absorption Materials

Three flexible sound absorption materials of different densities--Conwed 9525, 6198, and 11330*--were tested in conjunction with 0.025 inch aluminum panels. The noise level reduction mechanism of the sound absorption materials is due to the viscous shear losses that occur when the vibrating air enters through the porous material.

*manufactured by Conwed Corporation

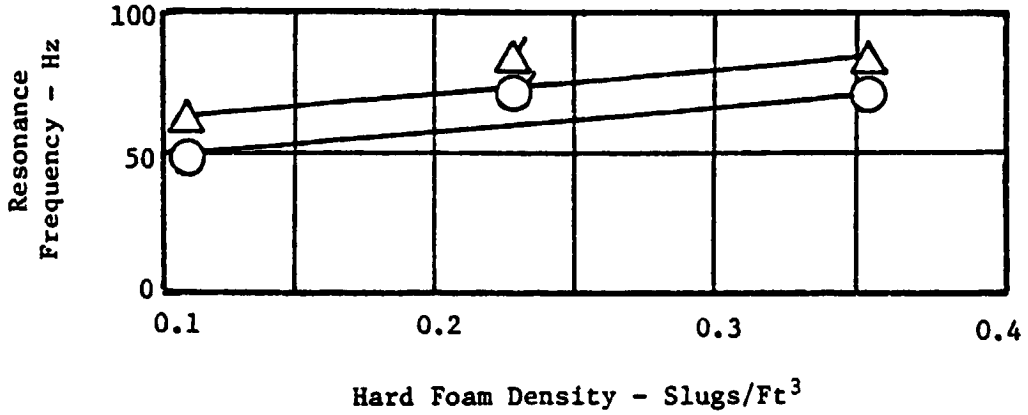

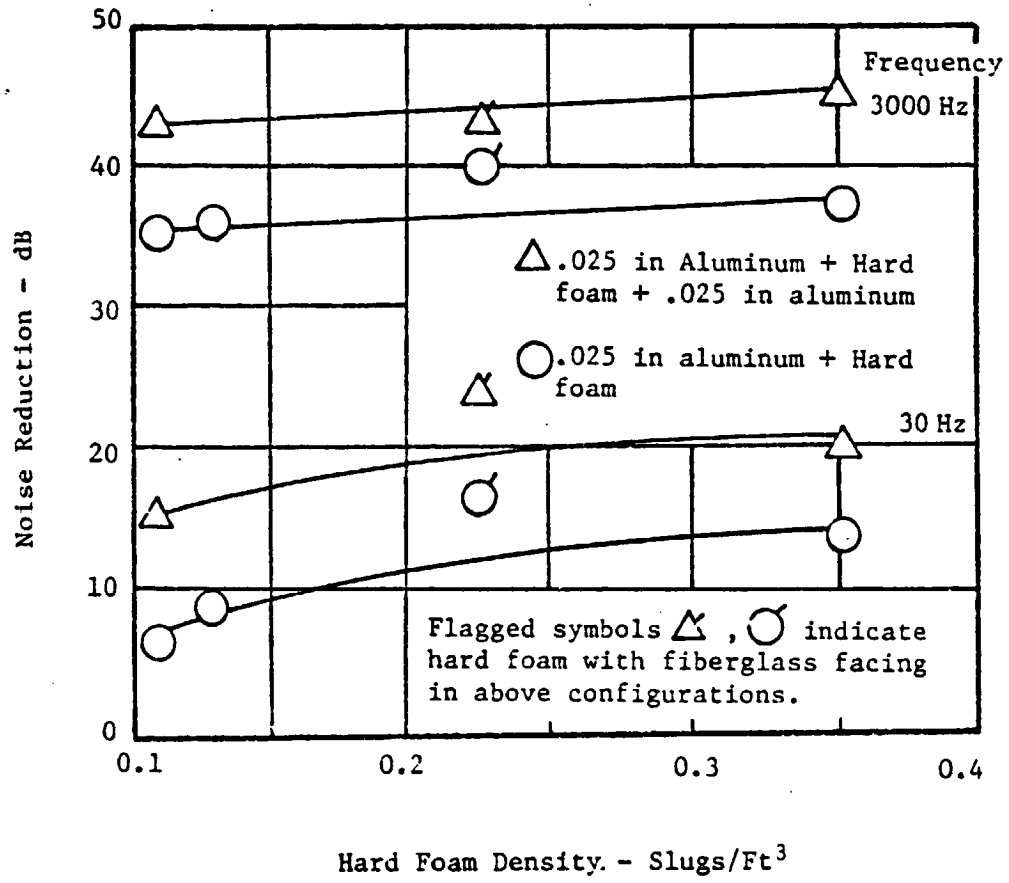

Figure 2.4: Effect of Rigid P.V.C. Foam Density on the Noise Reduction and the Fundamental Resonance Frequency of a Multilayered Panel

Two types of sound absorption systems were tested: (a) sound absorption material attached to a 0.025" aluminum panel, and (b) sound absorption material sandwiched between two 0.025 inch aluminum panels. The noise reduction curves are presented in Appendix B (Figures B.7 through B.12). The noise reduction values obtained at 30 and 3000 Hz are plotted in Figure 2.5 as a function of the density of the material tested. Also shown in the same figure is the fundamental resonance frequency observed. Increase in sound absorption material density increased the noise reduction very slightly in both the low and high frequency ranges (approximately 3 dB for the range of density tested). In general the noise reduction of these panels is better than that of foam panels, in both the double and triple layered configurations tested.

Sandwiching the panels increased the noise reduction by 20 dB. The noise reduction values at 30 Hz, in this configuration, varied from 35 to 37 dB. The resonance frequency also increased from ∿60 to ∿105 Hz.

2.2.3.2 Effect of Polyurethene Foam

Soft polyurethene foam was another sound absorption material tested. Two thicknesses of the same density (0.0469 slugs/ft^3) were investigated. The results are presented in Appendix B (Figures B.13 through B.15). As in the case of rigid P.V.C. foam, the attachment of soft polyurethene foam to a 0.025 inch aluminum panel did not produce any significant increase in noise reduction compared to a bare aluminum panel. Also, an increase in thickness of foam did

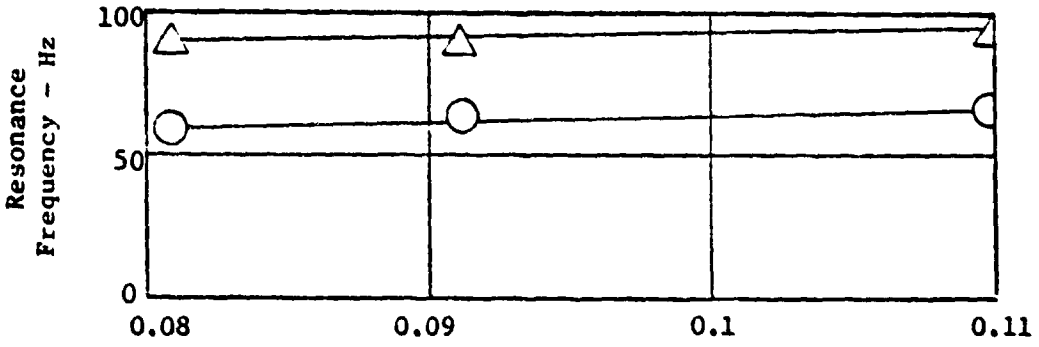

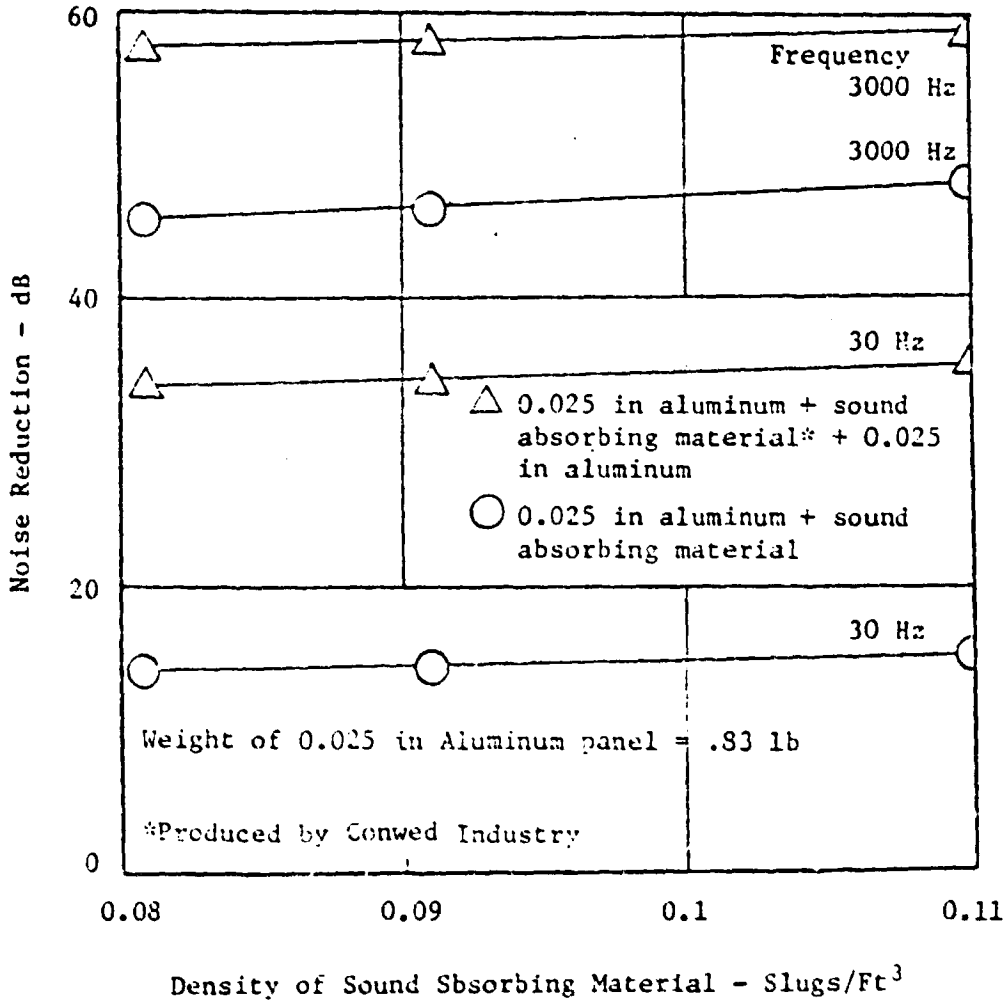

Figure 2.5 : Effect of Sound Absorption Material Density on the Noise Reduction and the Fundamental Resonance Frequency of a Multilayered Panel

not increase the noise reduction. The cross-plot of results is given in Figure 2.6. Sandwiching the foam between the two aluminum panels increased the noise reduction by 10 dB.

2.2.3.3 Effect of Matte Fiberglass

Fiberglass batting of one inch thickness was sandwiched between two 0.020 inch aluminum panels to study the effect of fiberglass. The density of the fiberglass was 3.5 lb/ft^3. The result is given in Appendix B (Figure B.17). The result indicates that the minimum noise reduction is 8 dB at its fundamental resonance frequency. The noise reduction of a bare aluminum panel is around zero at the resonance frequency (Reference 6).

2.2.4 Combined Effect of Rigid P.V.C. Foam and Sound Absorption Material

Sub-subsection 2.2.3.2 showed encouraging results in applying the concept of sandwiching two aluminum panels with a viscoelastic core material. In an attempt to produce significant noise reduction with a relatively light-weight multilayered panel, the rigid P.V.C. foam and fibrous sound absorption material were combined into a multiple structure noise reduction system. Specifically, the P.V.C. foam and sound absorbing material were sandwiched between a 0.025 inch outer panel and a 0.016 inch inner panel. The lower inner panel thickness was chosen to keep the panel weight low. However, the effect of inner panel thickness was also investigated and is discussed in Subsection 2.2.5.

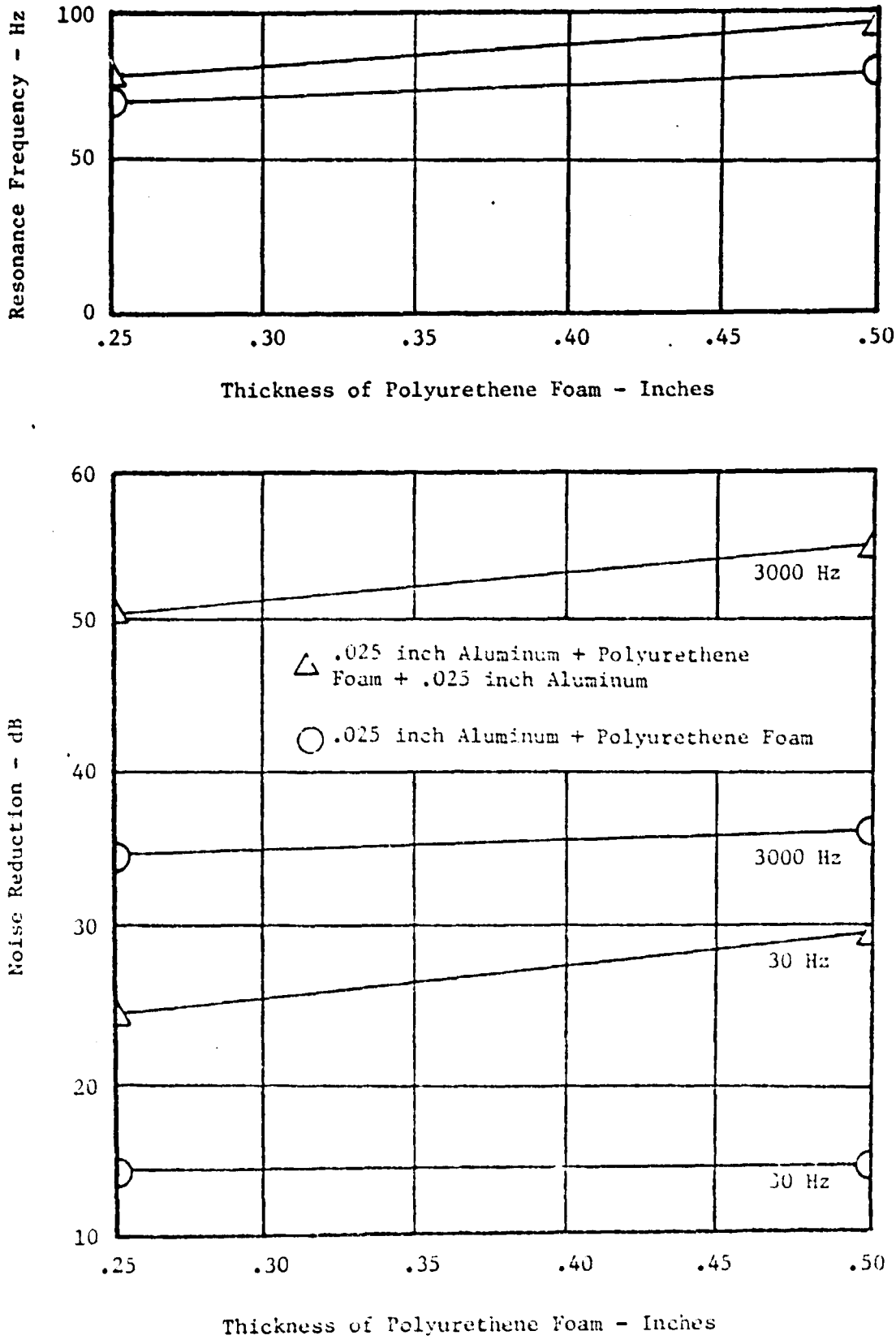

Figure 2.6: Effect of Soft Polyurethene Foam Thickness on the Noise Reduction and Resonance Frequency of a Multilayered Panel

Two different sound absorbing materials and rigid P.V.C. foam densities were tested. The noise reduction results obtained are presented in Appendix B (Figures B.18 through B.21). The cross-plot of the results is shown in Figure 2.7. Increase in either foam or sound absorbing material density increased the noise reduction slightly (2-3 dB). The noise reduction value at 30 Hz varied from 42-48 dB for all the materials tested in this configuration.

2.2.5 Effect of Inner Panel Thickness

An attempt was made to determine the effect of reducing the thickness of the inner aluminum panel of a multiple structure in order to reduce the overall panel weight.

Three different inner panel thicknesses--0.016 inch, 0.020 inch, and 0.025 inch--and two different sound absorption material densities were tested. The noise reduction test results are given in Appendix B (Figures B.22 through B.27). The cross-plot of results is shown in Figure 2.8. An increase in noise reduction of only 2-3 dB at low frequency is observed for an increase in thickness of 0.009 inch. This would indicate that for these sandwiched panels, the total panel weight can be reduced without a substantial decrease in low frequency noise reduction, by reducing the inner panel thickness. In the high frequency region, which is mass controlled, the decrease in noise reduction is higher (7 dB for the reduction of 0.009 inch of inner aluminum panel).

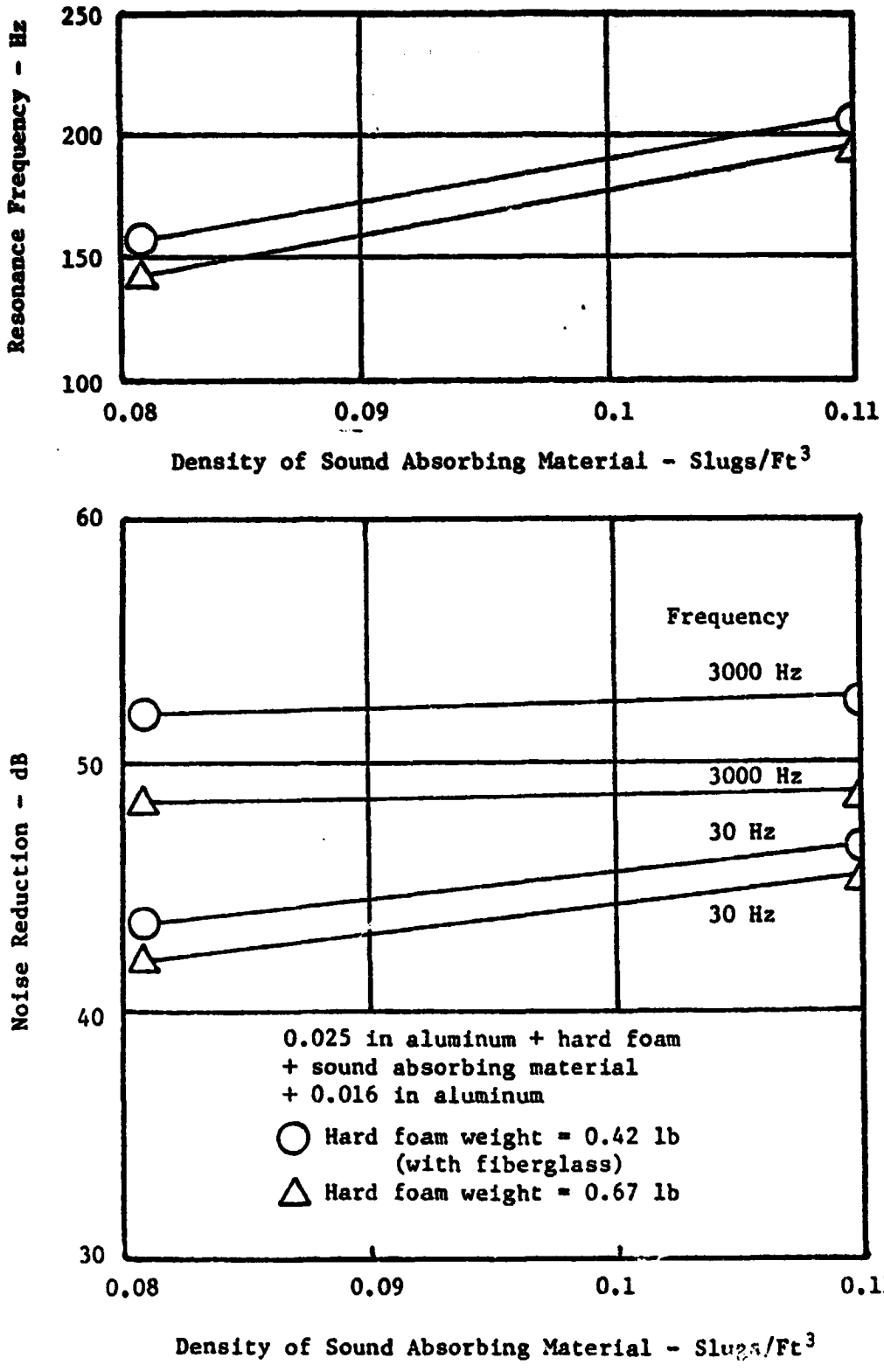

Figure 2.7 : Noise Reduction and Fundamental Resonance Frequency Characteristics of a Multilayered Panel Built of 0.025 Inch Aluminum Panel, 1/4 Inch P.V.C.-Based Foam, 1 Inch Thick Sound Absorption Material, and 0.016 Inch Aluminum Panel

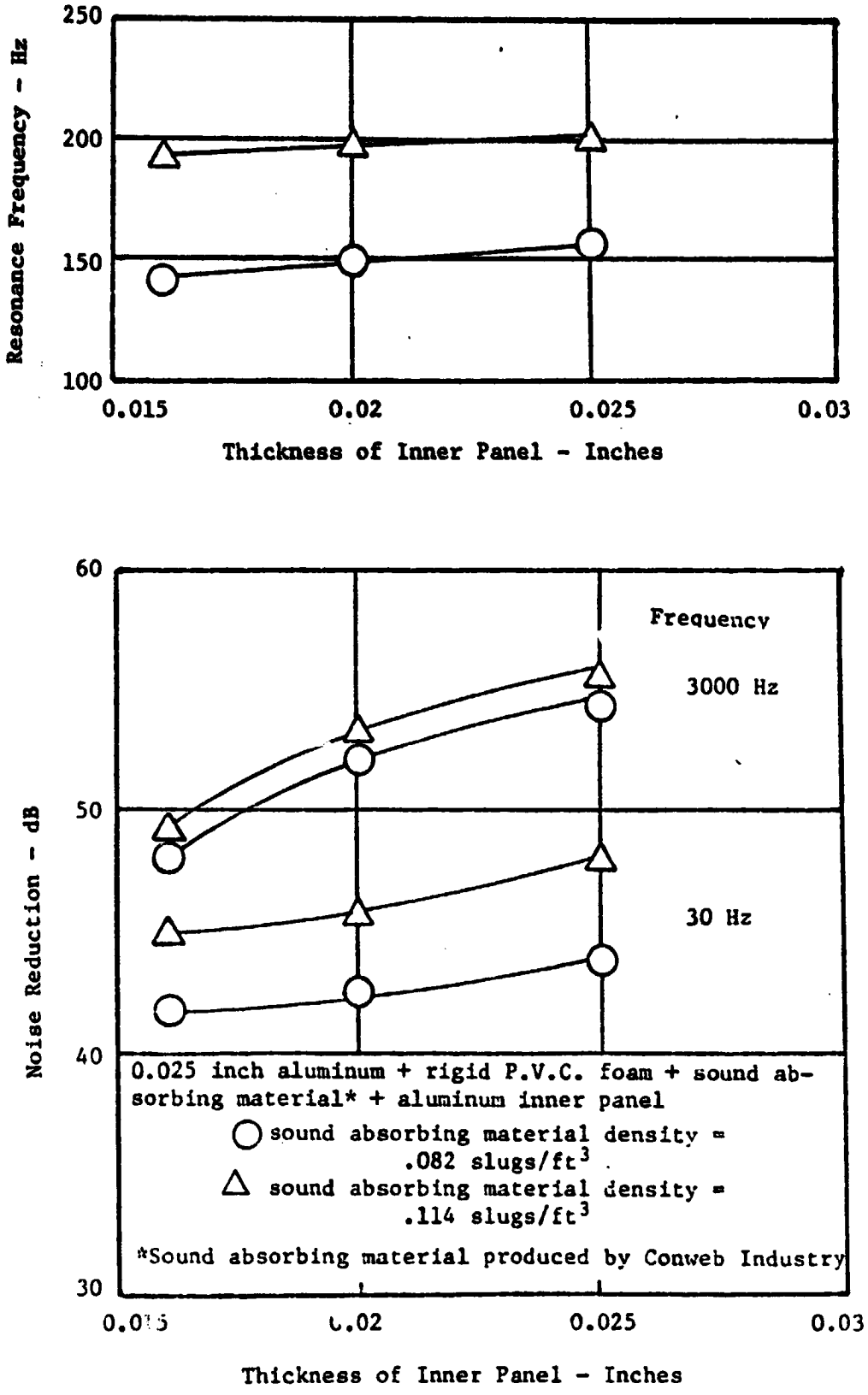

Figure 2.8 : Effect of Inner Panel Thickness on the Noise Reduction and the Resonance Frequency of a Multilayered Panel

2.2.6 Effect of Air Gaps

The effect of an air gap as a layer in the multilayered panel was investigated for 4 thicknesses (1/16, 3/16, 3/8, and 3/4 inch). The results of the tests are presented in Appendix B (Figures B.28 through B.31). The cross-plot of results is shown in Figure 2.9.

During the investigation the air in between the layers was sealed along the edges, using vinyl foam strips, preventing any air leak. At low frequencies, air gaps did not have any effect on the noise reduction. This trend is consistent with the results obtained for the double window tests (References 17 and 18). The panels vibrate in phase, as the cavity in between is not vented. However, an additional resonance--of 150 to 250 Hz, depending upon air gap width--is produced in the interval. This is due to the panel-air-panel resonance. In the mass-controlled region the least squares averaged noise reduction is constant because no mass is added.

2.2.7 Honeycomb Panels

Five different honeycomb panels were tested. The effects of thickness and core material were investigated. Core thicknesses of 0.125, 0.25 and 0.5 inches and core materials of aluminum and Nomex were tested. In all the tests, the facing sheet was fiberglass. The results of these five tests are presented in Appendix B (Figures B.32 through B.36). The cross-plot of results is shown in Figure 2.10.

The honeycomb panels have very high stiffness-to-mass ratio and therefore have very good low-frequency noise attenuation charac-

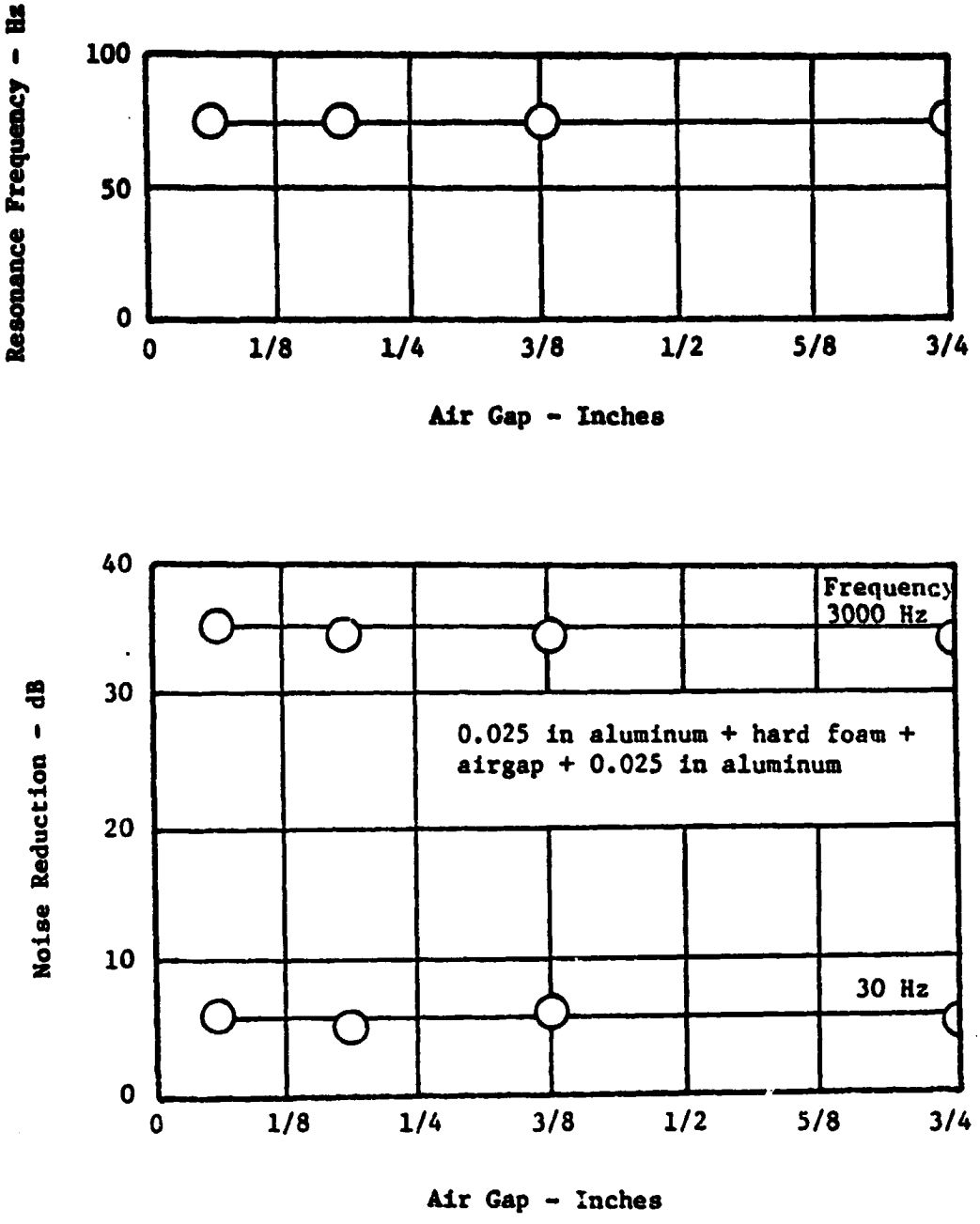

Figure 2.9 : Effect of Airspace Thickness on Noise Reduction Characteristics of a Multilayered Panel

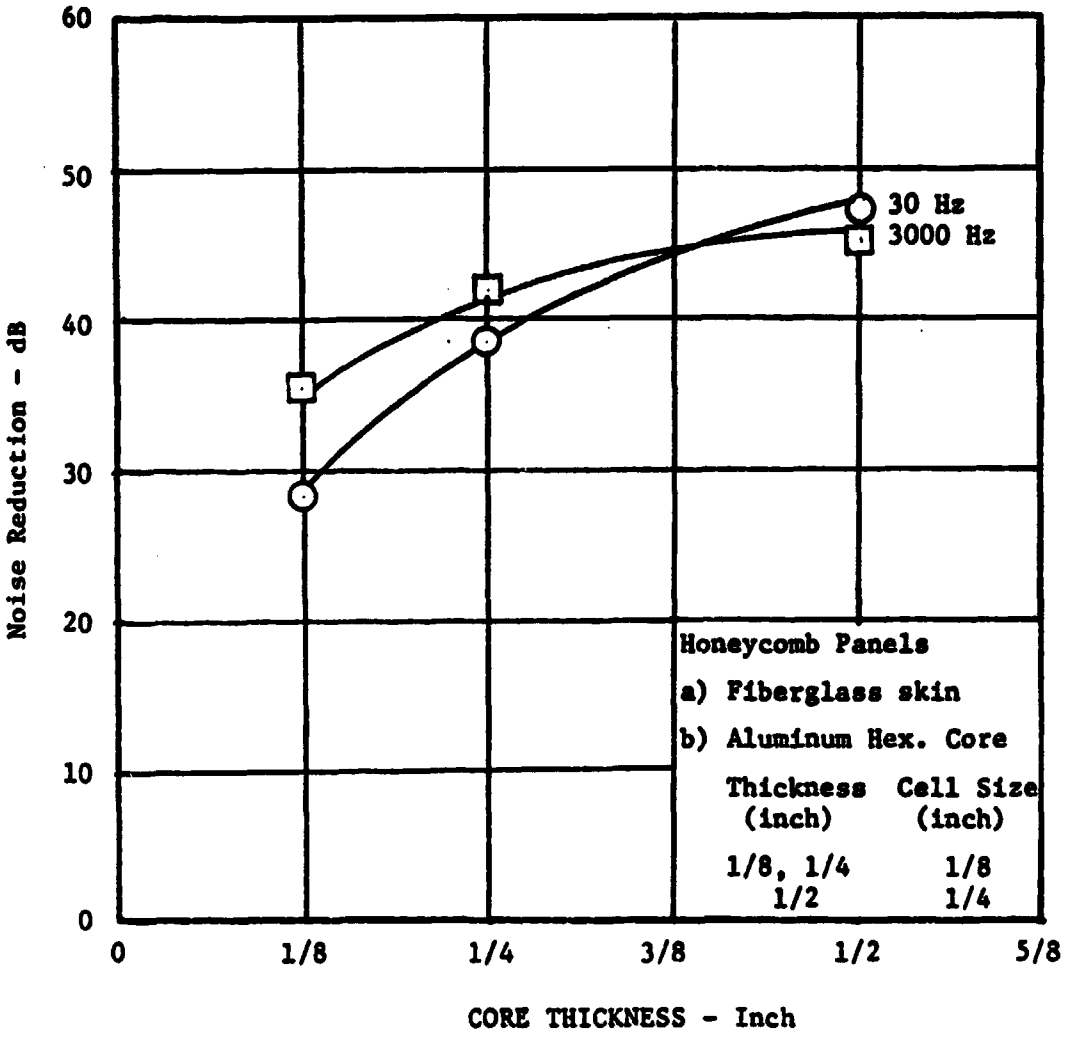

Figure 2.10: Effect of Core Thickness on Noise Reduction Characteristics of a Honeycomb Panel

teristics. The resonance frequency is also high due to the same reason. For the same facing material, the thickness of the core material appears to be the most important factor. The effect of core stiffness, or Young's modulus, has no significant effect at low frequency. In the mass law region, the effect of thickening of the core is seen to be small.

2.2.8 Summary

The effects of individual layers and stiffeners have been discussed in Subsections 2.2.2 through 2.2.6. The results of 30 Hz are cross-plotted for various panels as a function of mass in Figure 2.11. As can be seen, the noise reduction of sandwiched panels is in general higher. The study of an individual noise reduction curve shows an increase in fundamental resonance frequency for these panels. While the increased stiffness for the honeycomb and stiffened panels is easily predicted (Subsections 2.3.3 and 2.3.4), the increase in low frequency noise reduction of P.V.C.-based rigid foam and fibrous sound absorbing material is not predicted. The increased stiffness can also be due to the following causes:

(i) The edge conditions may not have been simply supported for both face plates.

(ii) The clamping of the panel in the Beranek tube may have introduced some membrane stresses, which could have increased the stiffness.

(iii) The actual mechanism of sound transmission may lie in between shear resistant and non-shear resistant core.

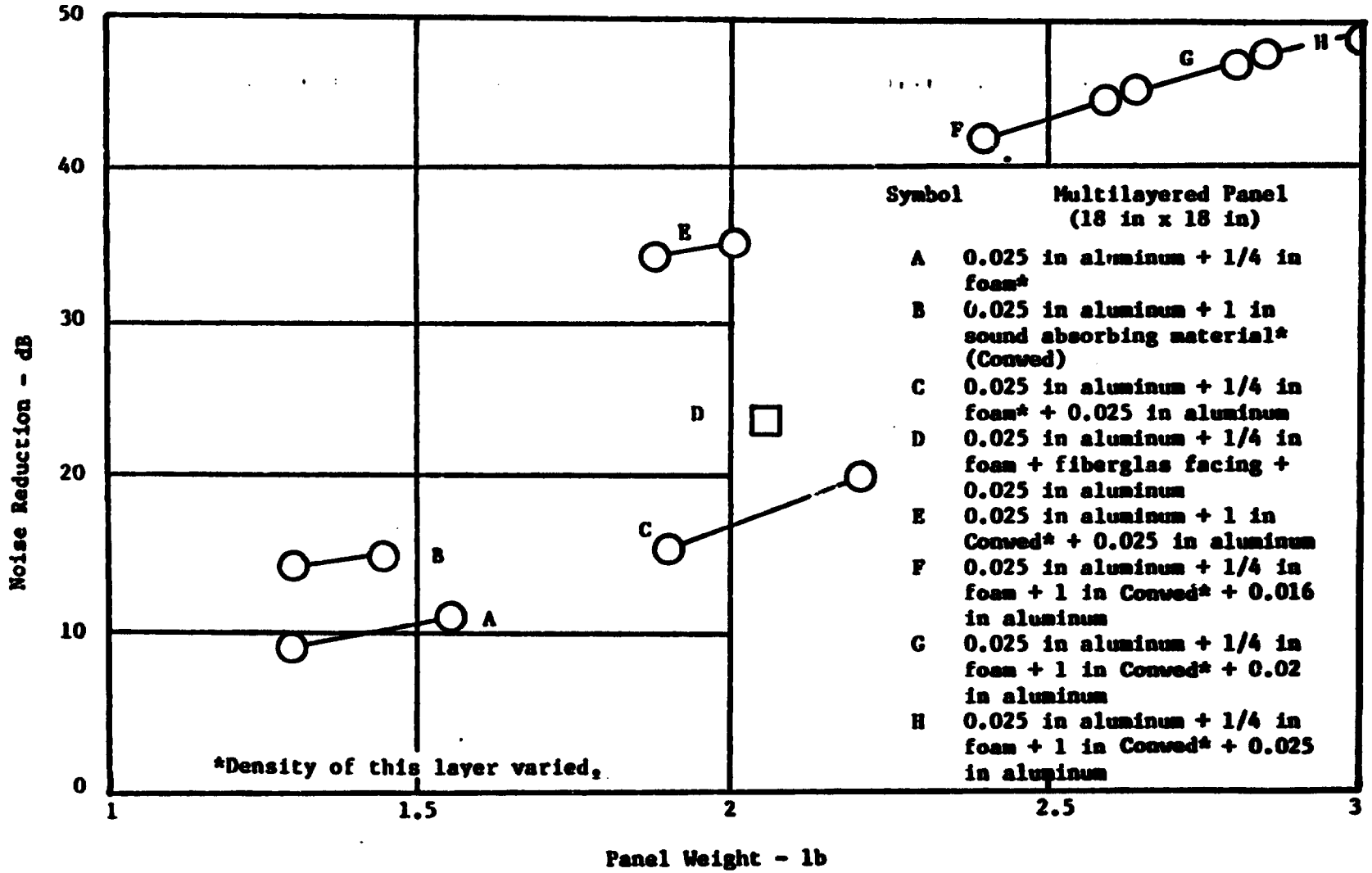

Figure 2.11: Effect of Mass on Low Frequency Noise Reduction of Multilayered Panels

In summary, honeycomb panels offer the best noise reduction in the low frequency region. Sandwich panels with fibrous sound absorbing materials offer good noise reduction characteristics in both low and high frequency regions.

2.3 THEORETICAL ANALYSIS

The theoretical analysis of low frequency noise transmission of multilayered panels is very complex due to the number of variables involved. The noise reduction of panels at low frequencies is very much dependent upon the mounting details (or edge conditions). The method of attachment between the layers (and hence the ability to transmit shear stresses) also affects noise reduction to a great extent in the low frequency region.

In the following two subsections, two extreme cases of attachment between two layers will be considered. In Subsection 2.3.1 noise reduction/transmission loss of a sandwich panel in which there is no sliding between the layers present will be derived. The characteristics of a sandwich panel in which there is perfect sliding (no shear constraints) will be considered in Subsection 2.3.2. The results from these two subsections will be used to calculate noise reduction values to be compared with the experimental values obtained for some of the panels tested.

2.3.1 Shear Resistant Sandwich Panel

In this subsection an analytical expression will be derived for noise reduction through a triple-layered panel in which there is no

sliding between the panels. A honeycomb panel is a perfect example of such a panel. The method is based on theoretical considerations presented in Reference 7.

The dynamic equilibrium of the multilayered panels is used for writing the governing differential equations of the motion. The sound pressures acting on the structure are shown schematically in Figure 2.12.

The following assumptions are made:

(a) The deflection of the structure is small so the small deflection theory can be used.

(b) The individual layers are isotropic.

(c) Sliding between the layers is prevented.

In this case, the governing differential equation of equilibrium for layered plates is given by Reference 19:

$$D^* \nabla^2 \nabla^2 w(x,y) = p_z(x,y) \tag{2.1}$$

where:

D^* = transformed flexural rigidity

w = lateral displacement of the panel

p_z = lateral forcing function.

The transformed flexural rigidity of the layered plate is given by (Ref. 19):

$$D^* = (AC - B^2)/A \tag{2.2}$$

where:

$$A = \sum_{k=1}^{3} \frac{E_k}{1-\nu_k^2} (z_k - z_{k-1}) \tag{2.3}$$

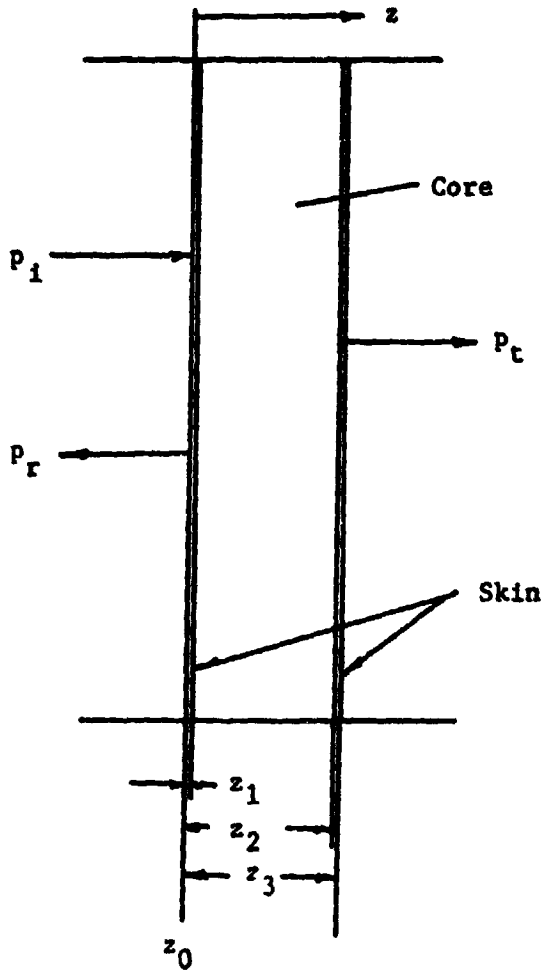

Figure 2.12: Geometry of Sound Pressures Acting on a Shear-Resistant Sandwich Panel

$$B = \sum_{k=1}^{3} \frac{E_k}{1-\nu_k^2} \left(\frac{z_k^2 - z_{k-1}^2}{2}\right) \tag{2.4}$$

$$C = \sum_{k=1}^{3} \frac{E_k}{1-\nu_k^2} \left(\frac{z_k^3 - z_{k-1}^3}{3}\right) \tag{2.5}$$

where:

E_k = Young's modulus of k^{th} layer

ν_k = Poisson's ratio of k^{th} layer

z_k, z_{k-1} = z coordinates of layers k and k-1, respectively (see Fig. 2.12)

The transferred flexural rigidity, D*, can be simplified in case Young's modulus of the core is far less than that of the facings and also if the facing materials are the same. (See Section 2.3 for D* of honeycomb panels.)

In the dynamic equilibrium of a plate element, the inertial forces associated with the translation of the plate element is:

$$-m \frac{\partial w^2}{\partial t^2}$$

For simplicity of analysis, only viscous damping will be assumed to be present. The structural damping term, which is proportional to the deflection rather than the velocity, is neglected. This assumption is being made because the viscous damping due to the core material will be greater than the structural damping of facings.

The forces due to damping then are given by:

$$-a\dot{w}$$

Extending the differential equation of static equilibrium by adding force terms due to inertia and damping forces, the differential equation of forced, damped motion of the panel is obtained.

$$D^*\nabla^2\nabla^2 w(x, y, t) + m\frac{\partial^2 w}{\partial t^2} + \alpha\frac{\partial w}{\partial t} = p(x, y, t) \qquad (2.6)$$

The lateral forcing function, p(x, y, t), is in this case time dependent. Under steady state conditions the pressures shown in Figure 2.12, which are the lateral forcing functions, may be represented by:

$$P_i(x, y, z, t) = A(x, y)\, e^{j(\omega t - kz)} \qquad (2.7)$$

$$P_r(x, y, z, t) = B(x, y)\, e^{j(\omega t + kz)} \qquad (2.8)$$

$$P_t(x, y, z, t) = C(x, y)\, e^{j(\omega t - kz)} \qquad (2.9)$$

where:

A, B, C are the steady state sound pressure amplitudes;

k, the wavenumber ($=\omega/c$);

ω, the angular frequency;

c, the speed of sound.

The time invariant parts of the sound pressure functions in Equations (2.7) through (2.9) can be represented by a double trigonometric series.

In general,

$$p(x, y) = \sum_{m=1}^{\infty}\sum_{n=1}^{\infty} P_{mn} \sin\left(\frac{m\pi x}{a}\right) \sin\left(\frac{n\pi y}{b}\right) \qquad (2.10)$$

where m and n are integers and a and b the panel dimensions.

If the core is considered incompressible, the faces of the multilayered panel will vibrate in phase, and hence the entire panel

may be assumed to vibrate as a single unit. (The implications of this assumption are discussed later on in this section.) With this assumption, Navier's method can be used to find the solution to Equation (2.6).

In accordance with this method, the solution is to be considered of the form:

$$w(x, y, t) = e^{j\omega t} \sum_{m=1}^{\infty} \sum_{n=1}^{\infty} W_{mn} \sin\left(\frac{m\pi x}{a}\right) \sin\left(\frac{n\pi y}{b}\right) \qquad (2.11)$$

Substituting Equations (2.10) and (2.11) in Equation (2.6) gives for a simply supported square panel whose side is a:

$$D^* W_{mn} \left(\frac{\pi}{a}\right)^4 (m^4 + 2m^2n^2 + n^4) - m\omega^2 W_{mn} + j\alpha\omega W_{mn} = P_{mn} \qquad (2.12)$$

where:

$m = 1, \infty$

$n = 1, \infty$

The undamped free panel resonance frequency for the (m, n) mode of a simply supported square panel is given by:

$$\omega_{mn} = \left(\frac{\pi}{a}\right)^2 (m^2 + n^2) \sqrt{D^*/m} \qquad (2.13)$$

For the multilayered panel the RHS in Equation (2.12) is given from Equations (2.7) through (2.9) as:

$$P_{mn} = A_{mn} + B_{mn} - C_{mn} \qquad (2.14)$$

Equations (2.11), (2.12) and (2.13) generate:

$$W_{mn} = \frac{A_{mn} + B_{mn} - C_{mn}}{m(\omega_{mn}^2 - \omega^2) + j\alpha\omega^2} \qquad (2.15)$$

Another boundary condition to be satisfied is that the particle velocity of the air and the panel velocity have to match at the boundary of air and panel. This results in:

$$u = \frac{P_i - P_r}{\rho c} = \frac{P_t}{\rho c} \tag{2.16}$$

or:

$$j\omega W_{mn} = \frac{A_{mn} - B_{mn}}{\rho c} = \frac{C_{mn}}{\rho c} \tag{2.17}$$

Noise reduction through a multilayered panel is defined as:

$$NR = 10 \log \left| \frac{P_i + P_r}{P_t} \right|^2 \tag{2.18}$$

With Equations (2.7) through (2.9) this becomes:

$$NR = 10 \log \left| \frac{\sum (A_{mn} + B_{mn})}{\sum C_{mn}} \right|^2 \tag{2.19}$$

Considering only a single-degree-of-freedom model:

$$NR = 10 \log \left| \frac{A_{11} + B_{11}}{C_{11}} \right|^2 \tag{2.19a}$$

Equations (2.15), (2.17) and (2.19a) generate for m = 1, and n = 1.

$$NR = 10 \log \left[(1 + \frac{\alpha}{\rho c})^2 + \{ \frac{m(\omega_{11} - \omega^2)}{\omega \rho c} \}^2 \right] \tag{2.20}$$

In a single-degree-of-freedom model, with the damping factor defined as:

$$\zeta = \frac{\alpha}{2m\omega_n} \text{ , where } \omega_n = \omega_{11} \tag{2.21}$$

we get:

$$NR = 10 \log \left[\{ 1 + \frac{2m\omega_n \zeta}{\rho c} \}^2 + \{ \frac{m(\omega_n^2 - \omega^2)}{\omega \rho c} \}^2 \right] \tag{2.22}$$

For this single-degree-of-freedom model, the damped natural frequency is given by:

$$\omega_{n_D} = \sqrt{1 - \zeta^2}\,\omega_n \tag{2.23}$$

where:

ω_n is given by Equation (2.13) for m = 1, n = 1

ω_{n_D} = damped natural frequency of the SDOF system.

Transmission loss (TL) of this SDOF system is given by:

$$TL = 10 \log \left[\frac{P_i}{P_t}\right]^2 \tag{2.24}$$

From Equations (2.7), (2.8), (2.9), (2.15), (2.17), (2.19), (2.21) and (2.24) we get:

$$TL = 10 \log \left[\left\{1 + \frac{m\omega_n\zeta}{\rho c}\right\}^2 + \left\{\frac{m(\omega_n^2 - \omega^2)}{2\omega\rho c}\right\}^2\right] \tag{2.25}$$

In deriving Equations (2.22) and (2.25) it had been assumed that the core is incompressible. Such an assumption is not normally valid for core materials such as foams and honeycomb (References 20 and 21). Most of the core materials will have a finite value of Young's modulus. Therefore, in addition to the flexural modes of vibrations which are obtained from Equation (2.6) and in which the faces of a sandwich panel vibrate in phase, dilatational modes, in which the panel can no longer be considered as a single unit, occur. In this mode the face plates vibrate independently of each other, amplitudes and frequency being dependent upon Young's modulus of the core. When there is a 180° phase difference between the two faces, dilatational resonances occur. At these resonance frequencies the noise reduction becomes very low.

Once again a single-degree-of-freedom approximation can be made to model this mode of vibration. The first dilatational resonance in which the faces act as a single mass connected by a springlike core is given by Reference 8:

$$f_d = \frac{1}{2\pi} \left[\frac{4E_2}{h_2(m_1 + m_3 + m_2/3)}\right]^{1/2} \tag{2.26}$$

where:

f_d is the first dilatational resonance frequency

E_2 is the effective Young's modulus in compression of the core

m_1 m_2 m_3 are the mass per unit areas of the individual layers 1, 2 and 3.

Table 2.1 gives the effect of varying Young's Modulus of the core on the first dilatational frequency for the type of sandwich constructions tested. These frequencies are calculated using Equations (2.13) and (2.26). As the table indicates, even with a low Young's modulus, the dilatational frequency is higher than the range of frequency of our interest.

2.3.2 Panel with Non-Shear-Resistant Core

In the second limiting case considered, no mechanical coupling between the faces is assumed. Under these conditions the core is free to slide between the faces. In order to analyze this case, the following model is proposed:

Table 2.1 Effect of Young's Modulus of the Core on First Dilatational Frequency

Sandwich Panel

Skin: 0.025 Inch Aluminum

Density = $\rho_1 = \rho_3 = 2700$ kg/m^3

Young's Modulus = $1.05 \times 10^7 \times 6895$ N/m^2

Core

Thickness, $t_2 = 0.5 \times 0.0254$ m

Density, $\rho_2 = 67.5$ kg/m^3

Young's Modulus = Ec_2 = Varied

$$\text{First Dilatational Frequency} = \frac{1}{2\pi}\sqrt{\frac{4Ec_2}{t_2(m_1 + m_3 + m_{2/3})}} \quad \text{(Equation 2.26)}$$

where: $m_i = \rho_i * t_i$

Young's Modulus of the Core (psi)	Calculated Dilatational Frequency (Hz)
10	384
100	1217
200	1721
500	2721
1000	3848
5000	8605

[1 psi = 6895 N/m^2]

(a) The sandwiched panel can be considered as a flexible double wall with the core acting as a (porous) medium transmitting acoustic energy.

(b) There is no resistance offered by the core to the movements of the face plates.

(c) There is no mechanical transport of acoustic energy between the faces. This means that the sound transmission through structures (structure borne flanking path) is neglected.

The analytical approach is based on References 7 and 22. A typical sandwich panel and the pressure forces acting it, under the above assumptions, are given in Figure 2.13. In addition, the following assumptions will be made:

(a) The thickness of the face is small compared to the thickness of the core.

(b) The deflections are small.

Along the lines of Subsection 2.3.1 the homogeneous biharmonic differential equation of the individual face of a sandwich panel is given by:

$$D_i \nabla^2 \nabla^2 w_i(x, y) = p(x, y)$$

where:

D_i = flexural rigidity of the face, i

w_i = lateral displacement of the face, i

p = lateral forcing function

i = subscript denoting face 1 or 2.

The dynamic equilibrium of the individual faces can be written in a similar way as:

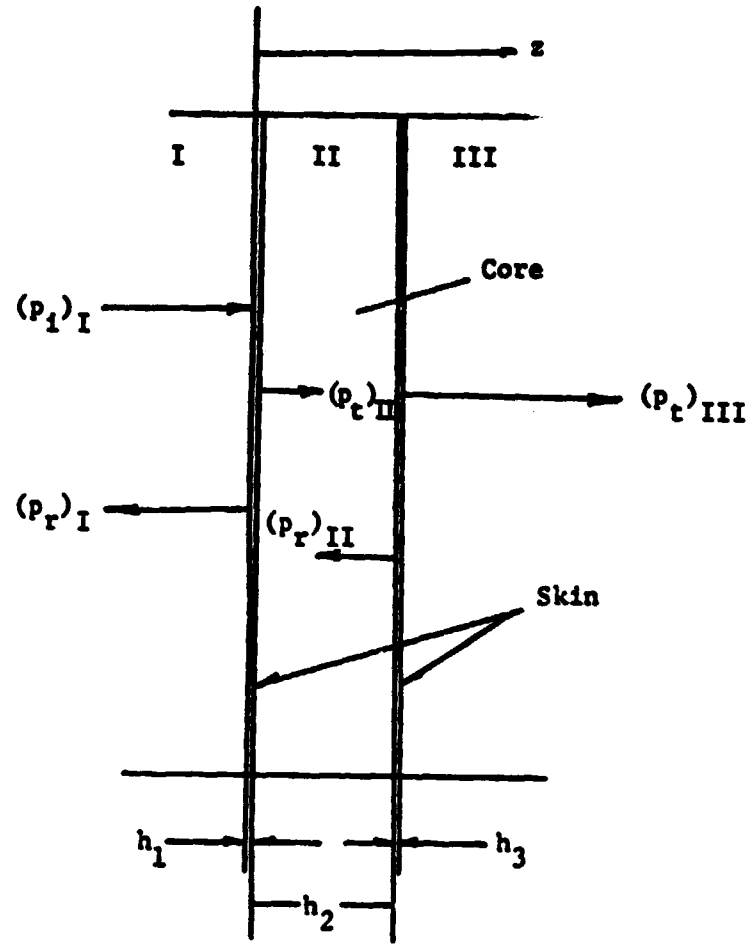

Figure 2.13: Geometry of Sound Pressure Forces Acting on a Non-Shear-Resistant Sandwich Panel

$$D_i \nabla^2 \nabla^2 w_i(x, y, t) + m_i \frac{\partial w_i^2}{\partial t^2} + j\alpha w_i = p(x, y, t) \qquad (2.28)$$

where:

m_i is the mass per unit area of face i

$j = \sqrt{-1}$

α_i is the structural damping factor of face i (proportional to displacement) (Reference 19)

Both displacement w_i and the lateral forcing function, p, are time dependent. Under steady state conditions the pressures shown in Figure 2.13, which form the forcing functions, may be expressed as:

$$(P_i)_I(x, y, z, t) = A(x, y)e^{j(\omega t - k_1 z)} \qquad (2.29)$$

$$(P_r)_I(x, y, z, t) = B(x, y)e^{j(\omega t + k_1 z)} \qquad (2.30)$$

$$(P_t)_{II}(x, y, z, t) = C(x, y)e^{j(\omega t - k_2 z)} \qquad (2.31)$$

$$(P_r)_{II}(x, y, z, t) = D(x, y)e^{j[\omega t + k_2 (z-h_2)]} \qquad (2.32)$$

$$(P_t)_{III}(x, y, z, t) = E(x, y)e^{j[\omega t - k_3 (z-h_2)]} \qquad (2.33)$$

where:

A, B, C, D and E are the steady state sound pressure amplitudes

I, II and III are subscripts referring to regions depicted in Figure 2.13.

z is the coordinate perpendicular to the plane of the panel

h_2 is the thickness of the core material

k_1, k_2, k_3 are the wave numbers in mediums I, II, and III

$$(k_i = \frac{\omega}{c_i})$$

c_1, c_2, c_3 are the speed of sound in the mediums I, II, and III

ω is the angular frequency.

The time invariant parts of the sound pressure functions in Equations (2.29) through (2.33) can be represented by:

$$p(x, y) = \sum_{m=1}^{\infty} \sum_{n=1}^{\infty} P_{mn} \sin \frac{m\pi x}{a} \sin \frac{n\pi y}{b} \qquad (2.34)$$

where:

m, n are integers;

a, b are panel dimensions.

In accordance with Navier's method (Reference 19), the solution is to be considered of the form:

$$w_i(x, y, t) = e^{j\omega t} \sum_{m=1}^{\infty} \sum_{n=1}^{\infty} W_{mn_i} \sin \frac{m\pi x}{a} \sin \frac{n\pi y}{b} \qquad (2.35)$$

Substituting Equations (2.34) and (2.35) in (2.28) gives, for a simply supported square face at z = 0,

$$D_i W_{mn_i} (\frac{\pi}{a})^4 (m^4 + 2m^2n^2 + n^4) - m_i \omega^2 W_{mn_i} + j\alpha_i W_{mn_i} = P_{mn} \qquad (2.36)$$

where:

m = 1, 2, . . . ∞

n = 1, 2, . . . ∞

For face 1, from Figure 2.13, the time invariant part of the forcing function is written as:

$$P_{mn_1} = A_{mn} + B_{mn} - C_{mn} - D_{mn} e^{-jk_2 h_2} \qquad (2.37)$$

The panel resonance frequency for the (m, n) mode of a simply supported square panel is given by Reference 23.

$$\omega_{mn} = \left(\frac{\pi}{a}\right)^2 (m^2 + n^2)\sqrt{D_1/m_1} \tag{2.38}$$

Equations (2.36), (2.37) and (2.38) generate:

$$W_{mn_1} = \frac{A_{mn} + B_{mn} - C_{mn} - D_{mn}^{-jk_2h_2}}{m_1(\omega_{mn}^2 - \omega^2) + j\alpha} \tag{2.39}$$

For aluminum, the structural damping α is of the order of 0.02 (References 7 and 22). Although structural damping is theoretically present in all plate vibrations, it will be ignored in further treatment of this problem. Then:

$$W_{mn_1} = \frac{A_{mn} + B_{mn} - C_{mn} - D_{mn}e^{-jk_2h_2}}{m_1(\omega_{mn}^2 - \omega^2)} \tag{2.39a}$$

One other boundary condition that has to be satisfied is that the particle velocity of the core and the velocity of the panel have to match at the boundary of air and core at $z = 0$.

$$u_1 = \frac{(P_i)_I - (P_r)_I}{Z_1} = \frac{(P_t)_{II} - (P_r)_{II}}{Z_2} \tag{2.40}$$

where:

u_1 is the particle velocity at $z = 0$

Z_1 is the impedance of the air ($= \rho c$)

ρ is the density of air

c is the velocity of sound

Z_2 is the impedance of the core.

The impedance of an absorptive porous core will, in general, be complex and will be discussed in detail later in this section.

From Equations (2.29) through (2.32) and (2.40) we get, at $z = 0$:

$$j\omega W_{mn_1} = \frac{A_{mn} - B_{mn}}{\rho c} = \frac{C_{mn} - D_{mn}e^{-jk_2h_2}}{Z_2} \tag{2.41}$$

Equations (2.39a) and (2.41) yield:

$$A_{mn} + B_{mn} = \{1 - j(\frac{\rho c}{Z_2})q_1\}C_{mn} + \{1 + j(\frac{\rho c}{Z_2})q_1\}D_{mn}e^{-jk_2h_2} \tag{2.42}$$

$$A_{mn} = \frac{1}{2}\{1 + (\frac{\rho c}{Z_2}) - j(\frac{\rho c}{Z_2})q_1\}Cmn + \{1 - (\frac{\rho c}{Z_2}) + j(\frac{\rho c}{Z_2})q_1\}D_{mn}e^{-jk_2h_2} \tag{2.43}$$

where:

$$q_i = \frac{m(\omega_{mn}^2 - \omega^2)}{\omega\rho c} \qquad i = 1, 2 \tag{2.43a}$$

The same approach is used to determine the pressure amplitudes for the second face of the sandwich panel at h_2. The time dependent lateral panel deflection is given by:

$$w_2(x, y, t) = W_2(x, y)e^{j(\omega t - \phi)} \tag{2.44}$$

where ϕ is the phase difference between the vibrations of face 1 and face 2.

Analogous to Equation (2.39a) at $z = h_2$:

$$W_{mn_2}e^{-j\phi} = \frac{C_{mn}e^{-jk_2h_2} + D_{mn} - E_{mn}}{m_2(\omega_{mn}^2 - \omega^2)} \tag{2.45}$$

Equating the particle velocity and plate velocity at $z = h_2$:

$$u_2 = \frac{(P_t)_{II} - (P_r)_{II}}{Z_2} = \frac{(P_t)_{III}}{Z_3} \tag{2.46}$$

where:

Z_3 is the impedance of air ($= Z_1 = \rho c$)

or:

$$j\omega W_{mn_2} e^{-j\phi} = \frac{C_{mn} e^{-jk_2h_2} - D_{mn}}{Z_2} = \frac{E_{mn}}{\rho c} \tag{2.47}$$

and

$$E_{mn} = j\omega\rho c W_{mn_2} e^{-j\phi} \tag{2.48}$$

Equations (2.45), (2.46) and (2.47) generate:

$$C_{mn} = \frac{e^{jk_2h_2}}{2} \{1 - jq_2 + (\frac{Z_2}{\rho c})\} E_{mn} \tag{2.49}$$

$$D_{mn} = \frac{1}{2} \{1 - jq_2 - (\frac{Z_2}{\rho c})\} E_{mn} \tag{2.50}$$

Substituting Equations (2.49) and (2.50) into Equations (2.42) and (2.43), we get:

$$\frac{A_{mn} + B_{mn}}{E_{mn}} = \frac{e^{jk_2h_2}}{2} [\{1 - j(\frac{\rho c}{Z_2})q_1\}\{1 - jq_2 + (\frac{Z_2}{\rho c})\} + \{1 + j(\frac{\rho c}{Z_2})q_1\}\{1 - jq_2 - (\frac{Z_2}{\rho c})\}e^{-jk_2h_2}] \tag{2.51}$$

$$\frac{A_{mn}}{E_{mn}} = \frac{e^{jk_2h_2}}{4} [\{1 + (\frac{\rho c}{Z_2}) - j(\frac{\rho c}{Z_2})q_1\}\{1 - jq_2 + (\frac{Z_2}{\rho c})\} + \{1 - (\frac{\rho c}{Z_2}) + j(\frac{\rho c}{Z_2})q_1\}\{1 - jq_2 - \frac{Z_2}{\rho c})e^{-jk_2h_2}] \tag{2.52}$$

By definition:

$$\text{Noise Reduction} = 10 \log \left|\frac{(P_i)_I + (P_r)_I}{(P_t)_{III}}\right|^2 \tag{2.53}$$

$$NR = 10 \log \left| \frac{\sum_{m,n=1}^{\infty} (A_{mn} + B_{mn})}{\sum_{m,n=1}^{\infty} E_{mn}} \right|^2 \qquad (2.54)$$

For a single-degree-of-freedom model:

$$NR = 10 \log \left| \frac{A_{11} + B_{11}}{E_{11}} \right|^2 \qquad (2.54a)$$

Substituting (2.51) in (2.54a):

$$NR = 10 \log \left| \tfrac{1}{2}\{(1 - j(\tfrac{\rho c}{Z_2})q_1)(1 - jq_2 + \tfrac{Z_2}{\rho c})e^{+jk_2h_2} + (1 + j(\tfrac{\rho c}{Z_2})q_1)(1 - jq_2 - \tfrac{Z_2}{\rho c})e^{-jk_2h_2}\} \right|^2 \qquad (2.55)$$

Similarly, transmission loss of a SDOF system is given by:

$$TL = 10 \log \left| \frac{A_{11}}{E_{11}} \right|^2 \qquad (2.56)$$

Substitution of (2.52) in (2.56) results in:

$$TL = 10 \log \left| \tfrac{1}{4}\{(1 + (\tfrac{\rho c}{Z_2}) - j(\tfrac{\rho c}{Z_2})q_1)(1 - jq_2 + (\tfrac{Z_2}{\rho c}))e^{+jk_2h_2} + (1 - (\tfrac{\rho c}{Z_2}) + j(\tfrac{\rho c}{Z_2})q_1)(1 - jq_2 - \tfrac{Z_2}{\rho c})e^{-jk_2h_2}\} \right|^2 \qquad (2.57)$$

Equations (2.55) and (2.57) represent the noise attenuation equations for a multilayered panel. In general, the value of the impedance of the core and the wave number k_2 of the core will be complex. The method of calculation of these two quantities is given in Reference (8). They depend upon the frequency, flow resistivity, porosity, and effective gas density of the core material. Appendix C gives the method to calculate the values based on Reference 8. Table 2.2 gives the values of the impedance for a typical fibrous core material at different frequencies. The propagation constant, b, can be written as:

Table 2.2 Calculation of Complex Impedance of PF105 Material (Based on Reference 8)

Bulk density = ρ_m = 9.6 kg/m^3

Gas in material, air, density = ρ_0 = 1.18 kg/m^3

Fiber diameter = d = 1.0 micron

Porosity = P = 0.99

Structures factor = s = 1.0

Flow resistivity = 4.1 x 10^4 MKS Rayls/m

Frequency	100	300	600	1000	3000	5000
f_1	67.5	83.9	2.8	1.67	1.07	1.03
f_2	608	68.4	17.9	7.07	1.67	1.24
α dB/m	3.0	27.3	79.5	156	367	446
λ_m m	.99	.347	.195	.138	.074	.053
R_2 MKS Rayls	1055	1030	943	821	542	466
X_2 MKS Rayls	-112	-162	-268	-325	-269	-202
$\|Z_2\|$ MKS Rayls	1057	1042	981	882	605	508
θ deg	-3.1	-8.9	-15.9	-21.6	-26.4	-23.44

f_1, f_2 defined in Appendix C

α attenuation constant, dB/m

λ_m wavelength in the material, m

R_2 real part of complex impedance, MKS Rayls

X_2 imaginary part of complex impedance, MKS Rayls

$|Z_2|$ absolute value of complex impedance, MKS Rayls

θ phase of Z_2, degrees

$$b = jk_2 = \alpha + j\beta \tag{2.58}$$

As can be seen from Appendix C and Table 2.2, at very low frequencies attenuation constant α is small for the range of thickness used ($\sim$0.05 m). Hence the wave number k_2 may be assumed to be real. With this assumption Equations (2.55) and (2.57) can be simplified as:

$$NR = 10 \log\left|\left\{\cos k_2h_2 - \frac{X_2}{\rho c}\sin k_2h_2 + \frac{q_1\rho c}{|z_2|^2}(R_2 - q_2X_2)\sin k_2h_2\right\} + \right.$$

$$\left. + j\left\{-(q_1 + q_2)\cos k_2h_2 + \frac{R_2}{\rho c}\sin k_2h_2 - \frac{q_1\rho c}{|z_2|^2}(R_2q_2 + X_2)\sin k_2h_2\right\}\right|^2 \tag{2.59}$$

$$TL = 10 \log\left|\frac{1}{2}\left[\left\{\cos k_2h_2 + \left(\frac{\rho c\, X_2}{|z_2|^2} - \frac{X_2}{\rho c} - \frac{q_1q_2\rho cX_2}{|z_2|^2} + \frac{(q_1 + q_2)\rho cR_2}{|z_2|^2}\right)\sin k_2h_2\right\} + \right.\right.$$

$$\left.\left. + j\left\{-(q_1 + q_2)\cos k_2h_2 + \left(\frac{R_2}{\rho c} + \frac{\rho cR_2}{|z_2|^2} - \frac{q_1q_2\rho cR_2}{|z_2|^2} - \frac{(q_1 + q_2)\rho cX_2}{|z_2|^2}\right)\sin k_2h_2\right\}\right]\right|^2 \tag{2.60}$$

The noise reduction and transmission loss characteristics of a twin layered panel, in which a sound absorbing material is attached to an aluminum panel, can be derived from the above analysis. A typical twin layered panel and the pressure forces acting on it under the same assumptions as for three-layered panels are given in Figure 2.14. The equations may also be developed along the same lines as a sandwich panel. Equation (2.29) through (2.43) are still applicable for the twin layered case also.

At the boundary between sound absorption material and air, the pressure forces acting are as shown in Figure 2.14. The boundary conditions that need to be satisfied are: (a) at the boundary, the pressure forces should be the same on both sides, and (b) the particle velocities should be the same on the boundary. This gives:

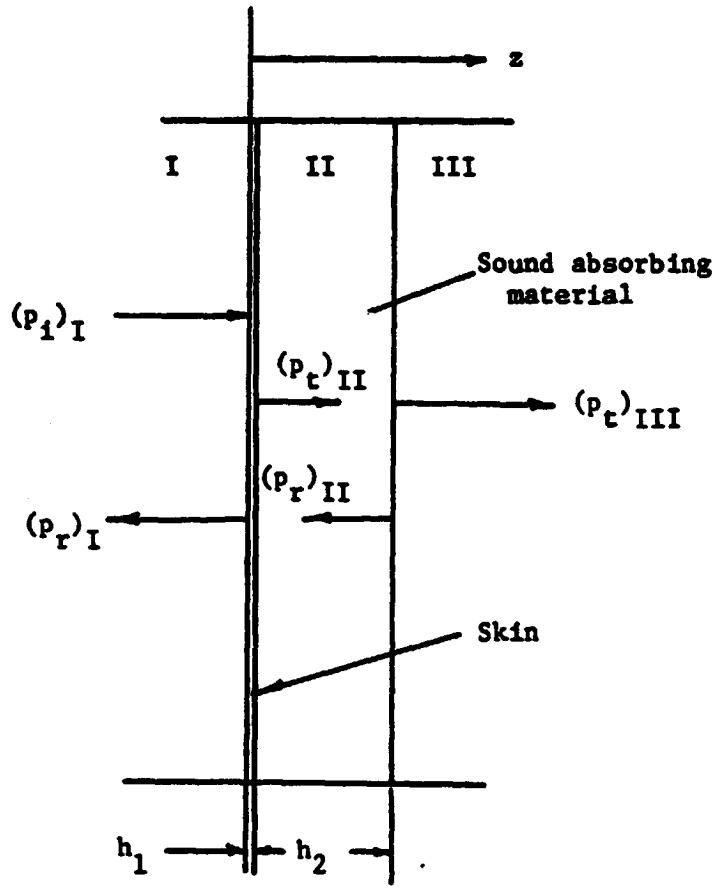

Figure 2.14: Geometry of Sound Pressure Forces Acting on a Twin Layered Panel

$$(P_t)_{II} + (P_r)_{II} = (P_t)_{III} \tag{2.61}$$

$$\frac{(P_t)_{II} - (P_r)_{II}}{Z_2} = \frac{(P_t)_{III}}{\rho c} \tag{2.62}$$

Substituting (2.31) through (2.33) in (2.61) and (2.62):

at $z = h_2$

$$Ce^{-jk_2h_2} + D = E \tag{2.63}$$

$$Ce^{-jk_2h_2} - D = (\frac{Z_2}{\rho c})E \tag{2.64}$$

Equations (2.63) and (2.64) generate:

$$C = \frac{e^{+jk_2h_2}}{2}\{1 + \frac{Z_2}{\rho c}\}E \tag{2.65}$$

$$D = \frac{1}{2}\{1 - \frac{Z_2}{\rho c}\}E \tag{2.66}$$

Substituting Equations (2.65) and (2.66) into (2.42) and (2.43), we get:

$$\frac{A + B}{E} = \frac{e^{jk_2h_2}}{2}[\{1 - j(\frac{\rho c}{Z_2})q_1\}\{1 + \frac{Z_2}{\rho c}\} + \{1 + j(\frac{\rho c}{Z_2})q_1\}\{1 - \frac{Z_2}{\rho c}\}e^{-j2k_2h_2}] \tag{2.67}$$

$$\frac{A}{E} = \frac{e^{jk_2h_2}}{2}[\{1 + x(\frac{\rho c}{Z_2}) - j(\frac{\rho c}{Z_2})\}\{1 + \frac{Z_2}{\rho c}\} + \{1 - (\frac{\rho c}{Z_2}) + j(\frac{\rho c}{Z_2})q_1\}\{1 - \frac{Z_2}{\rho c}\}e^{-j2k_2h_2}] \tag{2.68}$$

The noise reduction and transmission loss are calculated using Equations (2.54a) and (2.58). This results in (for low frequencies):

$$NR = 10 \log|\{\cos k_2h_2 - \frac{X_2}{\rho c}\sin k_2h_2 + \frac{q_1\rho c}{|Z_2|^2}R_2 \sin k_2h_2\} +$$

$$j\{-q_1\cos k_2h_2 + \frac{R_2}{\rho c}\sin k_2h_2 - \frac{q_1\rho c}{|Z_2|^2}X_2\sin k_2h_2\}|^2 \tag{2.69}$$

$$TL = 10 \log\left|\frac{1}{2}\left[2\cos k_2 h_2 + \left(\frac{\rho c X_2}{|Z_2|^2} - \frac{X_2}{\rho c} + \frac{q_1 \rho c R_2}{|Z_2|^2}\right)\sin k_2 h_2 + j\left\{-q_1 \cos k_2 h_2 + \left(\frac{R_2}{\rho c} + \frac{\rho c R_2}{|Z_2|^2} - \frac{q_1 \rho c X_2}{|Z_2|^2}\right)\sin k_2 h_2\right\}\right]\right|^2 \quad (2.70)$$

The theoretical noise reduction characteristics of a triple layered panel with 0.025 inch aluminum skins and PF105 (Reference 8) fiberglass 1 inch thick was calculated using Equation (2.55). For this purpose Equation (2.55) was programmed into a Honeywell 66/60 series computer using time sharing Fortran. The low frequency approximation (Equation 2.59) was programmed into an Apple II micro-computer using Applesoft language. The calculated values are plotted in Figure 2.15. The noise reduction value at 20 Hz is nearly zero, as the fundamental resonance frequency of 0.025 inch aluminum is ∿17 Hz. There is one more resonance frequency at 460 Hz due to the skin-core-skin resonance. Because Equation (2.59) is complicated, this value of resonance cannot be found explicitly (as has been done in Section 3.1 for air gaps). The value was found by trial and error method. At high frequency, the noise reduction values are higher than the mass law due to absorption in the core (α) and due to reflection losses at the interfaces of surfaces.

2.3.3 Analysis of Results

2.3.3.1 Stiffened Aluminum Panel with Damping Material

For the analysis of the stiffened aluminum panel, the following assumptions will be made:

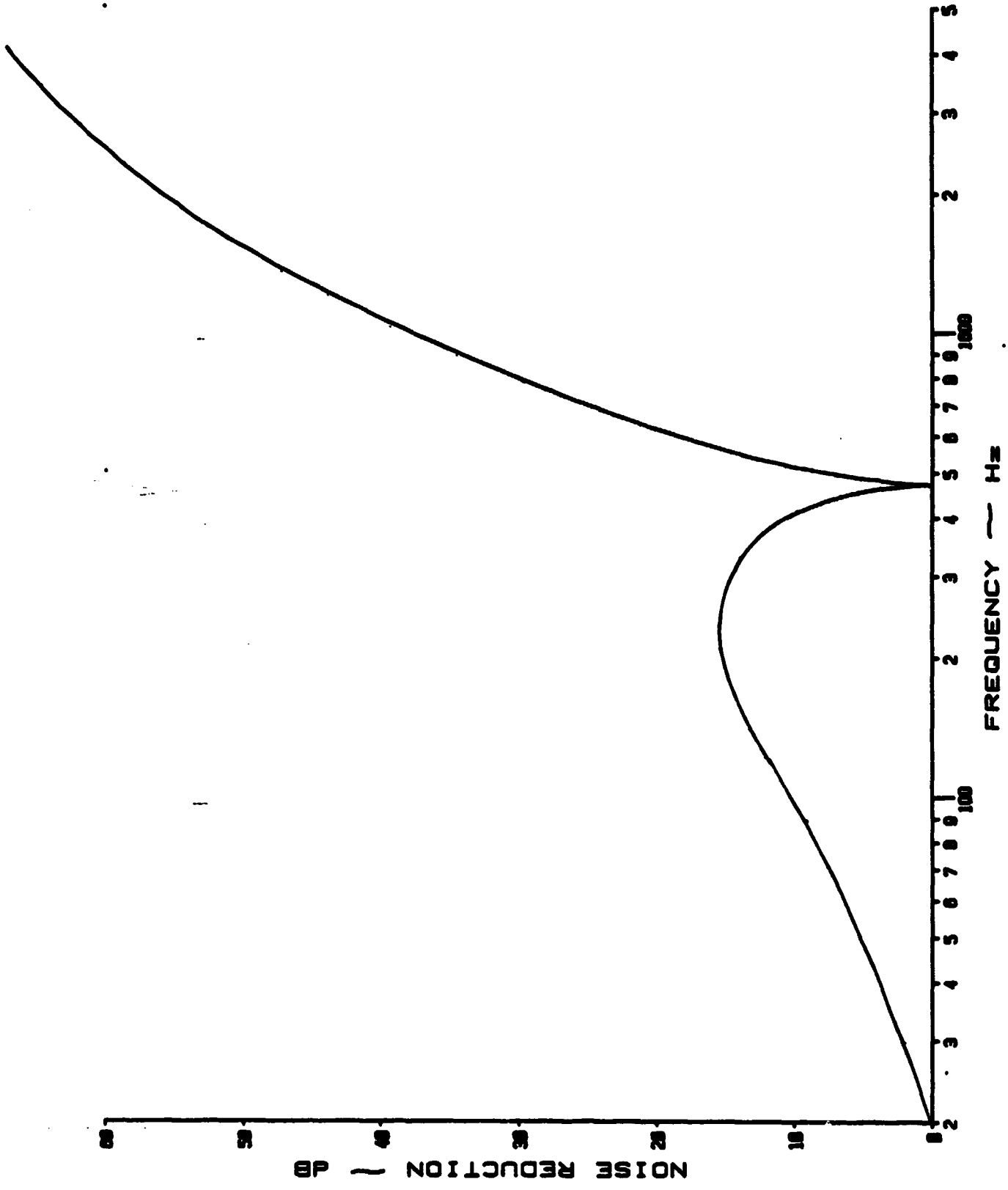

Figure 2.15: Theoretical Noise Reduction Curve of Sandwich Panel Constructed of 0.025 Inch Aluminum Skins and PF 105 Fiberglass Core

(a) panel is simply supported;

(b) small deflection theory is applicable;

(c) single degree of freedom will only be considered;

(d) the additional stiffness due to the stringers can be assumed to be "smeared" over the length of the panel.

Under the above assumptions the panel may be considered to be an orthotropic panel with different stiffness in X and Y directions. Equation (2.22) can still be applicable with the natural frequency being replaced with the fundamental resonance frequency of the stiffened panel. This is similar to the approach used by Getline (Reference 12).

Reference 23 gives the fundamental resonance frequency of the square orthotropic panel as:

$$f_n = \frac{\pi}{2a^2\sqrt{m}} \sqrt{D_X + H + D_Y} \qquad (2.71)$$

where:

a is the side of the panel

m is the mass per unit area of the plate

D_X

D_Y are orthotropic elastic constants.

H

For a panel with equidistant stiffeners, these elastic constants are approximated by Reference 24.

$$D_X = H = \frac{Et^3}{12(1 - \nu^2)} \qquad (2.72)$$

$$D_Y = \frac{Et^3}{12(1 - \nu^2)} + \frac{E'I}{S'} \qquad (2.73)$$

where:

E is Young's modulus of the sheet

ν is Poisson's ratio of the sheet

E' is Young's modulus of the stiffener

I is the moment of inertia of the stiffener cross section with respect to the middle surface of the sheet

S' is the spacing between the centerlines of the stiffeners

t is the thickness of the sheet.

The calculation of the resonance frequency of the stiffened panel tested in Subsection 2.2.1 is presented in Table 2.3. The cross section of the panel is sketched in Figure 2.16. The elastic constants for the panel are found using Equations (2.72) and (2.73). The mass of the panel is assumed to be the combined skin and stringer mass. The value of the resonance frequency calculated is 180 Hz, which compares well with the measured values (between 180 and 190 Hz). The theoretical noise reduction was calculated using Equation (2.22) with damping assumed to be zero (Figure 2.2). For frequencies well above the fundamental resonance frequencies, two cases are considered. In the first case the mass of the stringers is assumed to be smeared over the skin, and in the second case only skin mass in considered. The results are in reasonable agreement in the low frequency region. However, at high frequencies the single-degree-of-freedom model is no longer valid, as higher panel and cavity modes dominate. The

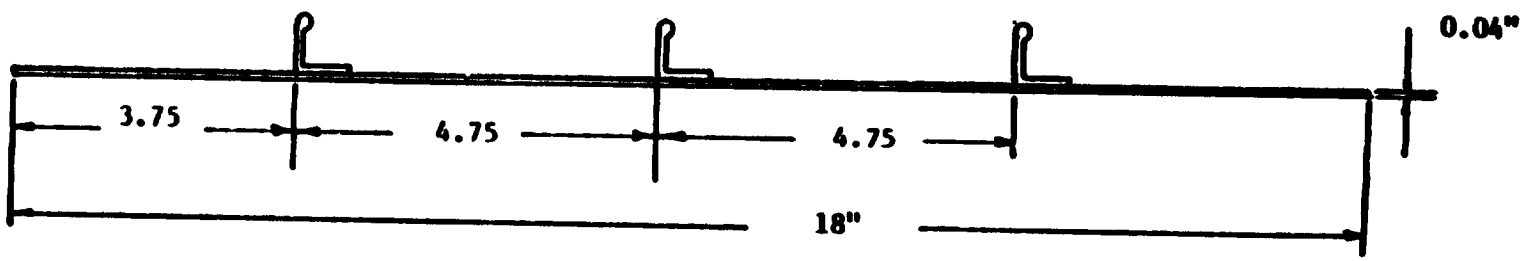

Stringer area = 0.0863 in^2

Moment of inertia about its neutral axis = I_{xx} = 0.00409 in^4

I_{yy} = 0.00621 in^4

Moment of Inertia about centerline = 0.0114 in^4

Figure 2.16: Cross Section of the Stiffened Panel Tested.

Table 2.3 Calculation of Resonance Frequency of a Stiffened Panel

Stiffener characteristics: $I_{XX} = 0.00409 * .0254^4$ [m^4]

$\bar{Y} = 0.2705 * .0254$ [m]

Area $= 0.0863 * .0254^2$ [m^2]

Moment of inertia of the stiffener about the centerline of sheet $\} = 0.0114 * .0254^4$ [m^4]

Length of the panel = a = 18 x .0254 [m]

Running moment of inertia per unit length $\} = \frac{3I}{a} = .0019 * .0254^3$ [m^3]

Young's Modulus of the sheet, Stiffener $\} = 7.24 \times 10^{10}$ [N/m^2]

Sheet thickness = t = 0.04 x .0254 [m]

$$\text{Elastic constant} = D_X = \frac{Et^3}{12(1 - \nu^2)} = 6.95 \text{ [Nm]}$$

$$\text{Elastic constant} = H = \frac{Et^3}{12(1 - \nu^2)} = 6.95 \text{ [Nm]}$$

$$\text{Elastic constant} = D_Y = \frac{Et^3}{12(1 - \nu^2)} + E\left(\frac{3I}{a}\right) = 2261 \text{ [Nm]}$$

Total mass of the panel = .8272 [kg] [measured]

Mass per unit area = m = 3.9573 [kg/m^2]

$$\text{Resonance frequency} = \frac{\pi}{2a^2\sqrt{m}} \sqrt{D_X + H + D_Y} \qquad (2.71)$$

$$= 180.1 \text{ Hz}$$

noise reduction value obtained with only the skin is closer to the experimental least squares line above 1000 Hz. Between 200 and 1000 Hz, the smeared mass approximation is closer to experimental results.

In conclusion, the resonance frequency is well predicted. In this case, the cavity effects of the Beranek tube are found to be negligible. The theory predicts low frequency noise reduction reasonably well. In the high frequency region, approximation of panel with only skin mass is closer to the least square line obtained during experimental investigation. In the mid-frequency region (just above the resonance frequency) the agreement is better when smeared mass approximation is used.

In order to model the stiffened panel with damping material, in addition to the above assumptions the damping material is assumed to add only the damping and mass, and no stiffening, in the entire frequency region. This assumption was made, as the damping material has been covered over the entire panel. The resonance frequency is reduced, since the mass is increased without any change in the stiffness. One other unknown was the damping ratio of the damping material. Hence the theoretical noise reduction curve could not be calculated without some input from the test results. This input was the damping ratio of the material. The damping ratio was calculated from the noise reduction value at the resonance frequency. At $\omega = \omega_n$ Equation (2.22) becomes:

$$NR\Big|_{\omega=\omega_n} = 10 \log\left[1 + \frac{2m\omega_n\zeta}{\rho c}\right]^2 \qquad (2.74)$$

For the panel tested (Subsection 2.2.1), the damping ratio was calculated from the damped natural frequency measured from Figure 2.3.

Equation (2.23) was used to calculate the natural frequency from the damped natural frequency. An interative procedure is needed to calculate the natural frequency. For the panel tested the damping ratio was observed to be 0.04.

Table 2.4 gives the calculation of noise reduction of the panel tested (same as in Subsection 2.2.1) with damping material Y-370. The decrease in the frequency at which the noise reduction is minimum is due to two factors: (a) increase in mass, and (b) increase in damping. As the stiffness remains the same and the mass increases, the natural frequency decreases. (For the test case it decreases from 180 to 156.0.) The difference between natural frequency and damped natural frequency is negligible for a damping ratio of 0.04. The value of the fundamental resonance frequency calculated from the experimental results differs from theoretical prediction only by $\sim$5 Hz. The theoretical noise reduction value calculated for damping ratio of 0.04 is also plotted in Figure 2.3, demonstrating once again that at low frequency region the theory is in reasonable agreement with the results, and the additional stiffness due to the cavity effects of the Beranek tube is negligible when the panel is "stiffer." The effect of damping is to reduce the resonance peaks and dips, as can be seen from Figures 2.2 and 2.3.

2.3.3.2 Fiberglass Material Sandwiched between Two 0.020 Inch Aluminum Panels

The theoretical noise reduction values for this panel were calculated using Equation (2.55). The values of resistivity and porosity are taken from Reference 7. The values of complex impedance

Table 2.4 Calculation of the Resonance Frequency of a Stiffened Panel with Damping Material

D_X	= 6.95	[Nm]	(Table 2.3)
H	= 6.95	[Nm]	(Table 2.3)
D_Y	= 2261	[Nm]	(Table 2.3)

Total mass of the panel = 1.125 [kg] [measured]

Mass per unit area = m = 5.3843 [kg/m^2]

Length of the panel = a = 18 x .0254 (m)

$$\text{Resonance frequency} = \frac{\pi}{2a^2\sqrt{m}} \sqrt{D_X + H + D_Y}$$

$$= 154.4 \text{ Hz.}$$

Damping ratio calculated based on Equation (2.74) = 0.04.

were calculated based on Subsection 2.2.2 and Appendix C. The values of impedance are shown in Table 2.5. The resulting noise reduction values are plotted in Figure 2.17, along with the experimental values. As can be seen, the agreement is very poor, especially in the low frequency region. This may be due to the cavity effects of the Beranek tube and the boundary conditions of the panel. This effect is predominant for this panel (Reference 7). The observed value of the first resonance frequency is aroung 90 Hz, while the calculated value is only 17 Hz. As discussed in Appendix A, the effect of the Beranek tube is to increase the stiffness of the panel, thereby increasing fundamental resonance frequency. Since the math model developed in Subsection 2.2.2 does not account for cavity effects, this can be overcome by using the observed value of the resonance frequency in the calculation of the noise reduction values. This has also been done and is shown in Figure 2.17 as a dotted line. With this assumption, the agreement between the theoretical value and the observed value is better. While skin-core-skin resonance frequency of 500 Hz is well predicted, the calculated values of noise reduction are still very much lower in the low frequency region. While part of it may be due to the deficiency of the model used, like neglecting the damping, etc., some of it may also be due to the average values of the resistivity, porosity, etc., used in the calculation. At high frequency the average noise reduction values seem to agree. The higher panel modes introduce peaks and dips, which are not modeled in the simple case considered. The very high values of noise reduction observed in the high frequency region are due to (a) mass effect (increase of 6 dB for doubling of frequency),

Table 2.5 Calculation of the Complex Impedance of the Core (Based on Reference 8)

DATA

Bulk density of the fiberglass	= 49.0 kg/m^3	
Density of gas in the core	= 1.18 m/sec	
Resistivity of the material	= 20000 MKS Rayls/m	(Reference 7)
Porosity	= 0.9	(assumed)
Structures factor	= 1.4	(Reference 8)
Thickness	= 1 * .0254 m	(Measured)

Frequency	100	300	600	1000	2000	3000	5000
f_1	1.61	1.07	1.02	1.01	1.00	1.00	1.00
f_2	19.57	3.06	1.52	1.19	1.05	1.01	1.00
α	37.5	94.45	134	163	194	207	209
λ_m	.67	.39	.276	.204	.125	.069	.0569
R_2	1730	1030	761	634	537	502	497
X_2	-801	-702	-518	-387	-238	-133	-108
$\|Z_2\|$	1905	1250	.921	734	588	519	509
θ_2 (deg)	-24.9	-34.2	-34.3	-31.4	-23.9	-14.8	-12.3

f_1, f_2 defined in Appendix C

α attenuation constant dB/m

λ_m wavelength in material m/sec

R_2 real part of complex impedance MKS Rayls

X_2 imaginary part of complex impedance MKS Rayls

$|Z_2|$ absolute value of Z_2

θ phase of Z_2 (degrees)

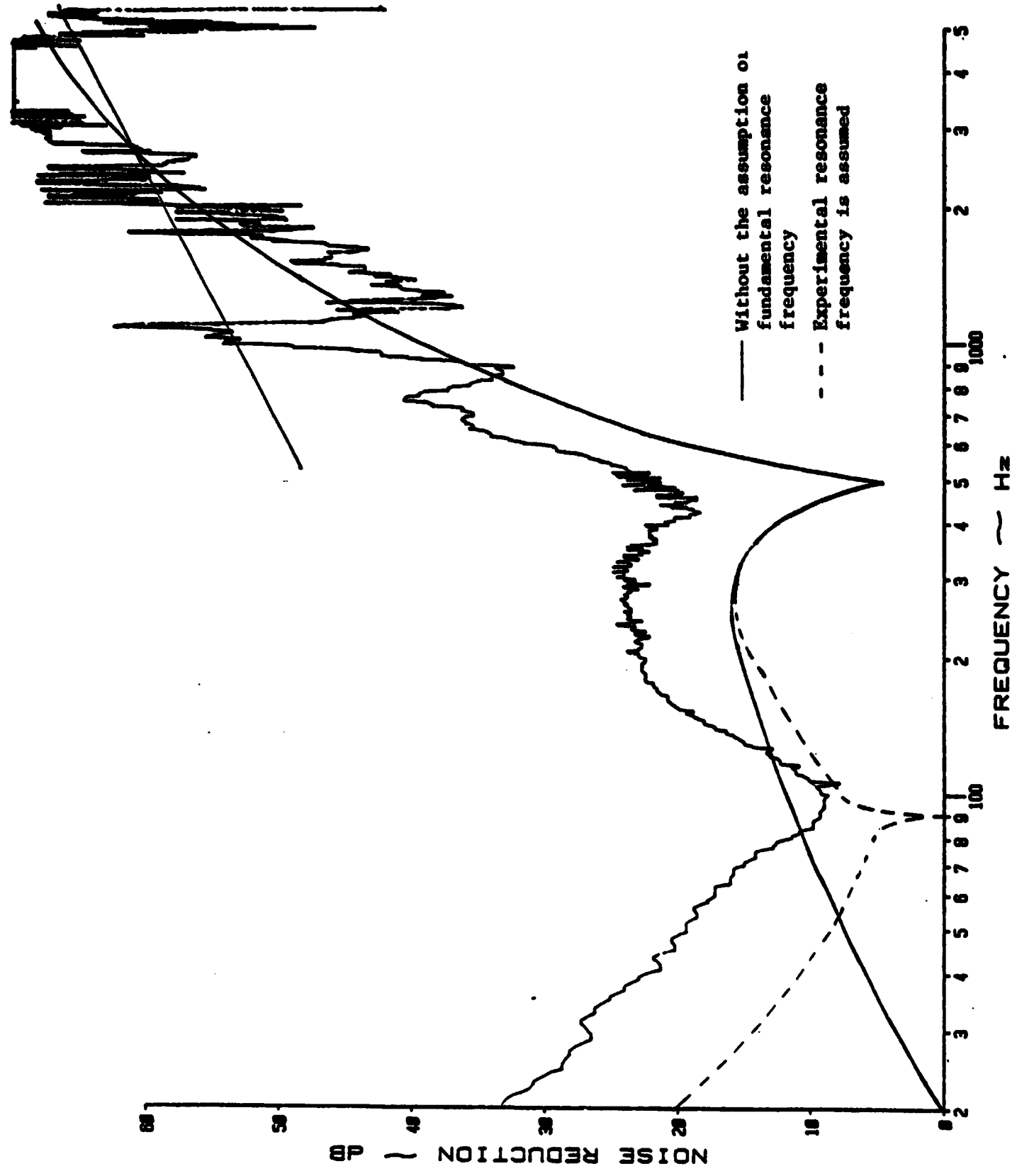

Figure 2.17: Theoretical and Experimental Noise Reduction Curve of Sandwich Panel Made of 0.020 Inch Aluminum Skins and 1 Inch Fiberglass Core

(b) the additional attenuation in the sound absorption material (contribution from α), and (c) reflection losses which change the slope of the noise reduction curves (Reference 8). In conclusion, the agreement is poor in the low frequency region unless the cavity effects are taken into account. The agreement is reasonable in the high frequency region. The theory reasonably predicts the trends of the experimental noise reduction curve.

2.3.3.3 Honeycomb Sandwich Panels

The honeycomb type sandwich panels are ideal examples for the shear resistant model. Equations (2.2), (2.13), and (2.22) will be used to calculate the noise reduction values. Equation (2.2) for the transformed flexural rigidity D* can be simplified if the Young's modulus of the facing sheet is far higher than that of the core material, which is normally the case.

In order to simplify Equations (2.2) through (2.5), the following assumptions will be made.

(a) The multilayered panel is made of three layers: two facing sheets and a core.

(b) The facing sheets are made of the same material ($E_3 = E_1$).

(c) The core has a low Young's modulus, compared to the facing sheet, and hence can be neglected ($E_2 << E_1$).

Then Equations (2.3) through (2.5) simplify to:

$$A = \frac{E}{1 - \nu^2} \{z_1 + z_3 - z_2\} \qquad (2.75)$$

$$B = \frac{E}{2(1 - \nu^2)} (z_1^2 + z_3^2 - z_2^2) \tag{2.76}$$

$$C = \frac{E}{3(1 - \nu^2)} (z_1^3 + z_3^3 - z_2^3) \tag{2.77}$$

From Figure 2.18:

$$z_1 = h_1 \tag{2.78}$$

$$z_2 = h_1 + h_2 \tag{2.79}$$

$$z_3 = h_1 + h_2 + h_3 \tag{2.80}$$

where:

h_1, h_2, h_3 = thickness of layers 1, 2, 3, respectively.

From Equations (2.2) and (2.75) through (2.80) we obtain:

$$D^* = \frac{E}{1 - \nu^2} \left[\frac{h_1^3}{12} + \frac{h_3^3}{12} + \frac{h_1 h_3}{h_1 + h_3} \left\{\frac{h_1}{2} + \frac{h_3}{2} + h_2\right\}^2\right] \tag{2.81}$$

This equation is similar to the equation for stiffness obtained by Barton (Reference 25). At this juncture it is pertinent to recall that one of the assumptions made in Subsection 2.3.2 is that the core is incompressible, which means that Young's modulus is extremely high. In practice, however, it can be seen from the sample calculations of dilatational frequency that even very small values of Young's modulus of the core are sufficient to satisfy the above conditions. And compared to the Young's modulus of the facing sheet for aluminum ($\sim$1.05 x 16^6 psi), the Young's modulus of the honeycomb core ($\sim$60000 psi) is very small, but enough to produce a very high dilatational frequency (Equation 2.26) for both the assumptions to be valid. This apparent contradiction thus does not exist in practical cases.

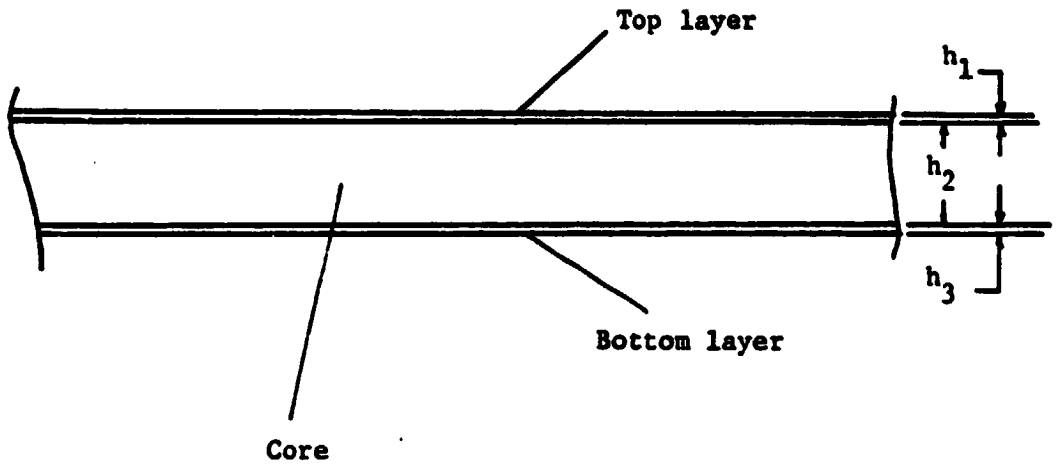

Figure 2.18: Typical Cross-Section of a Honeycomb Panel

n addition to the five honeycomb panels tested, the results
ch are presented in Appendix B, the experiments were also
d out with two more panels. The noise reduction character-
i of these panels are presented in Figures 2.19 and 2.20. The
ental resonance frequency has been calculated with the stiffness
ated from either Equation (2.2) or Equation (2.81). The details
c panel and the calculation are given in Table 2.6. The noise
ion values are calculated using single-degree-of-freedom model
tion 2.22) and are plotted in Figures 2.19 and 2.20 along with
perimental results. The calculated fundamental resonance fre-
o agrees well with the observed frequency for the honeycomb panel
luminum skin, whose material characteristics are well defined.
ation of 10 Hz between the calculated and observed frequencies
honeycomb panel with fiberglass facing was observed. For this
n average value for the material characteristics was used.
w frequencies the noise reduction values are comparable. The
e value of the noise reduction matches reasonably well. The
nd peaks in the high frequency range are not predicted. The
c modes and higher panel modes may also mask any dilatational
f transmission.

able 2.7 gives the resonance frequencies calculated and
bd for the five honeycomb panels whose noise reduction
are presented in Appendix B. As can be seen, the results
reasonable agreement.

Table 2.6 Calculation of Resonance Frequency and Noise Reduction Values of Honeycomb Panels

Panel 1 (Figure 2.19):

Skin = 0.016 inch thick aluminum			
Core = 1/4 inch cell, 1/2 inch thick aluminum			
Young's Modulus of the Skin	= 7.24×10^{10}	N/m^2	
Density of the Skin	= 2700	kg/m^3	
Thickness	= 0.016×0.0254	m	
Young's Modulus of the Core	= $90000 * 6.895 \times 10^3$	N/m^2	(Reference 26)
Density of the Core	= 3.4×16.08	kg/m^3	(Reference 26)
Thickness of the Core	= 0.5×0.0254	m	
Mass of the Panel	= 0.7577	kg	[measured]
Panel Width	= 18×0.0254	m	[measured]
Panel Resonance Frequency	= 425	Hz	(Equation 2.13; m = 1, n = 1)
First Dilatational Frequency	= ∿45000	Hz	(Equation 2.26)

Panel 2 (Figure 2.20):

Skin = USP-735 TYPE C Fiberglass			
Core = 1/8 inch cell, 1/4 inch thick aluminum			
Young's Modulus of the Skin	= 2.4×10^{10}	N/m^2	
Density of the Skin	= 1600	kg/m^3	
Young's Modulus of the Core	= $75000 * 6.895 \times 10^3$	N/m^2	(Reference 26)
Density of the Core	= 3.1×16.08	kg/m^3	(Reference 26)
Thickness of the Core	= 0.25×0.0254	m	
Mass of the Panel	= 0.293	kg	[measured]
Panel Width	= 18×0.0254	m	[measured]
Panel Resonance Frequency	= 187	Hz	(Equation 2.13; m = 1, n = 1)
First Dilatational Frequency	= ∿80000	Hz	(Equation 2.26)

Table 2.7 Comparison of Calculated and Measured Resonance Frequencies of Honeycomb Panels

Serial Number	Core	Resonance Frequency (Hz) Calculated	Measured from Noise Reduction Curve
1	0.125 inch aluminum	102	117
2	0.25 inch aluminum	182	191
3	0.5 inch aluminum	311	290
4	0.125 inch Nomex	103	117
5	0.25 inch Nomex	180	186

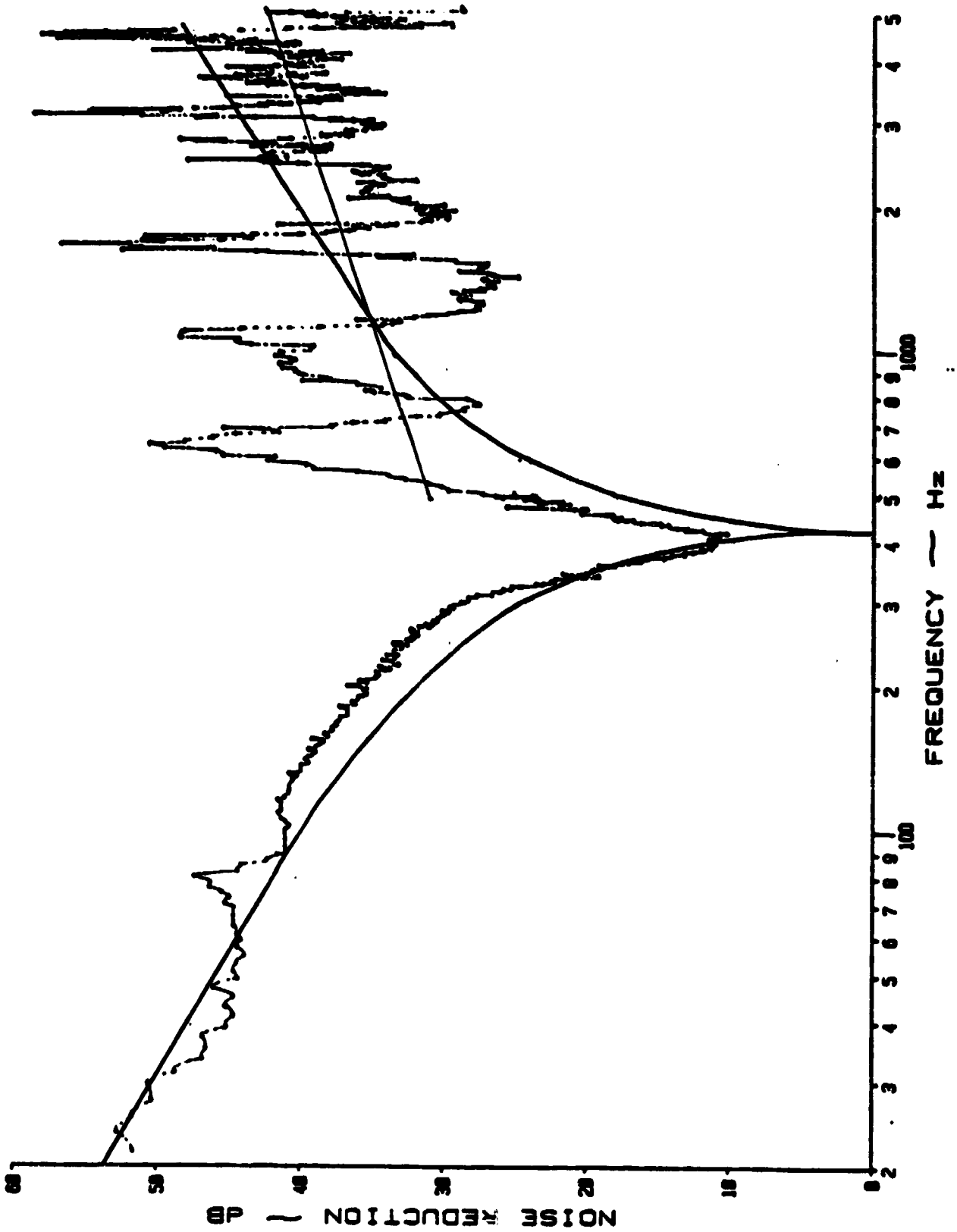

Figure 2.19: Noise Reduction Characteristics of Honeycomb Panel (0.016 Inch Aluminum Skin and 1/2 Inch Thick Aluminum Core)

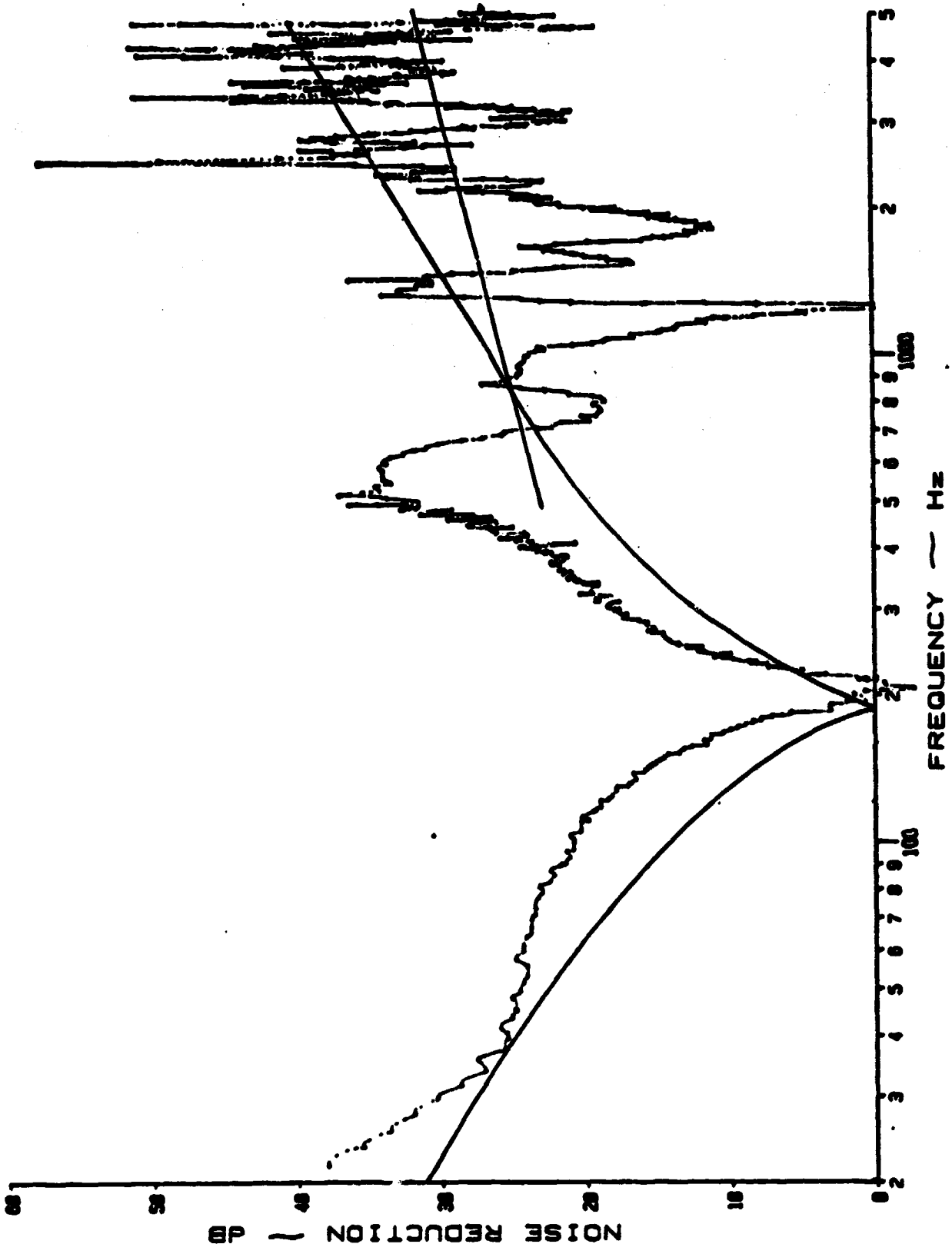

Figure 2.20: Noise Reduction Characteristics of Honeycomb Panel (Fiberglass Skin and 1/4 Inch Aluminum Core)

CHAPTER 3

HELMHOLTZ RESONATORS FOR DOUBLE WINDOWS

3.1 INTRODUCTION

The noise attenuation characteristics of existing single pane windows in general aviation aircraft are poor, especially at low frequencies, where the general aviation aircraft noise dominates. The use of double windows is one attempt to remedy this situation. However, the noise attenuation of conventional double windows is still low at low frequencies. Also, an additional resonance frequency due to pane-air-pane vibration is introduced at low frequencies, decreasing low frequency noise reduction. To increase the low frequency noise attenuation of conventional double windows, the concept of depressurization was investigated at the KU-FRL acoustic test facility (References 17 and 18). Due to the stiffening effect of depressurization, the fundamental resonance frequencies of the panes increase. This results in increased low frequency noise reduction. However, a depressurization system will, in practice, be costly and complex. The high values of deflections of the pane observed at pressure differentials greater than 1.5 to 2 psi may also limit its practical application (References 17 and 18).

Another concept that can be used to increase low frequency noise reduction around a very small frequency range is Helmholtz resonators. These resonators may be tuned to any selected frequency. The low noise reduction observed at the pane-air-pane resonance frequency can be eliminated by tuning the resonator to this frequency.

Helmholtz resonators can be constructed without much additional cost and complexity. In aircraft, the volume between the double windows and the adjacent frames and stringers may be used as the resonator volume. Figure 3.1 gives a schematic diagram of Helmholtz resonator installation in an aircraft.

The details of design and construction of a Helmholtz resonator for testing at the KU-FRL acoustic test facility are presented in Section 3.2. The results of the tests are analyzed and presented in Section 3.3.

3.2 DESIGN AND CONSTRUCTION OF HELMHOLTZ RESONATOR

The low frequency noise reduction characteristics of a conventional double window obtained at the KU-FRL acoustic test facility are given in Figure 3.2. As can be seen, two resonance frequencies exist in the frequency range considered. They correspond to the fundamental resonance frequency of the pane and the pane-air-pane of the window.

Equation (2.5) of Section 2.3 can be simplified to model a double window. In the present case, the core material is replaced by an air gap. The impedance Z_2 contains only the real term ($=\rho c$). In Equation (2.59), letting $R_2 = \rho c$ and $X_2 = 0$:

$$NR = 10 \log\left|\{\cos k\ell + q_1 \sin k\ell\} + j\{-(q_1 + q_2)\cos k\ell + \sin k\ell - q_1 q_2 \sin k\ell\}\right|^2 \quad (3.1)$$

One of the resonance frequencies occurs when q_1 or q_2 is equal to zero. This corresponds to the pane fundamental resonance frequency, since

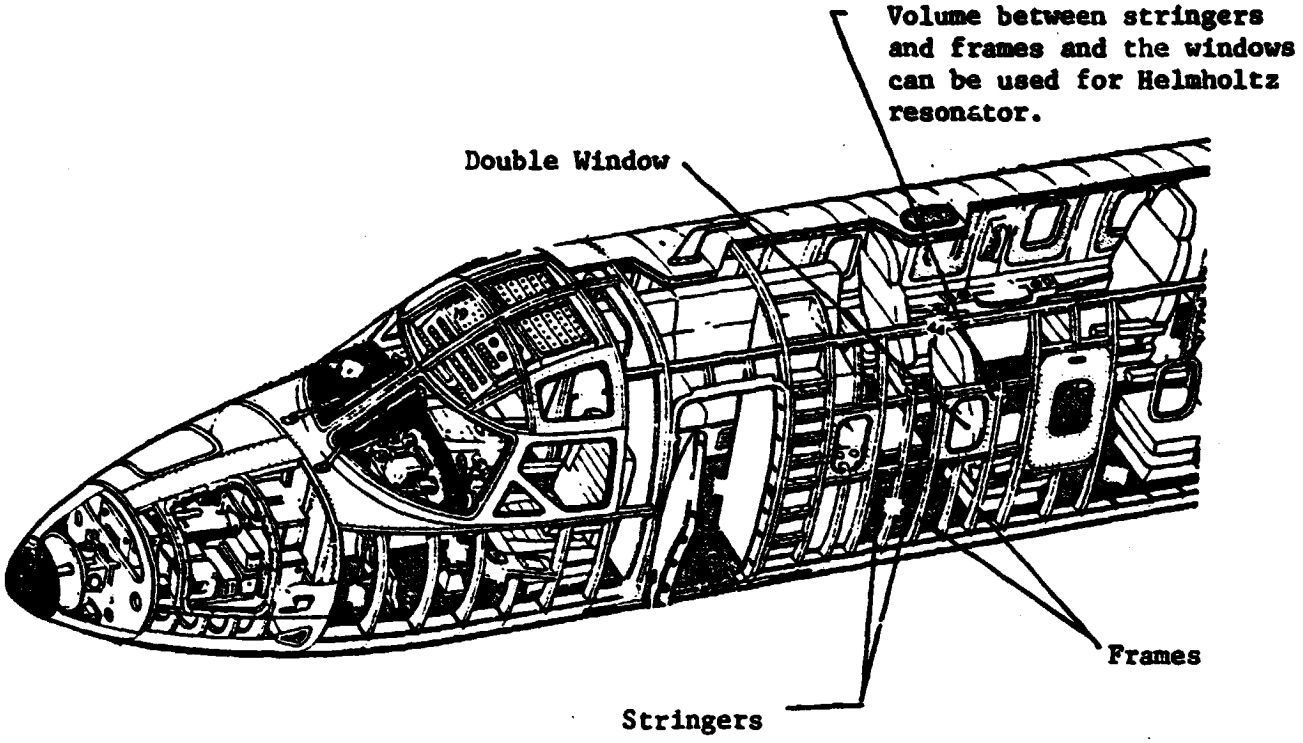

Figure 3.1: Schematic Diagram of the Helmholtz Resonator in an Aircraft

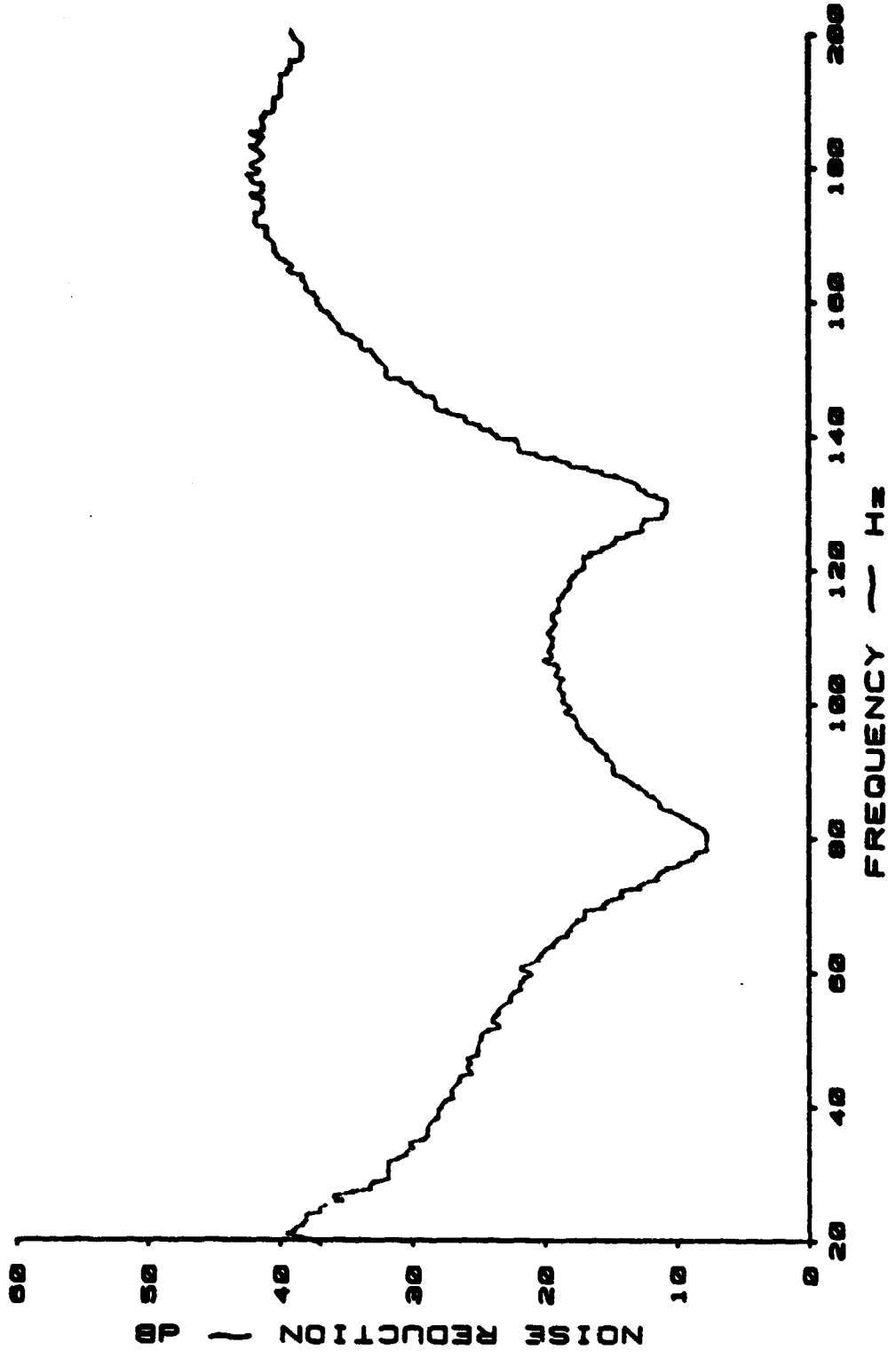

Figure 3.2: Noise Reduction Characteristics of the Double Window; 1/8 Inch Thick Panes, 4 Inch Spacing, and Pane Dimensions 13 x 13 Inches

$$q_i = \frac{m_i(\omega_n^2 - \omega^2)}{\omega\rho c} \qquad i = 1, 2 \tag{3.2}$$

In the particular case of two panes of similar mass, material, and edge conditions, Equation (3.1) reduces to:

$$NR = 10 \log|\{\cos k\ell + q\sin k\ell\} + j\{-2q\cos k\ell + (1 - q^2)\sin k\ell\}|^2 \tag{3.3}$$

where $q = q_1 = q_2$. (3.4)

The resonant condition is given by:

$$NR = 0 \tag{3.5}$$

or:

$$|\{\cos k\ell + q \sin k\ell\} + j\{-2q \cos k\ell + (1 - q^2)\sin k\ell\}|^2 = 1 \tag{3.6}$$

This reduces to:

$$4q^2(\cos k\ell + \frac{q}{2} \sin k\ell)^2 - 2q \sin k\ell(\cos k\ell + \frac{q}{2} \sin k\ell) = 0 \tag{3.7}$$

The condition for second resonance (pane-air-pane) is then:

$$\tan k\ell = -\frac{2}{q}. \tag{3.8}$$

At values $\omega > \omega_n$ q is negative; and at low frequencies $\tan k\ell \approx k\ell$. The lowest resonance frequency due to mass-air-mass is obtained from substituting (3.2) in (3.8).

$$k\ell = \frac{\omega_1}{c}\,\ell = -\frac{2X\omega_1\rho c}{m(\omega_n^2 - \omega_1^2)} \tag{3.9}$$

where c is the speed of sound.

This yields:

$$f_1 = \frac{1}{2\pi}\left(\frac{\rho c^2}{m\ell} + [2\pi f_n]^2\right)^{\frac{1}{2}} \tag{3.10}$$

This, when the stiffness effects of the pane are neglected, equals:

$$f_1 = \frac{1}{2\pi}\left(\frac{\rho c^2}{m\ell}\right)^{\frac{1}{2}} \tag{3.11}$$

Equation (3.11) is identical to the equation given in Reference 9. The theoretically calculated value of resonance frequency for the double window tested (Figure 3.2) was 127 Hz when small angle assumption was made (Equation 3.10) and 156 Hz when exact values were used (Equation 3.8). The experimental value was 135 Hz.

A Helmholtz resonator was designed for the dual pane window whose characteristics are given in Figure 3.2. A schematic sketch of the Helmholtz resonator is shown in Figure 3.3. The design was based on the method given in Reference 8. Equation (12.6) of Reference 8 gives the transmission loss of a volume resonator as:

$$TL = 10 \log_{10}\left[1 + \frac{\alpha + 0.25}{\alpha^2 + \beta^2(f/f_0 - f_0/f)^2}\right] \tag{3.12}$$

where:

α = resonator resistance (dimensionless) = $S_1 R_s / A_o \rho c$

β = resonator reactance (dimensionless) = $S_1 c / 2\pi f_0 V$

S_1 = area of double window, m^2

R_s = flow resistance in resonator tubes, MKS Rayls

V = volume of resonator, m^3

A_0 = total aperture area, m^2 = A*n

f_0 = resonance frequency, Hz

ρ = density of gas, kg/m^3

c = speed of sound, m/sec

A = area of single resonator tube, m^2

n = number of resonator tubes

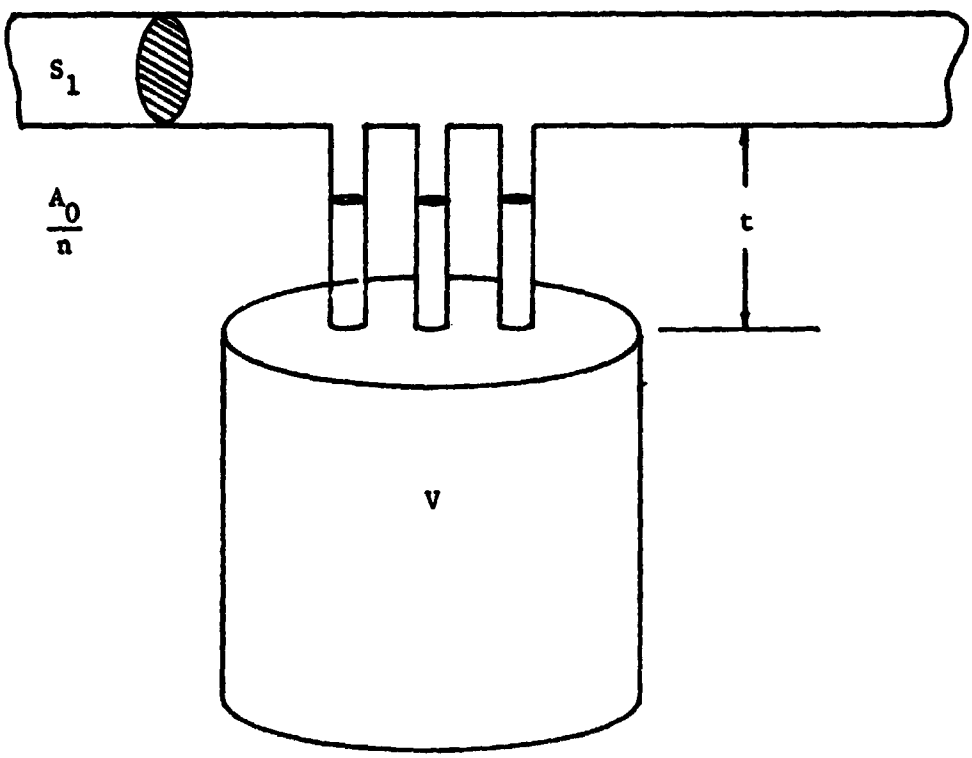

S_1 = Duct Area

A_0 = Total Resonator Tube Area

n = Number of Tubes

t = Tube Length

V = Volume of the Resonator

Figure 3.3: Schematic Diagram of a Helmholtz Resonator

The resonance frequency of a Helmholtz resonator is (Reference 8):

$$f_0 = \frac{c}{2\pi}\sqrt{\frac{A_0}{Vt'}} \qquad (3.13)$$

where:

t' = the equivalent resonator tube length $\approx t + 0.8\sqrt{\frac{A_0}{n}}$

t = the resonator tube length.

To test the concept of Helmholtz resonator, the same double window whose noise reduction characteristics are presented in Figure 3.2 was used. Equations (3.12) and (3.13) were programmed into an Apple II computer to check the effect of individual variables in those two equations on the theoretical transmission loss characteristics. Due to the restriction of size of the existing double window test specimens (15 x 15 inch) and the size limitation of the Beranek tube (18 x 18 inch), there was a severe restriction on the available resonator volume. The resonator volume was built all around the dual pane window, as shown in Figure 3.4. The only way the resonator volume could be increased was by increasing the spacing. Of the available spacings for a double window available at the KU-FRL acoustic test facility (i.e., 1, 2, or 4 inches), four inch spacing was chosen to have the maximum volume for the resonator (201 inch^3). This allowed the resonance frequency to be reduced to the desired value. Another constraint was the lack of space for the resonator tube length. This was overcome either by having no neck length ($\approx$ 0.1 inch) or having the resonator tube projecting into the resonator volume, as shown in Figure 3.4. Even though this may not be the best solution, it was considered that this offered a

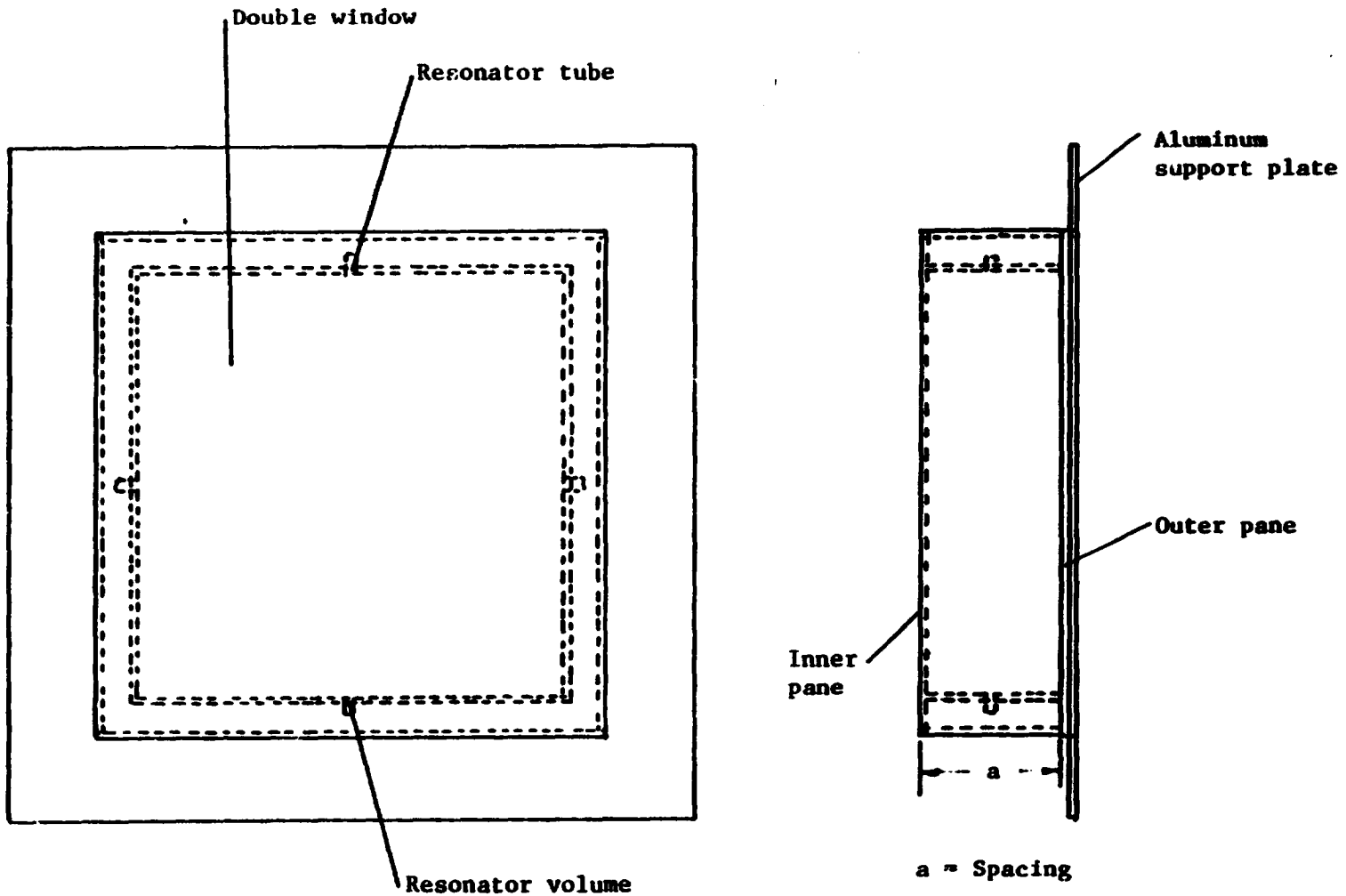

Figure 3.4: Schematic Diagram of a Double Window with Helmholtz Resonator, Tested at the KU-FRL Acoustic Test Facility

workable solution. The hole size, the number of holes, the neck length, and the resistivity were varied to observe the additional noise reduction at the second resonance frequency.

3.3 EXPERIMENTAL INVESTIGATION

The noise reduction test procedure for testing the double windows with the Helmholtz resonator was essentially similar to the tests described in Chapter 2. Since the frequency range of interest is very low, an additional sweep of frequency from 20 to 200 Hz was carried out. Narrow band width analysis using a band width of 0.6 Hz was performed and the noise reduction was plotted. The listing of the program used for the analysis of the microphone signals is given in Appendix D.

During the experimental investigation, the effects of hole sizes (i.e., aperture areas), the number of holes, neck length, and the resistivity on the minimum noise reduction value around 135 Hz (pane-air-pane resonance frequency) were checked. Even though a change of the hole size or the number of holes would change the resonance frequency of the Helmholtz resonator with constant resonator volume, this was still done, as the volume of the resonator could not be changed without changing the spacing and hence the pane-air-pane resonance frequency. So instead of tuning the resonance frequency of the resonator to that of the window, it was allowed to vary. The only justification for this approach is that in case such a resonator were to be installed in an aircraft, similar problems would be present. All the tests

were performed at lease twice, as even a very minor imperfection in the preparation of the double window caused a significant change in the noise reduction values obtained.

Table 3.1 gives the details of the tests carried out, the value of minimum noise reduction around 135 Hz, and the increase in noise reduction over the window without the resonator. A maximum of 8 dB increase was observed. The individual noise reduction curves obtained are presented in Figures 3.5 through 3.12.

Initial tests with four 7/64 inch diameter tubes (holes), which had a theoretical resonance frequency of 80 Hz, did not show any increase in noise reduction at either 80 Hz or around 135 Hz. Tests with twelve 7/64 inch diameter holes (theoretical resonance frequency ≈ 115 Hz) gave an increased noise reduction of 5 dB. When the diameter was increased to 3/16 inch (the theoretical resonance frequency 160 Hz), the noise reduction remained the same (Table 3.1). It is likely that due to the method of construction of the resonator, the calculated and the actual resonance frequencies of the resonator do not match. From the noise reduction curves it was difficult to judge the resonance frequency of the Helmholtz resonator. The resonator noise reduction characteristics could not be separated from the window noise reduction characteristics.

In order to avoid the ringing of the resonator, the resistivity of the resonator was changed. This was achieved in three ways: (a) resistive material (fiberglass) was placed inside the resonator volume, (b) the tube opening was covered with gauze (cloth screen), or (c) both of the above were done. When the volume of the resonator

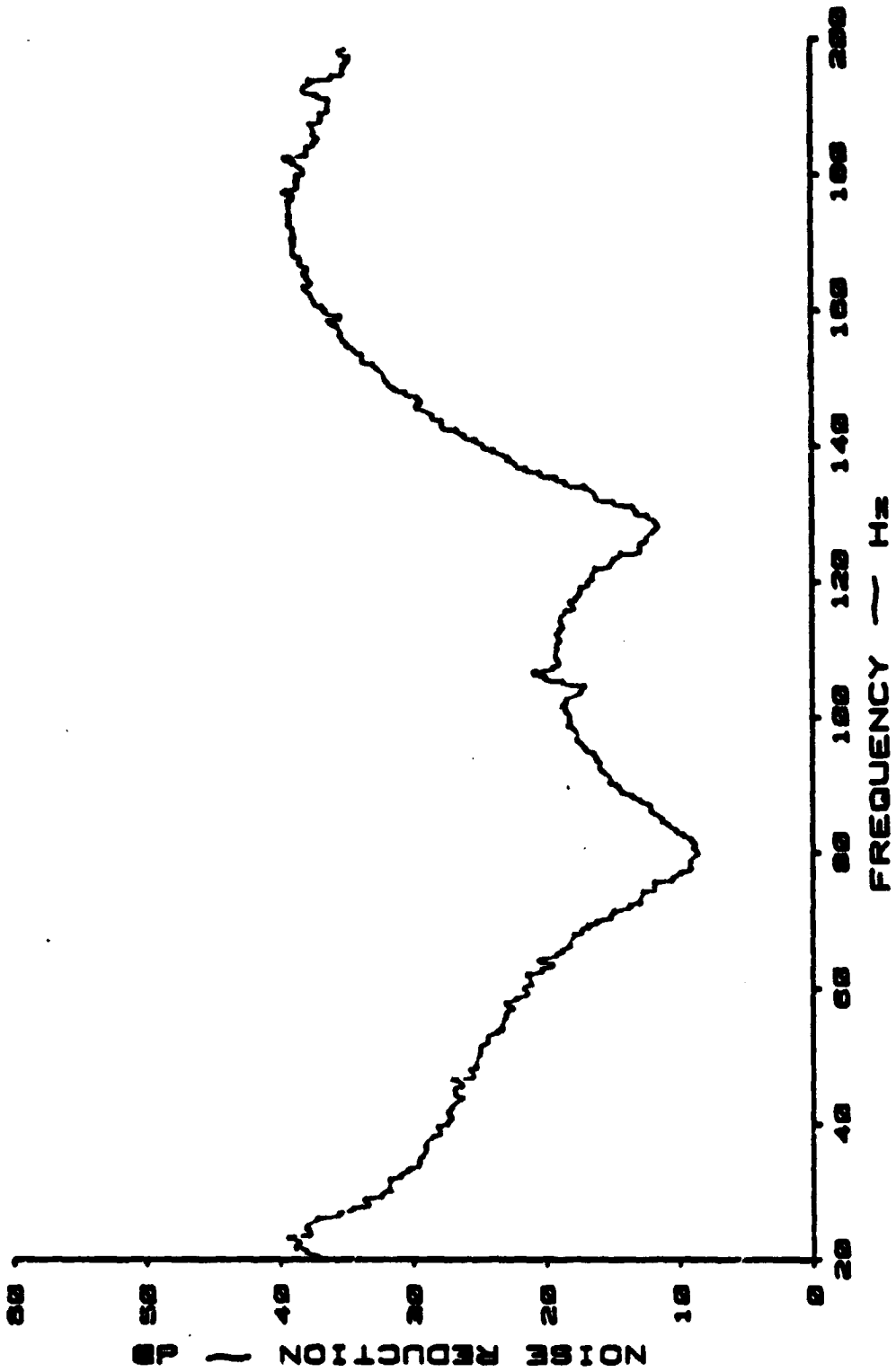

Figure 3.5: Low Frequency Noise Reduction Characteristics of a Dual Pane Window with Helmholtz Resonator; Tube Diameter 7/64 Inch, Number of Tubes 4, and Neck Length 0.1 Inch

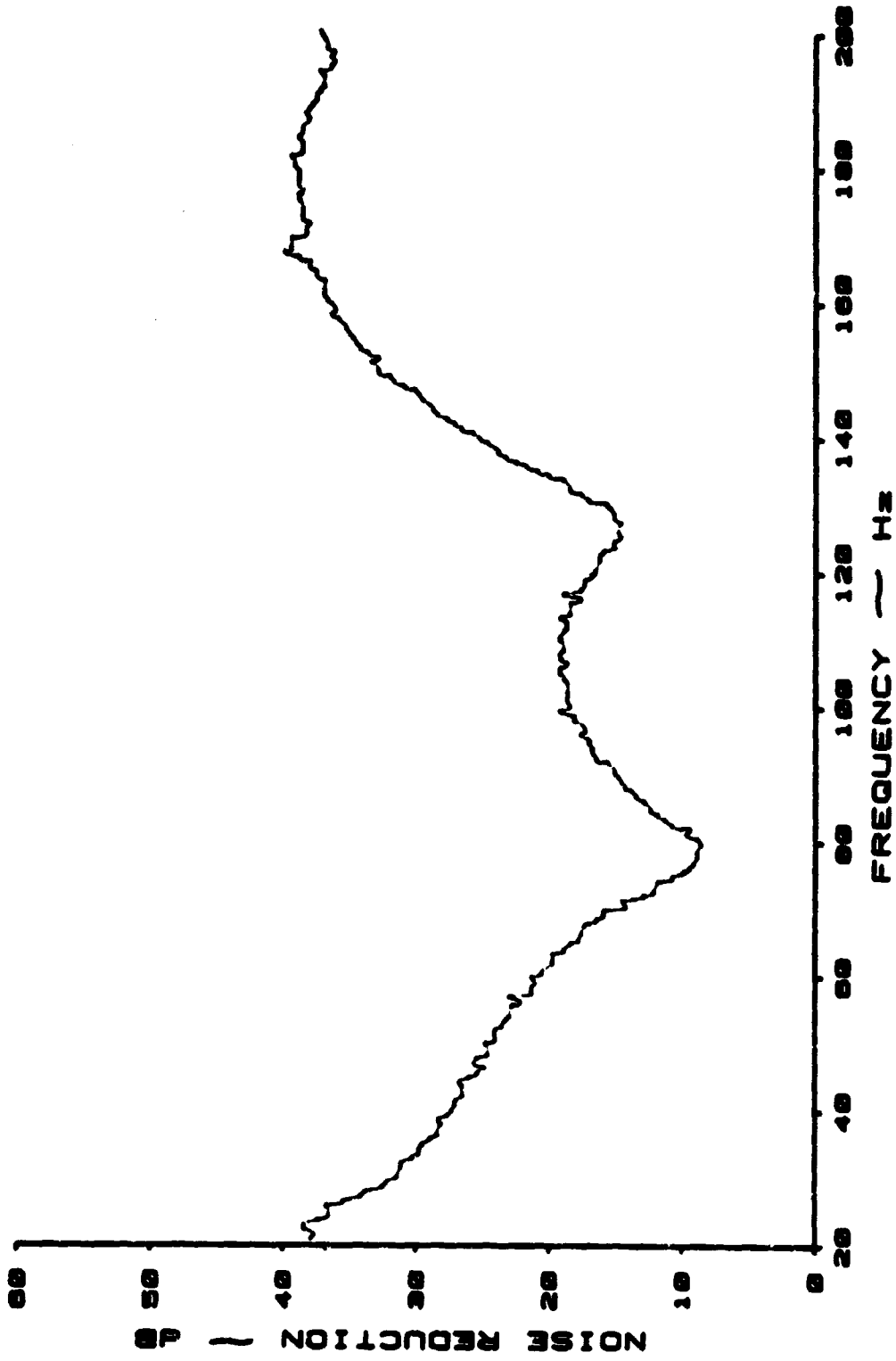

Figure 3.6: Low Frequency Noise Reduction Characteristics of a Dual Pane Window with Helmholtz Resonator; Tube Diameter 7/64 Inch, Number of Tubes 12, and Neck Length 0.1 Inch

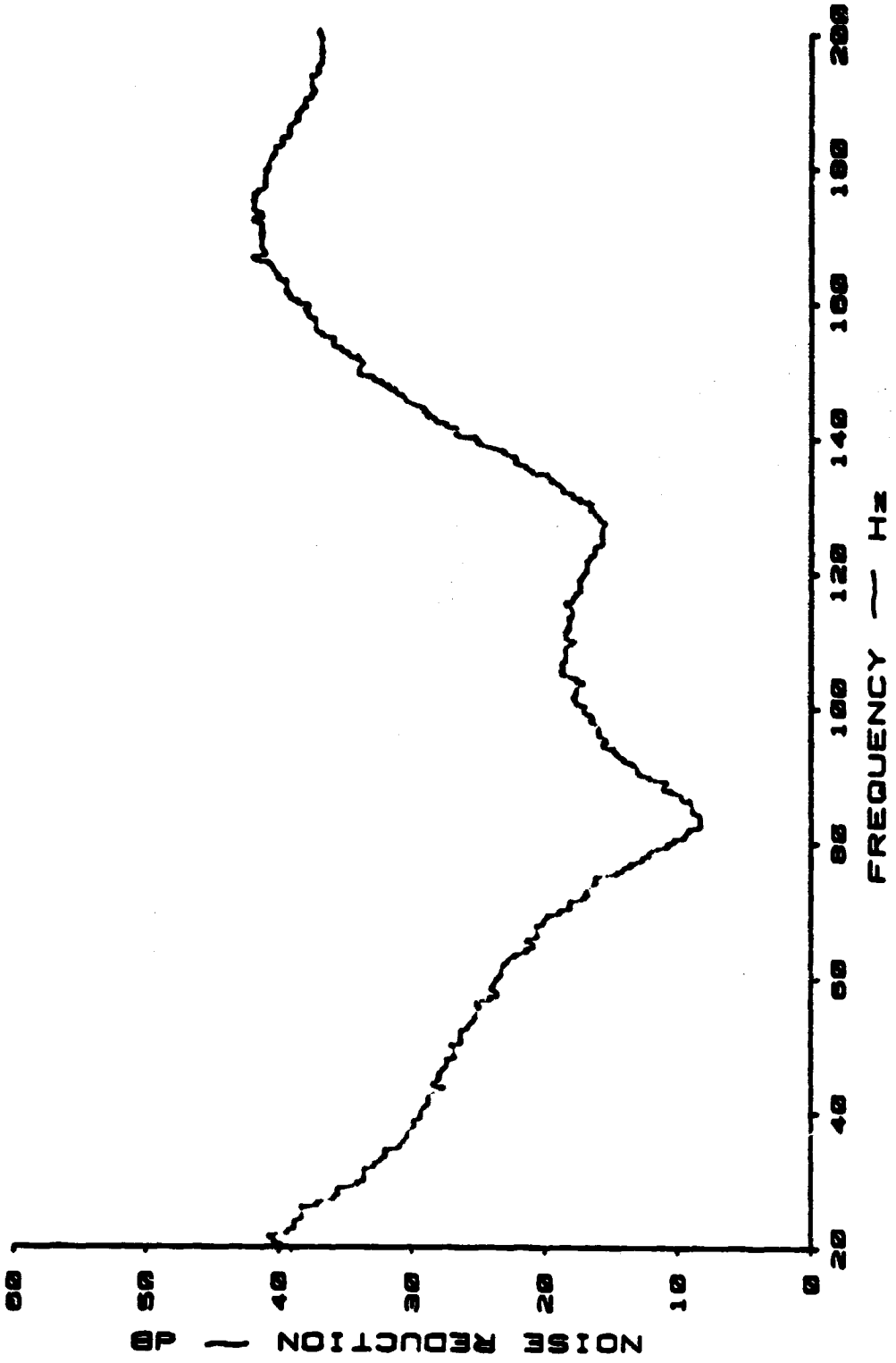

Figure 3.7: Low Frequency Noise Reduction Characteristics of a Dual Pane Window with Helmholtz Resonator; Tube Diameter 3/16 Inch, Number of Tubes 12, and Neck Length 0.1 Inch

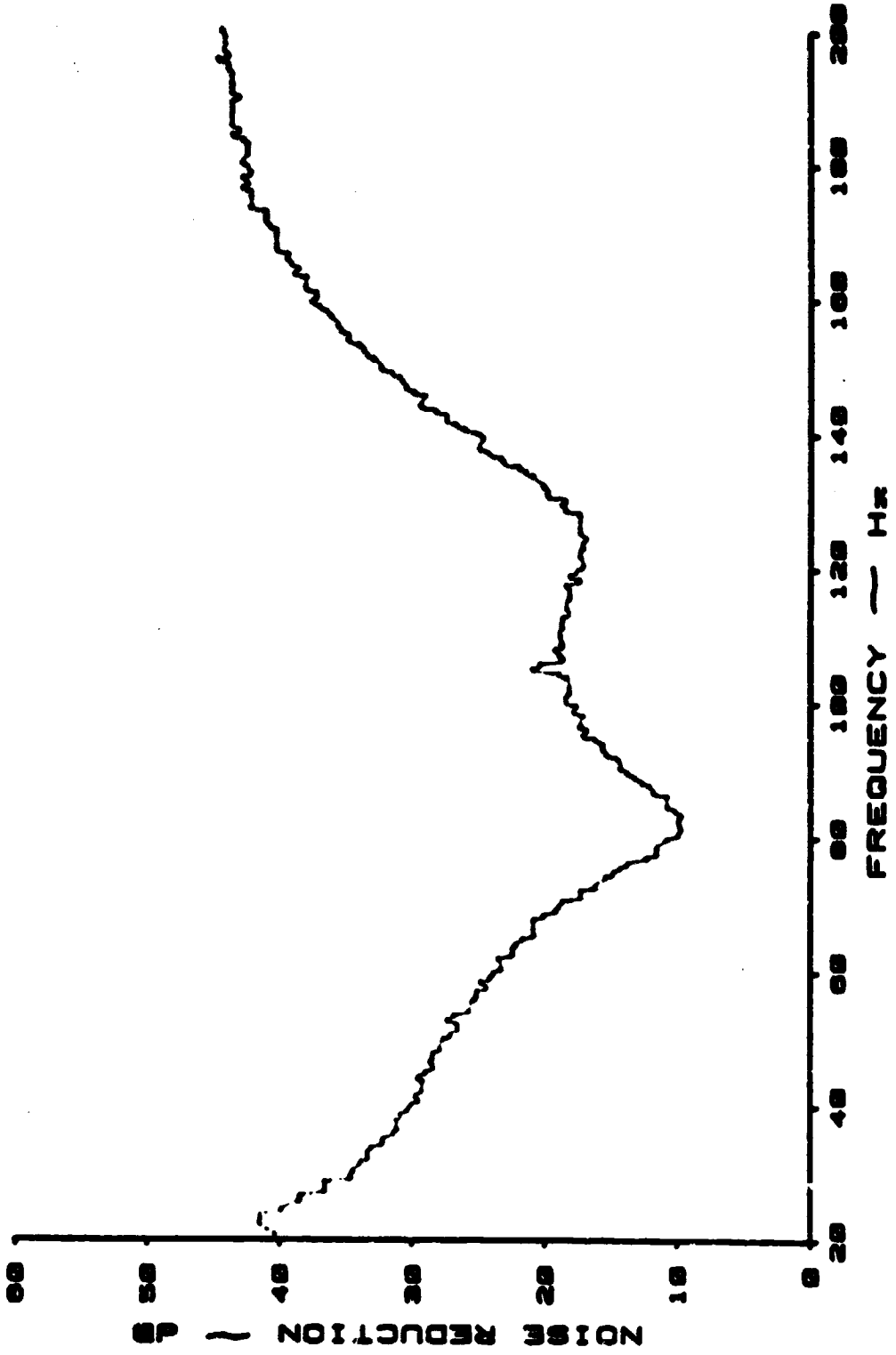

Figure 3.8: Low Frequency Noise Reduction Characteristics of a Dual Pane Window with Helmholtz Resonator; Tube Diameter 3/16 Inch, Number of Tubes 12, and Neck Length 0.1 Inch; 6 lb/ft^3 Fiberglass inside the Resonator Volume

C-2

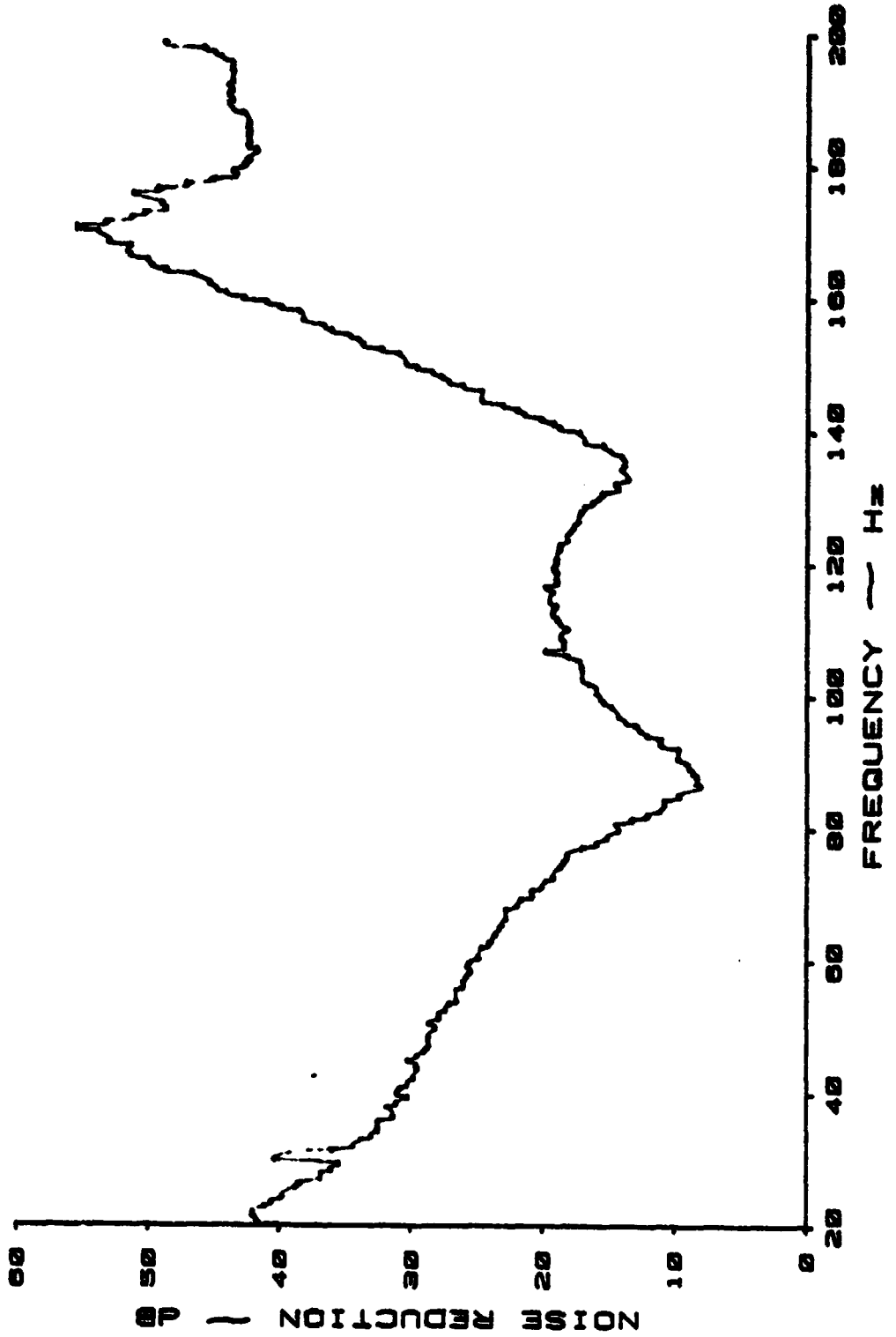

Figure 3.9: Low Frequency Noise Reduction Characteristics of a Dual Pane Window with Helmholtz Resonator; Tube Diameter 3/16 Inch, Number of Tubes 12, and Neck Length 0.1 Inch; 6 lb/ft^3 Fiberglass inside the Resonator Volume and Gauze (Cloth Screen) at the Tube Opening

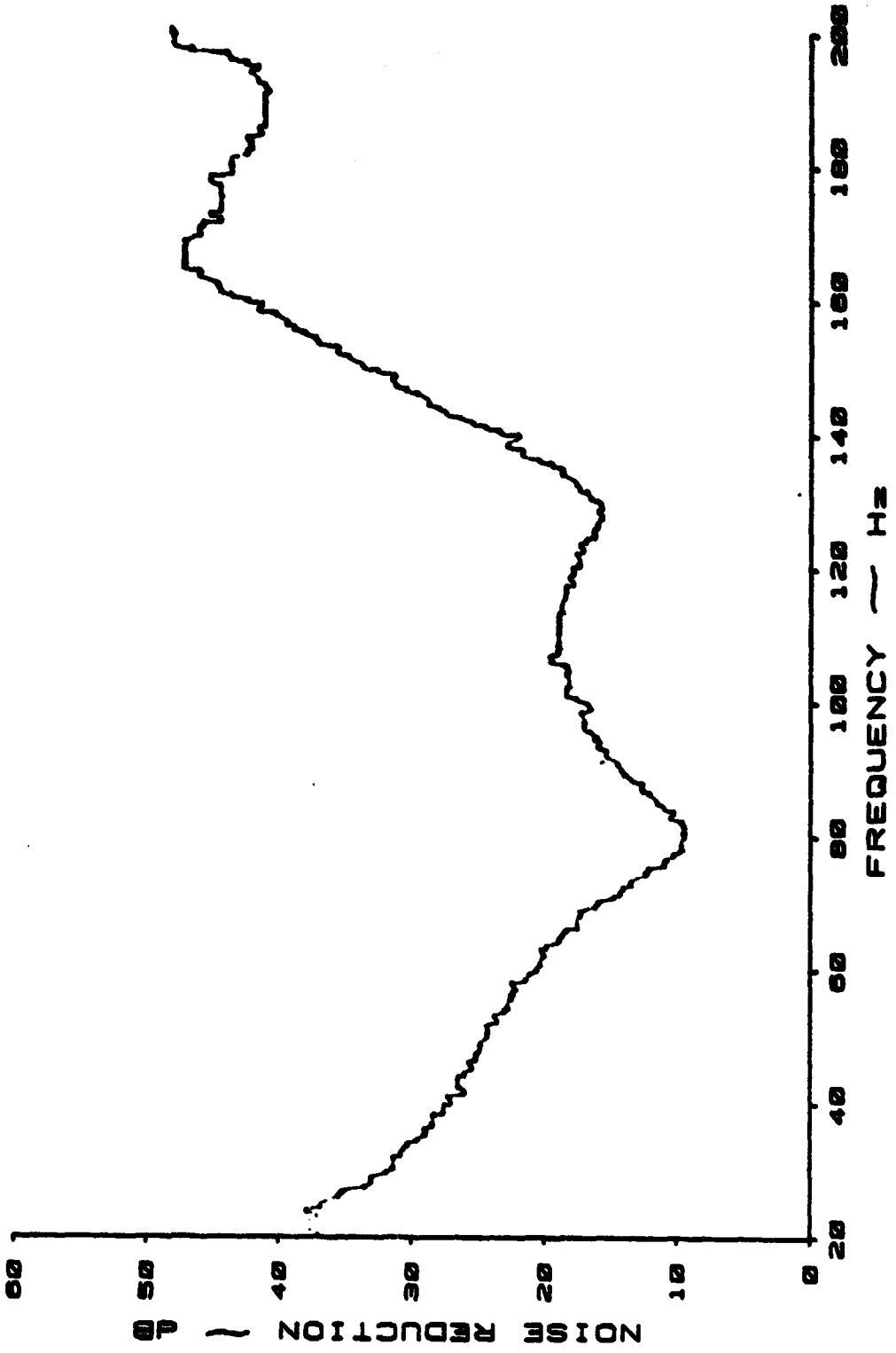

Figure 3.10: Low Frequency Noise Reduction Characteristics of a Dual Pane Window with Helmholtz Resonator; Tube Diameter 3/16 Inch, Number of Tubes 12, and Neck Length 0.1 Inch; Gauze (Cloth Screen) at the Tube Opening

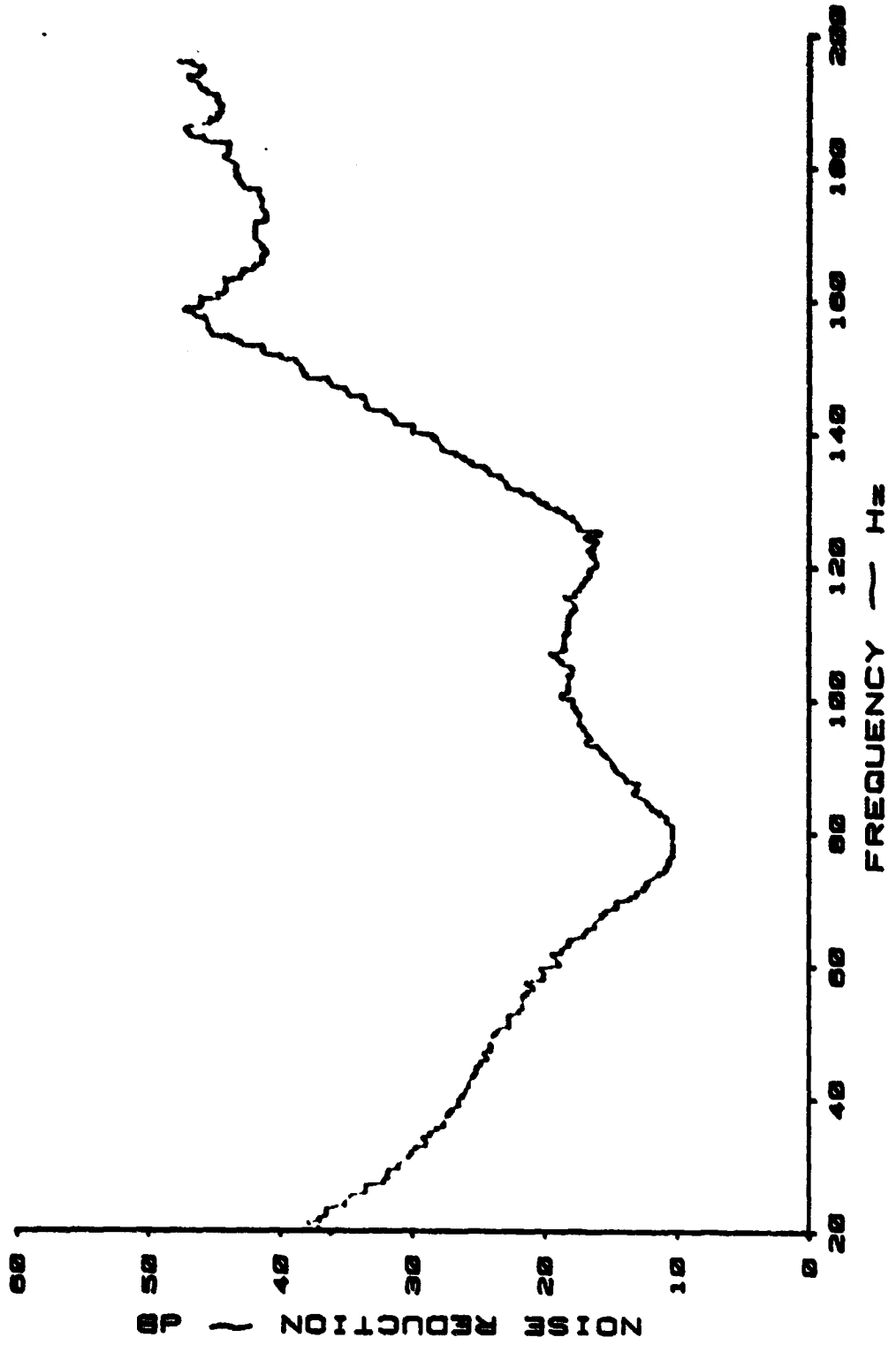

Figure 3.11: Low Frequency Noise Reduction Characteristics of a Dual Pane Window with Helmholtz Resonator; Tube Diameter 3/16 Inch, Number of Tubes 10, and Neck Length 0.1 Inch; Gauze (Cloth Screen) at the Tube Opening

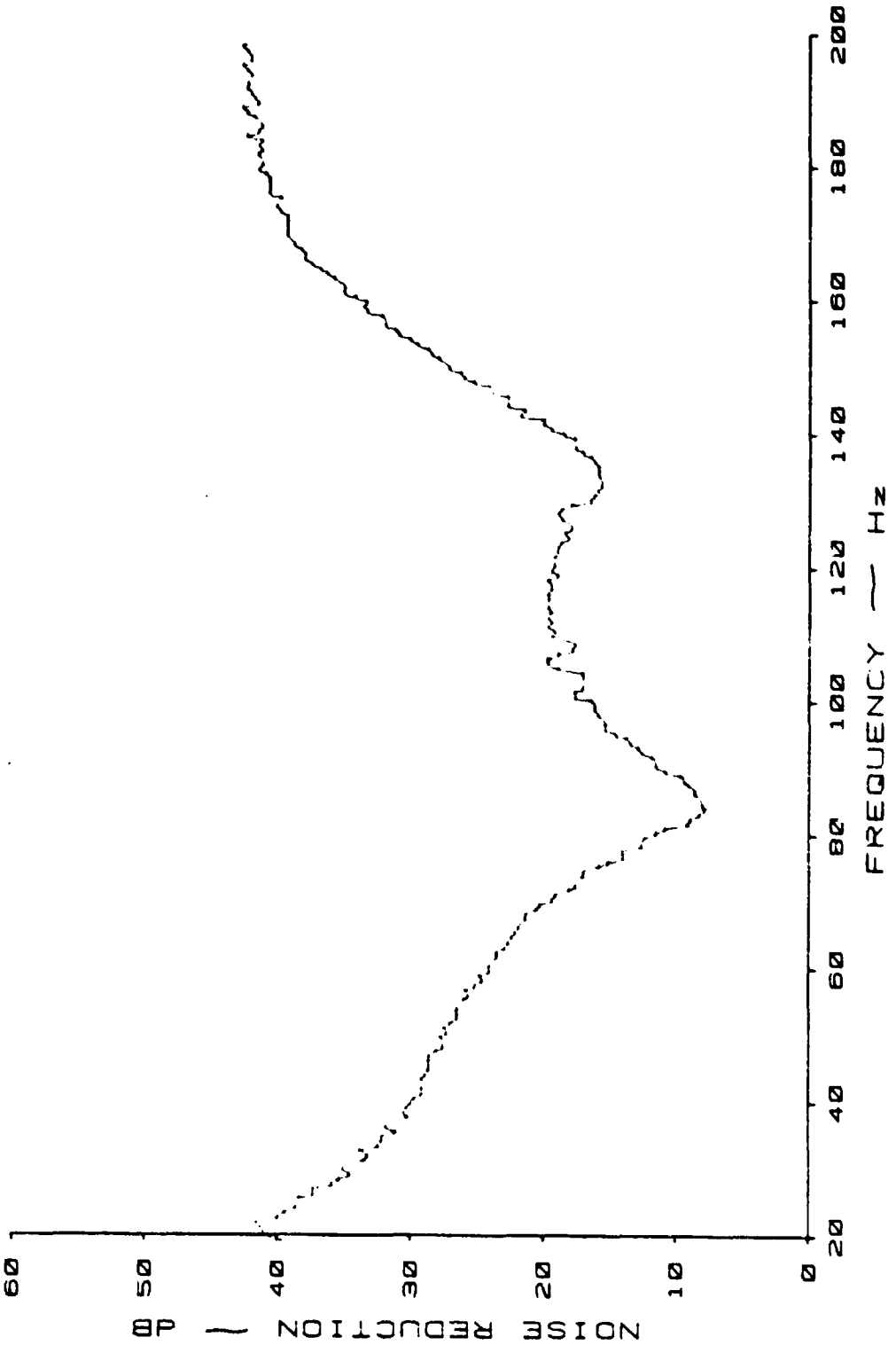

Figure 3.12: Low Frequency Noise Reduction Characteristics of a Dual Pane Window with Helmholtz Resonator Tube Diameter 3/16 Inch; Number of Tubes 12 and Neck Length 0.375 Inch

was filled with the resistive fiberglass (density 6 lb/ft^3), a maximum noise reduction of 8 dB was obtained. But the additional weight increase was 0.6 lb. Covering the hole with the gauze (cloth screen) did not increase weight; but the increase in noise reduction was also very small, 1 dB, which is within the experimental scatter. When the volume of the resonator and the tube were filled with fiberglass and the tube opening was covered with gauze, there was a decrease in noise reduction, compared with the case where there was no resistive material. Increasing the tube length to 0.375 inches as shown in Figure 3.4 did not significantly change the minimum noise reduction around 135 Hz.

It can be concluded from the experimental investigation that even within the constraints of the test facility and resonator volume restriction it is possible to increase the noise reduction of a dual pane window in a small frequency region by the use of the Helmholtz resonator concept, at low cost and complexity. Use of resistive materials tends to increase the range of frequency over which the resonator is effective, and the resistive material inside the resonator cavity gave the best increase of 8 dB around 135 Hz.

Table 3.1 Comparison of Minimum Noise Reduction Values of Dual Pane Windows with Helmholtz Resonators around 135 Hz

Test Number	Resonator Details: Tube Diameter inch	Number of Tubes	Tube Length inch	Resistive Material	Minimum Noise Reduction around 135 Hz	ΔNR
1	← without resonator →				10	-
2	7/64	4	0.1	-	11	1
3	7/64	12	0.1	-	15	5
4	3/16	12	0.1	-	15.5	5.5
5	3/16	12	0.1	6 lb/ft^3 fiberglass inside resonator cavity	18	8
6	3/16	12	0.1	6 lb/ft^3 fiberglass inside cavity and tube opening covered with gauze (cloth screen)	14	4
7	3/16	12	0.1	gauze (cloth screen) at the tube opening	16	6
8	3/16	10	0.1	gauze (cloth screen) at the tube opening	16.5	6.5
9	3/16	12	0.375	-	16	6.0

CHAPTER 4

CONCLUSIONS AND RECOMMENDATIONS

In this report the experimental noise attenuation characteristics of flat general aviation aircraft type multilayered panels are presented. Also single-degree-of-freedom theoretical models have been developed for sandwich panels with both shear-resistant and non-shear-resistant core material. The experimental investigation, performed to test the concept of Helmholtz resonators used in conjunction with dual pane windows in increasing the noise reduction around a small range of frequency, is also described.

From the experimental investigation it can be concluded that stiffening of the panels either by stiffeners or by sandwich construction increases the noise attenuation characteristics, in the low frequency region. Application of damping materials, while damping out the resonance peaks and dips in the high frequency region, lowers the fundamental resonance frequency. This results in decreased low frequency noise reduction. Of the materials tested, honeycomb sandwich panels produced the highest low frequency noise reduction for the given weight due to their high stiffness-to-mass ratio. Multilayered panels with sound absorbing materials showed increased noise reduction when sandwiched between two aluminum panels. This increase was achieved at a relatively high weight compared to honeycomb panels. They also produced increased high frequency noise reduction. The air gaps in the panel did not have any additional benefits in the frequency range of interest.

The theoretical models, within the constraints of the assumptions made in deriving them, predict the fundamental resonance frequency and the low frequency noise reduction fairly accurately, if the panel is inherently stiff. In such cases the effect of the cavity of the KU-FRL acoustic test facility is less pronounced. The prediction methods give reasonable results for stiffened panels and honeycomb panels. Modeling of damping materials to have only mass and damping is seen to agree well with the experimental results. The prediction method for non-shear-resistant core agrees with the earlier prediction methods (References 9 and 10), when the stiffness of the skin is neglected. The experimental results and the results of the present predictions show poor resemblance in the low frequency region. This, however, must be partly due to the cavity effects and unknown edge conditions of the skins of the panels. Even while accounting for the discrepancy of the fundamental resonance frequency, the predicted values are still conservative. This needs further investigation. At high frequency range the values predicted agree well with the average values obtained. The calculation of the complex impedances of the sound absorbing materials is still approximate and could have contributed to the inconsistencies.

From the experimental investigation carried out it can be concluded that the concept of Helmholtz resonators in conjunction with the dual pane windows offers an attractive low cost solution to increase the noise attenuation around a small range of frequency. These resonators can be tuned to the frequencies at which the pane or panel resonances occur. The prediction method presented gives reasonably accurate value of such frequencies.

In this report experimental investigation was limited to flat multilayered panels. It is recommended that this be extended to curved multilayered panels to determine their sound transmission characteristics.

Second, the experimental investigation was performed in laboratory conditions using 18 x 18 inch panels. It is recommended that the effect of such treatments on the overall interior noise be determined either analytically or experimentally.

Third, the prediction of noise reduction values of sound absorbing materials was limited to sandwich panels with fibrous materials. This can be extended to semi-rigid materials.

Fourth, the tests with Helmholtz resonators were limited by the volume of the resonator. It is recommended that further investigation be done to check the effect of the volume in increasing the effectiveness of these resonators.

REFERENCES

1. Catherines, J. J., and Mayes, W. H., "Interior Noise Levels of Two Propeller-Driven Light Aircraft," NASA TM X-72716, July 1975.

2. Rudrapatna, A. N., and Jacobson, I. D., "Impact of Interior Cabin Noise on Passenger Acceptance," SAE Paper 760466, 1976.

3. Mixson, J. S., Barton, C. K., and Vaicaitis, R., "Investigation of Interior Noise in a Twin Engine Light Aircraft," J. of Aircraft, Volume 15, No. 4, April 1978.

4. Peschier, T. D., "General Aviation Interior Noise Study," Doctor of Engineering Dissertation, University of Kansas, Lawrence, Kansas, August 1977.

5. Catherines, J. J., and Jha, S. K., "Sources and Characteristics of Interior Noise in General Aviation Aircraft," NASA TM X-72839, April 1976.

6. Roskam, J.; Grosveld, F.; and Van Aken, J., "Summary of Noise Reduction Characteristics of Typical General Aviation Materials," KU-FRL-317-P6; SAE Paper 790627, presented at the Business Aircraft Meeting, Wichita, Kansas, April 3-6, 1979.

7. Grosveld, F., "Study of Typical Parameters that Affect Sound Transmission through General Aviation Aircraft Structures," Doctor of Engineering Dissertation, University of Kansas, Lawrence, Kansas, August 1980.

REFERENCES (continued)

8. Beranek, L. L., Noise and Vibration Control, McGraw-Hill Book Co., New York, 1971.

9. Richards, E. J., and Mead, D. J., Noise and Acoustic Fatigue in Aeronautics, John Wiley & Sons Ltd., New York, 1968.

10. Mangiarotty, R. A., "Optimization of the Mass Distribution and the Airspaces in Multiple Element Sound Proofing Structures," J. Acoust. Soc. Amer., 35, 1023 (1963).

11. Beranek, L. L., and Work, G. A., "Sound Transmission through Multiple Structures Containing Flexible Blankets," J. Acoust. Soc. Amer., 21, 419 (1949).

12. Getline, G. L., "Low Frequency Noise Reduction of Light Weight Airframe Structures," NASA CR 145104, August 1976.

13. Vaicaitis, R., "Noise Transmission by Viscoelastic Sandwich Panels," NASA TN D-8516, August 1976.

14. Henderson, T. D., "Design of an Acoustic Panel Test Facility," Master of Engineering Project Report, University of Kansas, Lawrence, Kansas, August 1977.

15. Grosveld, F., and Van Aken, J., "Investigation of the Characteristics of an Acoustic Panel Test Facility," KU-FRL-317-9, Flight Research Laboratory, University of Kansas, Lawrence, Kansas 66045, September 1978.

REFERENCES (continued)

16. Emme, H. J., "Composite Materials for Noise and Vibration Control," Reprint from Sound and Vibration.

17. Grosveld, F., and Navaneethan, R., "Noise Reduction Characteristics of Flat, General Aviation Type Dual Pane Windows," KU-FRL-417-12, University of Kansas Flight Research Laboratory, Lawrence, Kansas, February 1980.

18. Grosveld, F.; Navaneethan, R.; and Roskam, J., "Noise Reduction Characteristics of General Aviation Type Dual Pane Windows," AIAA Paper No. 80-1874, presented at the 1980 AIAA Aircraft Systems and Technology Meeting, Anaheim, California, August 4-6, 1980.

19. Szilard, R., Theory and Analysis of Plates, Prentice-Hall, Inc., Englewood Cliffs, New Jersey, 1974.

20. Ford, R. D.; Lord, P.; and Walker, A. W., "Sound Transmission through Sandwich Constructions," J. Sound Vib., 5 (1), 1967.

21. Smolenski, C. P., and Krokosky, E. M., "Dilational Mode Sound Transmission in Sandwich Panels," J. Acoust. Soc. Amer., 54, 1449, 1973.

22. Unz, H., "Acoustic Plane Waves Normally Incident on a Clamped Panel in a Rectangular Duct," KU-FRL-417-11, University of Kansas Flight Research Laboratory, Lawrence, Kansas, August 1979.

23. Leissa, A. W., "Vibration of Plates," NASA SP-160, Scientific and Technical Information Division, Office of Technology Utilization, NASA, Washington, D.C., 1969.

24. McFarland, D. E.; Smith, B. L.; and Bernhart, W. D., Analysis of Plates, Spartan Books, New York, 1972.

25. Barton, C. K., "Structural Stiffening as an Interior Noise Control Technique for Light Twin-Engine Aircraft," Doctor of Philosophy Dissertation, North Carolina State University, Raleigh, 1979.

26. Anon., "Mechanical Properties of Hexcel Honeycomb Materials," TSB 210 Hexcel Dublin California, 1976.

APPENDIX A

DETAILS AND CHARACTERISTICS OF THE KU-FRL ACOUSTIC TEST FACILITY

The design and construction of the KU-FRL acoustic test facility have been described in Reference 14. Reference 15 describes the investigation carried out to determine the characteristics of the test facility.

A.1 DESIGN AND CONSTRUCTION OF THE KU-FRL ACOUSTIC TEST FACILITY (BERANEK TUBE)

The test panel is mounted between two chambers: the source chamber and the receiver chamber. The source chamber, consisting of a massive brick wall, concrete collar and a steel box, contains nine evenly spaced loudspeakers. This chamber can be considered to be a speaker box. Its purpose is to support the speakers and to prevent radiation of sound to the rear and the sides. It contains sound absorbing materials to minimize standing waves. These can induce undesired speaker-sound radiation characteristics. A small distance, about one inch, separates the test panel from the front side of the speaker baffle. This arrangement prevents standing waves between the baffle and the test panel at frequencies in the range of interest, 20-5,000 Hz. Other standing waves, parallel to the panel and the speaker baffle, could disturb the desired uniformity of excitation at the panel surface. The strength of these standing waves, however, is reduced by sound absorbing material, which nearly fills all the space between the baffle and the test panel.

The receiving chamber is an acoustic termination, which absorbs almost all the acoustic energy. To facilitate the installation of test specimens between this termination and the speaker box, the receiving chamber is mounted on wheels and rests on a steel table. Figures A.1 and A.2 show the details of the test facility.

The loudspeakers can be driven by the amplified signal of a pure-tone generator, a white-noise generator, or a tape recording of in-flight boundary layer fluctuations (Figure A.3). An equalizer is included in this noise generating system to obtain a reasonably flat frequency spectrum. The noise measuring system includes two microphones, one on each side of the test panel. The output signals of the microphones are fed into a real-time analyzer. The resulting spectra are plotted by an X-Y recorder. Next, these curves are put into a desk-top computer, having curve digitizing capabilities, which subtracts one spectrum from the other, applies corrections and plots final test results. To test the effect of pressurization on the sound transmission loss of a panel, a depressurization system has been installed. With this system the pressure in the source chamber can be reduced, while in the receiver chamber the atmospheric pressure exists.

A.2 CHARACTERISTICS OF THE KU-FRL ACOUSTIC TEST FACILITY

Based on the investigations carried out to determine the characteristics of the test facility, the following conclusions were reached (References 7 and 15).

1. Although all the walls have been covered very carefully with high quality absorption material, standing waves in

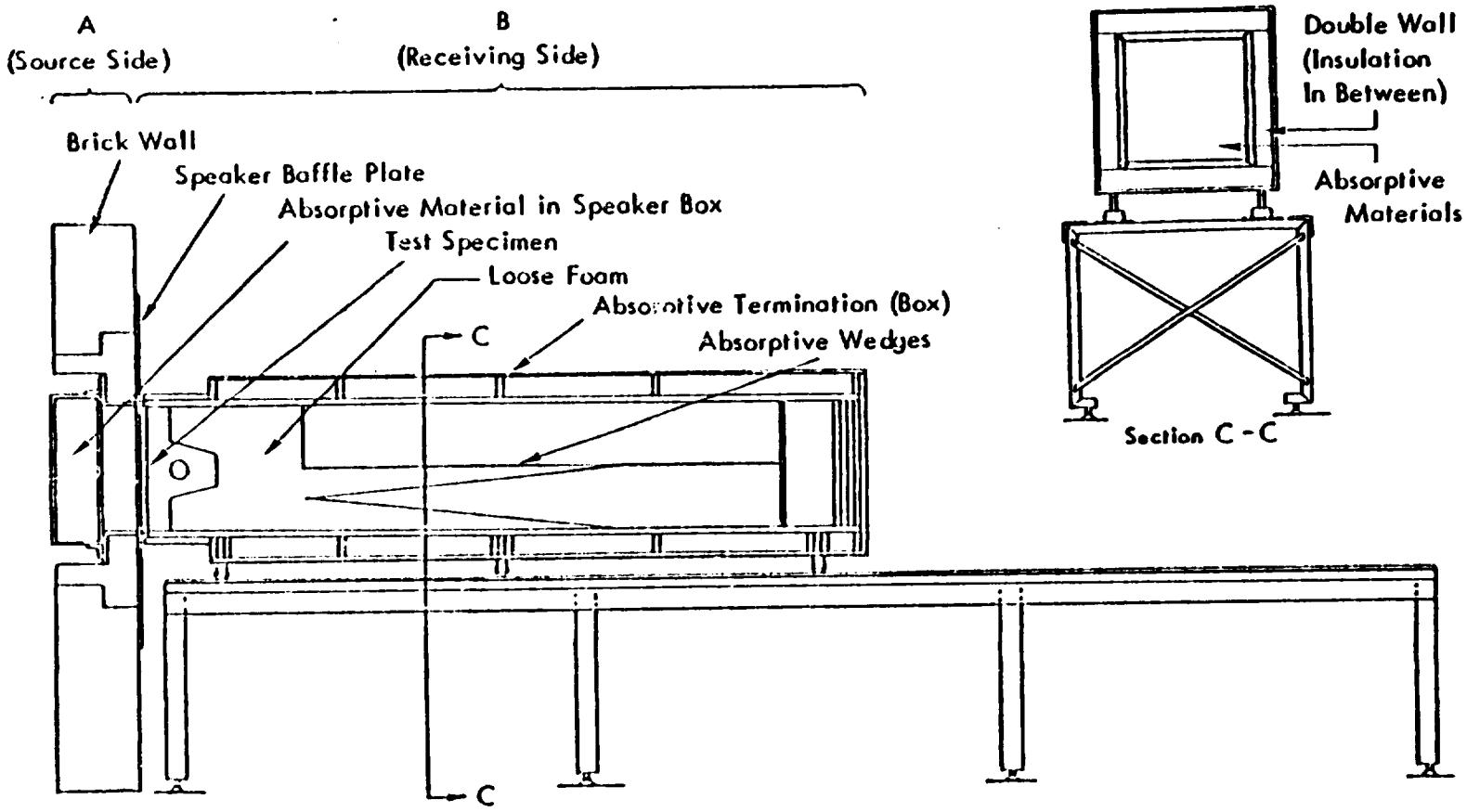

Figure A.1: Plane Wave Tube

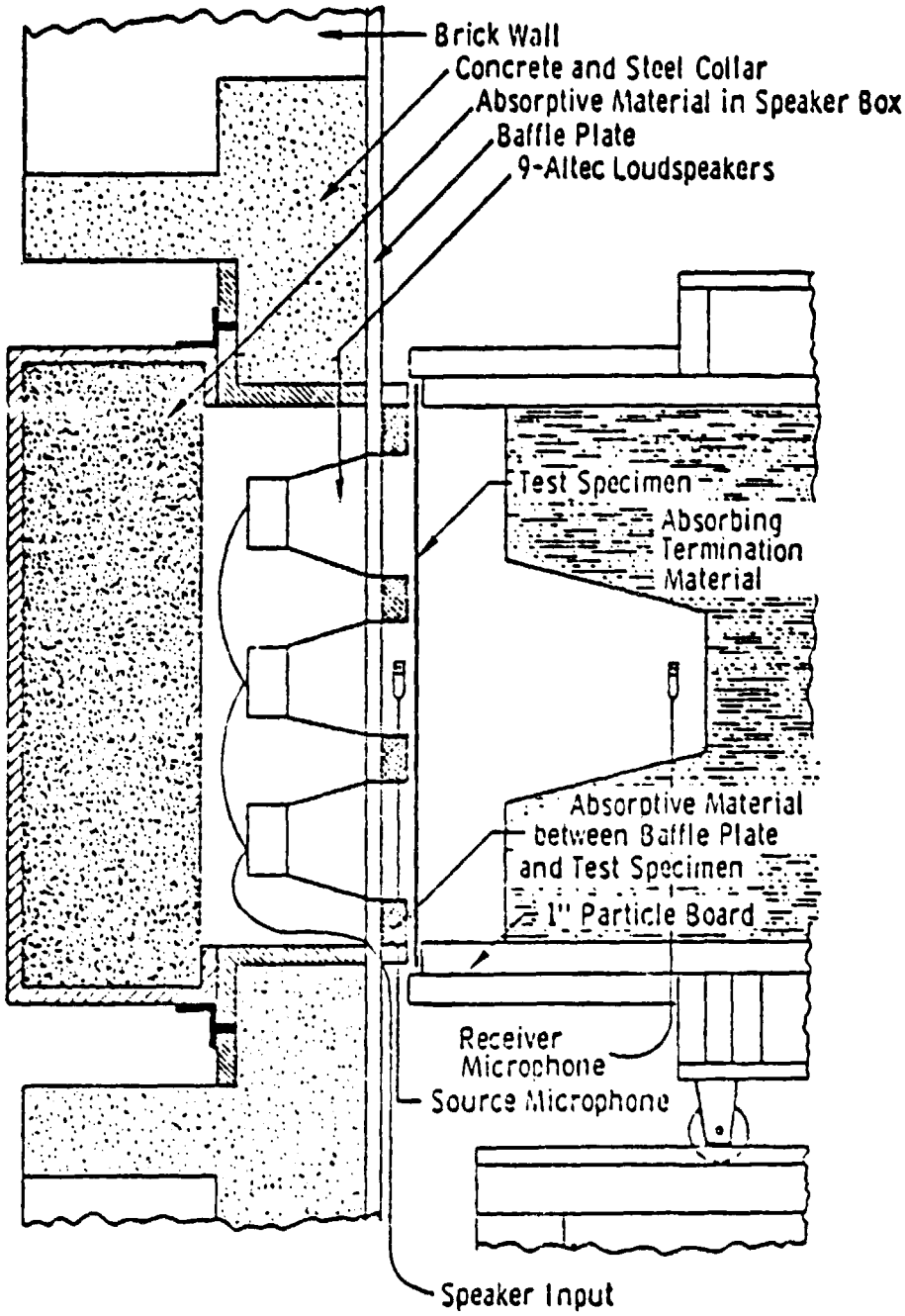

Figure A.2: KU-FRL Acoustic Test Facility
Showing Placement of Test Specimen

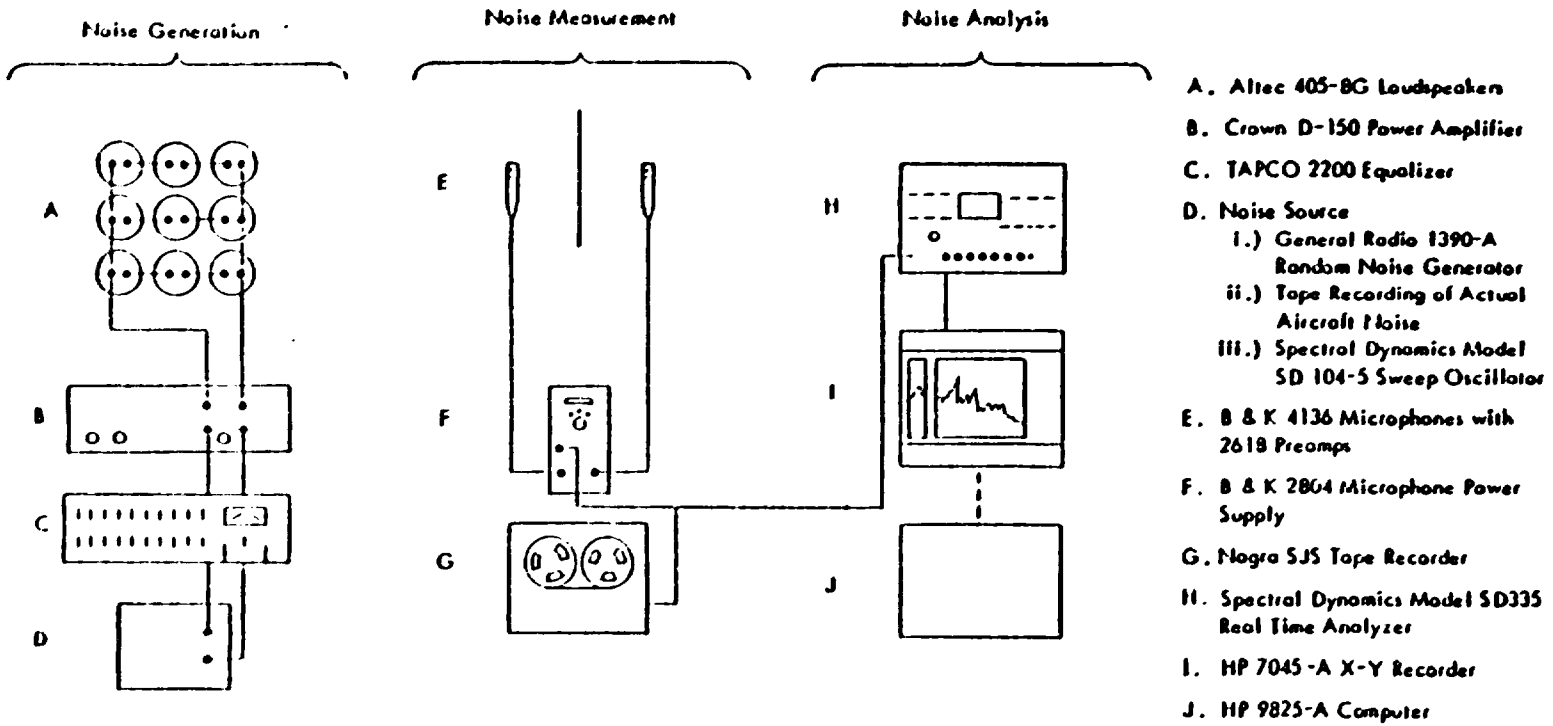

Figure A.3: General Arrangement of Electronic Equipment

between and reflections off the walls and absorption wedges cannot be prevented.

2. In addition, inside the Beranek Tube, behind the test panel, standing waves occur and reflections from the side walls influence the signal measured by the receiver microphone.
3. Energy dissipation by absorption material, walls and test panel is not negligible.
4. The plane wave approximation is only justified below a frequency of 800 Hz at short distances from the speaker baffle. It is also justified over the entire frequency range (20 Hz-5000 Hz) if the distance from the source is at least 34 inches.
5. The use of a pure tone generator as a sound source, instead of white noise or real aircraft noise, appeared to be a satisfactory substitute to measure sound transmission through aircraft structures.
6. The microphone position (Section 3.5) has its greatest influence on the measured sound pressure level in the frequency range between, roughly, 150 Hz and 800 Hz.
7. Each of the nine loudspeakers has its own frequency response characteristics.
8. Possible reflections off the back panel of the Beranek tube are not measured by the receiver microphone. Since the same sound pressure levels are measured with and without a back panel, the absorption material reduces the reflecting sound energy to non-measurable levels.

9. Above the frequency of 60 Hz the effect of removing the speaker back panel is minor. Below this frequency a change in sound pressure level is measured by the microphone. Because of the large wavelength in this low frequency region, it is assumed that this is due to reflections off the laboratory room walls.

10. The air in a closed cavity backing a flexible panel acts as an additional stiffness, raising the fundamental panel resonance frequency. The analytical model gives a pretty accurate prediction (withih 5% accuracy) of this cavity effect.

11. The air in a cavity between the test panel and the speaker baffle acts as a "virtual mass," decreasing the fundamental panel resonance frequency by an average of 3 Hz for the test cases considered.

12. The properties of the KU-FRL acoustic panel test facility are hard to define. Edge conditions of the test panels are somewhere between clamped and simply supported. The absorption material absorbs quite a lot of the sound energy, but not all the sound energy is absorbed. It is not known how much sound reflects from the panel, the walls and the sound absorption materials (at higher frequencies). This complicates any comparison of measured sound transmission with theoretical predictions.

APPENDIX B

EXPERIMENTAL NOISE REDUCTION DATA FOR MULTILAYERED PANELS

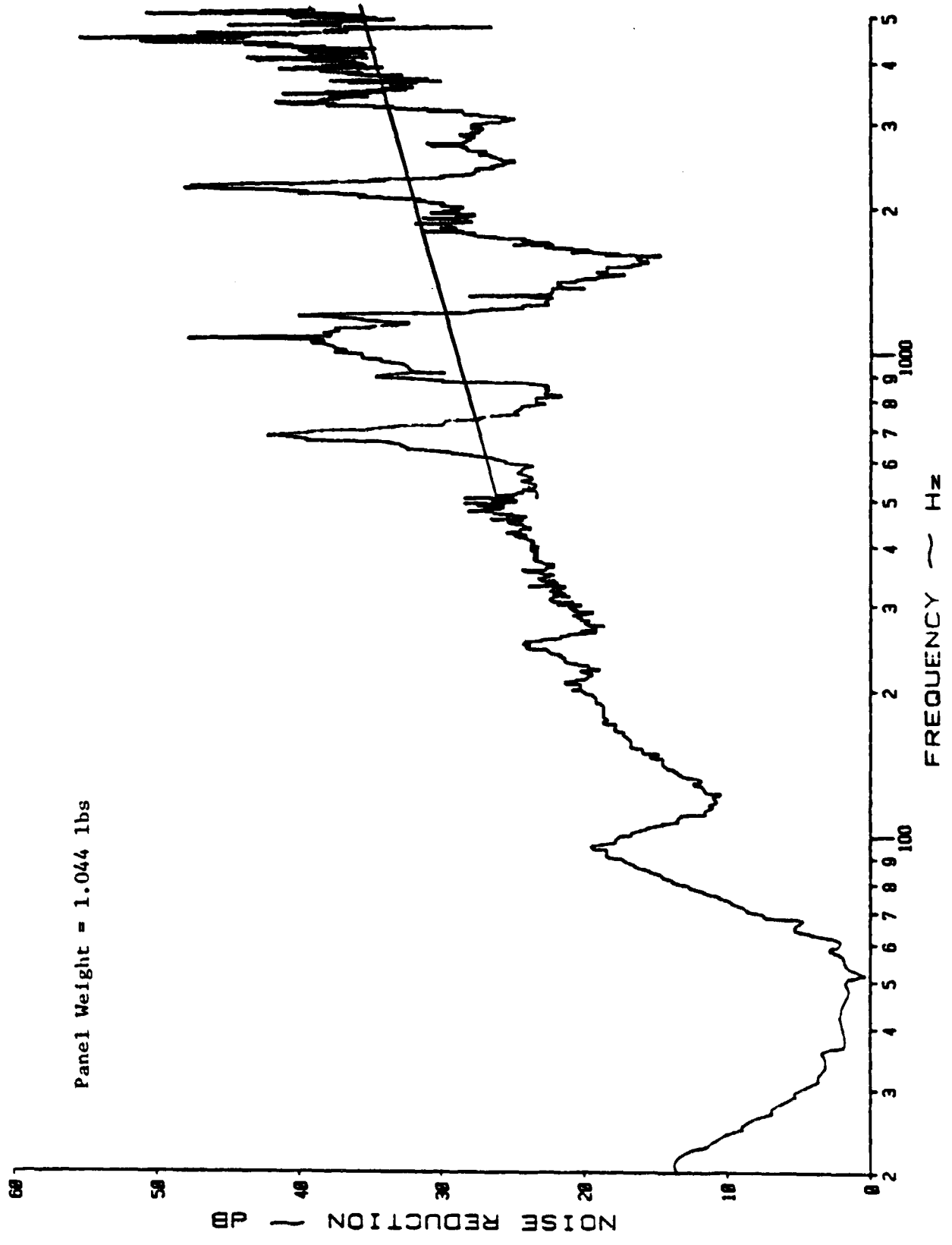

(a) Narrow Band Analysis

Figure B.1: Noise Reduction Characteristics of a Multilayered Panel with Rigid P.V.C.-Based Foam of Density 0.1073 Slugs/ft^3 Attached to a 0.025 Inch Aluminum Panel

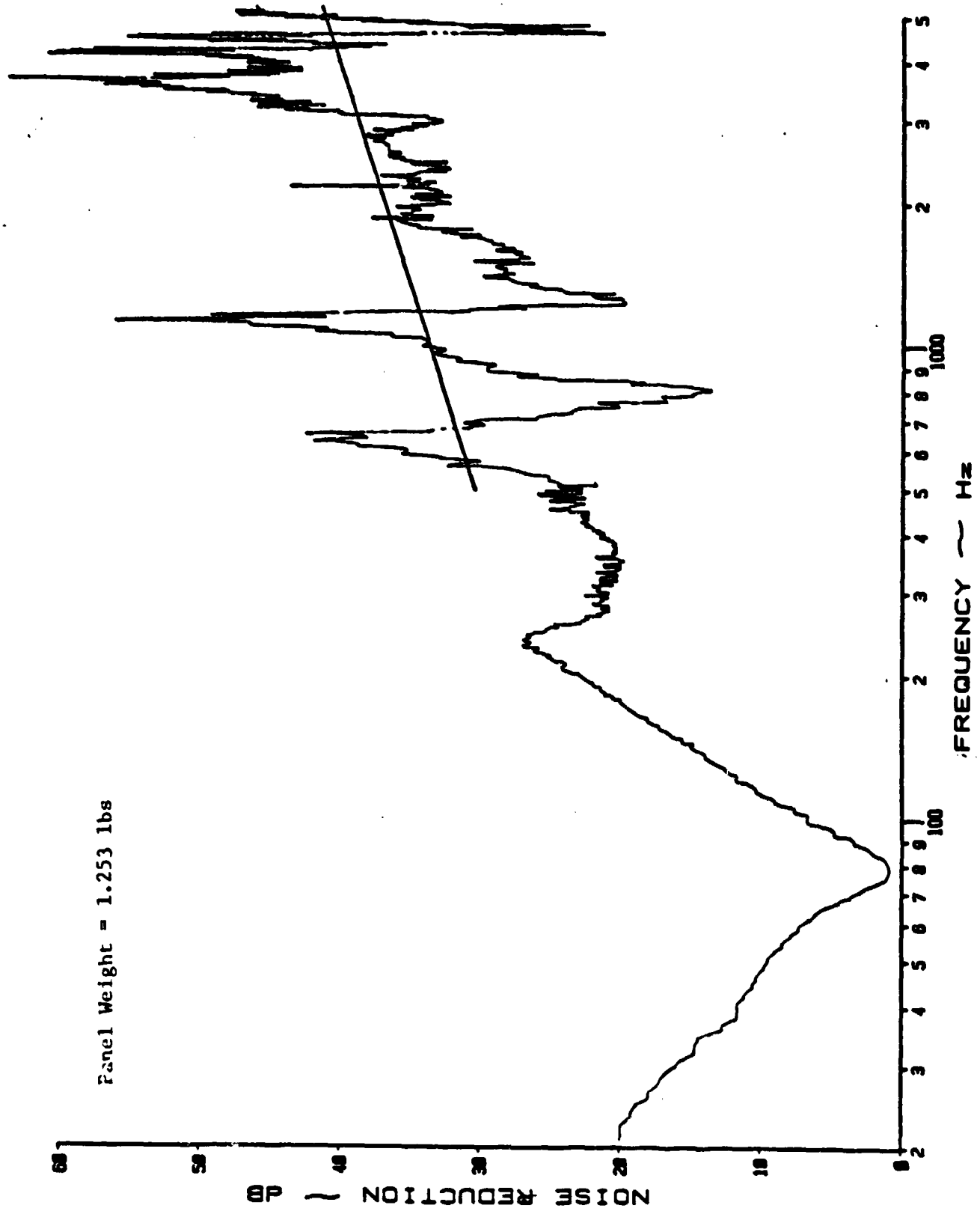

(a) Narrow Band Analysis

Figure B.2: Noise Reduction Characteristics of a Multilayered Panel with Rigid P.V.C.-Based Foam of Density 0.1287 Slugs/ft^3 Attached to 0.025 Inch Aluminum Panel

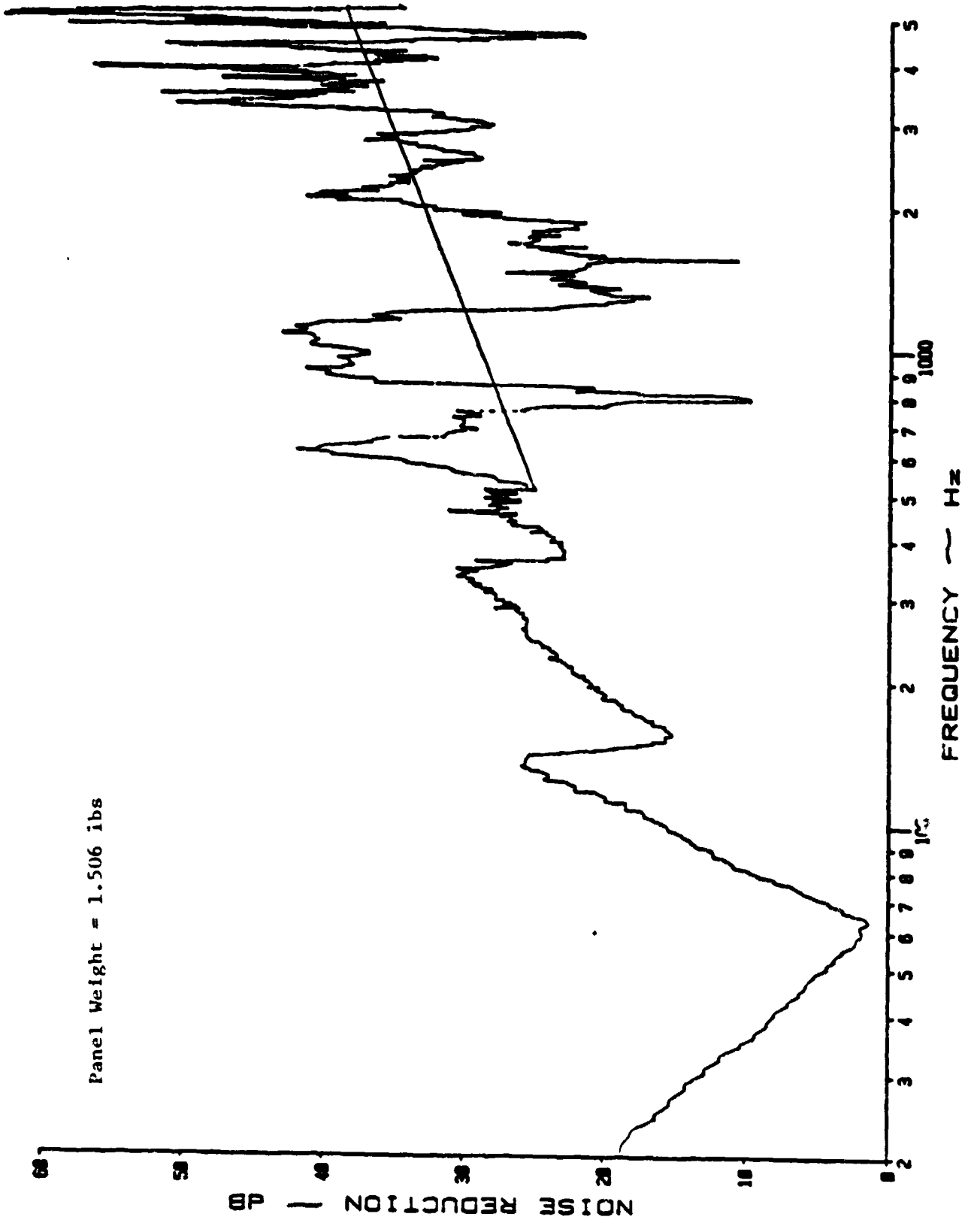

(a) Narrow Band Analysis

Figure B.3: Noise Reduction Characteristics of a Multilayered Panel with Rigid P.V.C.-Based Foam of Density 0.3594 Slugs/ft^3 Attached to 0.025 Inch Aluminum Panel

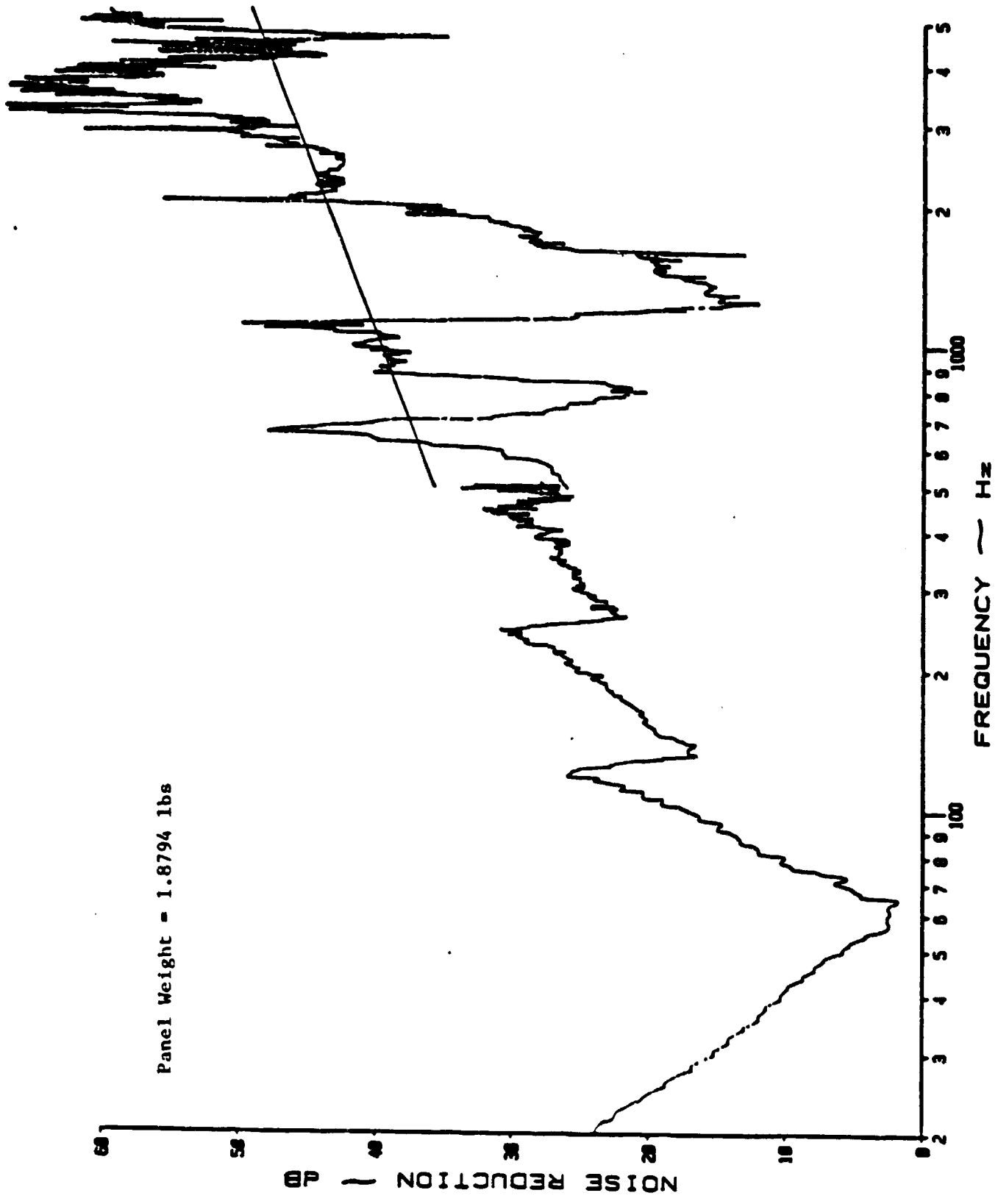

(a) Narrow Band Analysis

Figure B.4: Noise Reduction Characteristics of a Multilayered Panel with Rigid P.V.C.-Based Foam of Density 0.1073 Slugs/ft^3 when Sandwiched between Two 0.025 Inch Aluminum Panels

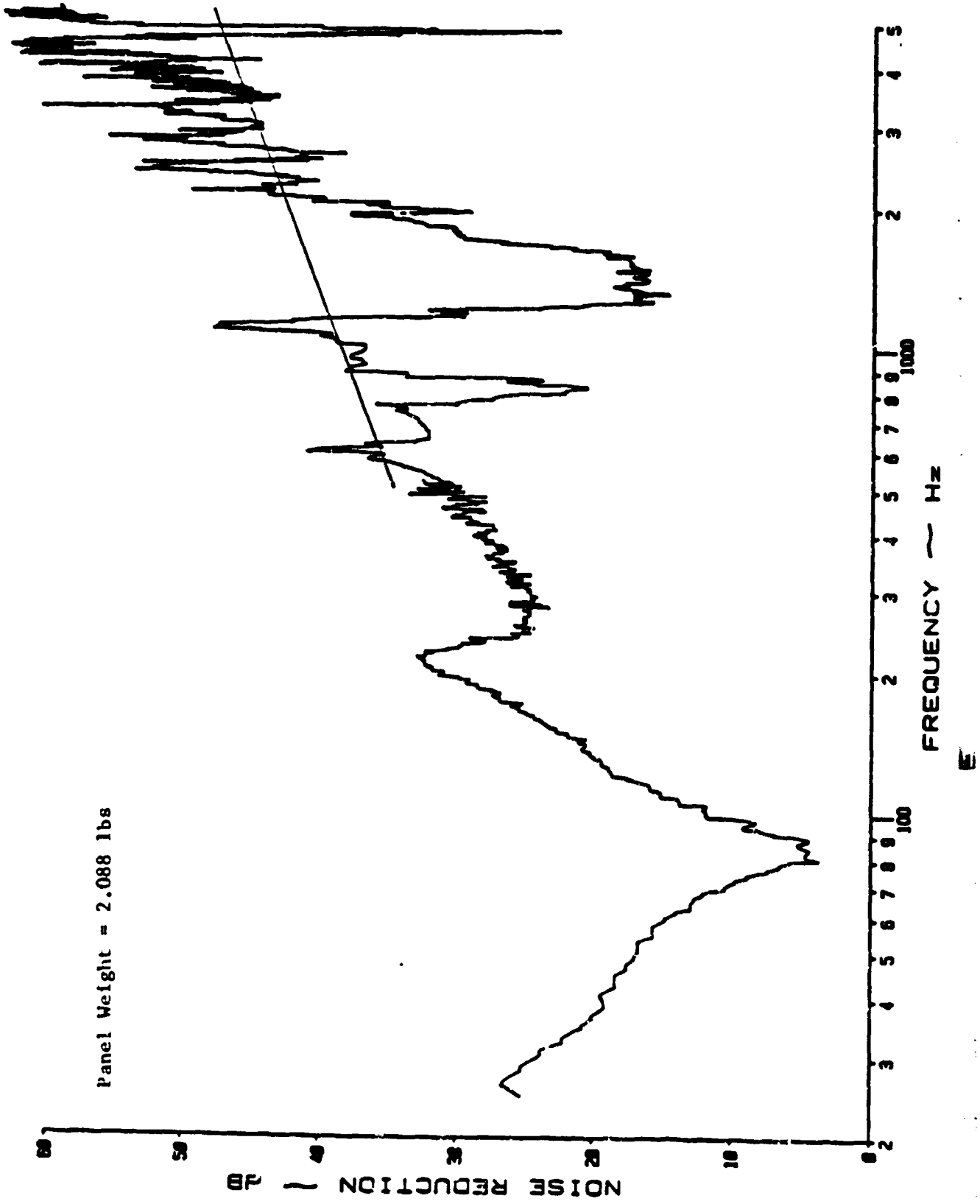

(a) Narrow Band Analysis

Figure B.5 : Noise Reduction Characteristics of a Multilayered Panel with Rigid P.V.C.-Based Foam of Density 0.1287 Slugs/ft^3 when Sandwiched between 0.025 Inch Aluminum Panels

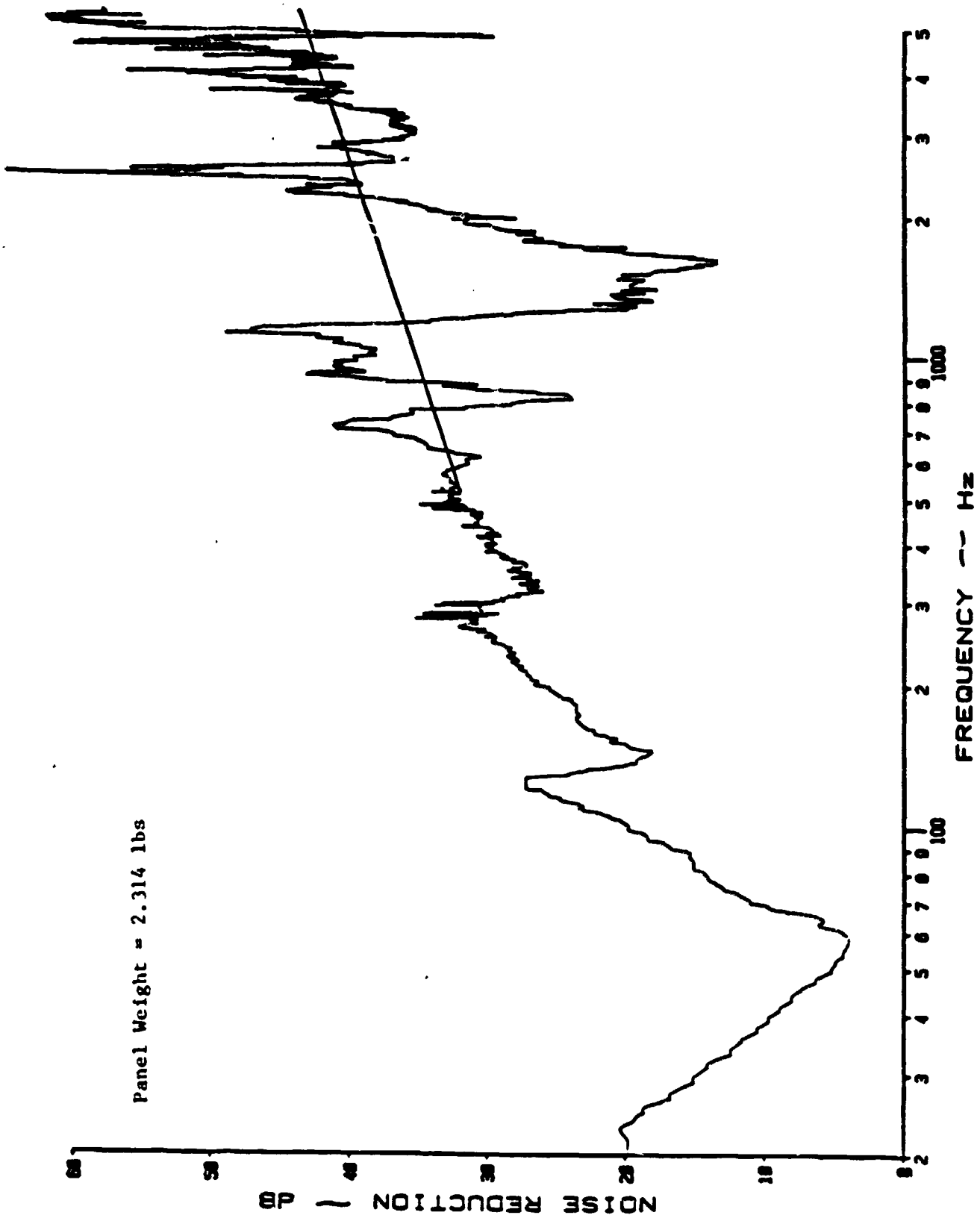

(a) Narrow Band Analysis

Figure B.6: Noise Reduction Characteristics of a Multilayered Panel with Rigid P.V.C.-Based Foam of Density 0.3594 Slugs/ft^3 when Sandwiched between 0.025 Inch Aluminum Panels

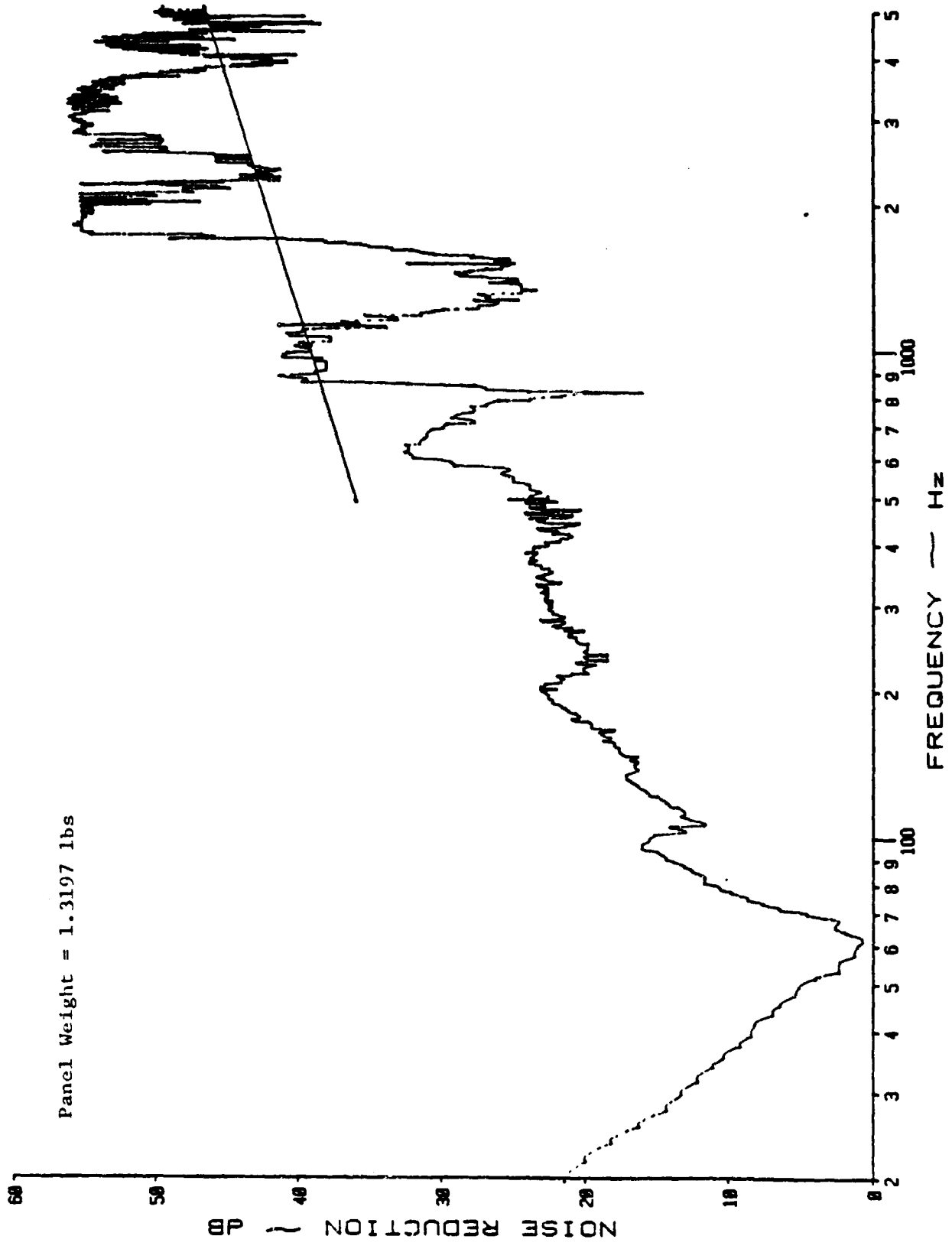

(a) Narrow Band Analysis

Figure B.7 : Noise Reduction Characteristics of a Multilayered Panel with Sound Absorption Material of Density 0.082 Slugs/ft^3 when Attached to 0.025 Inch Aluminum Panel

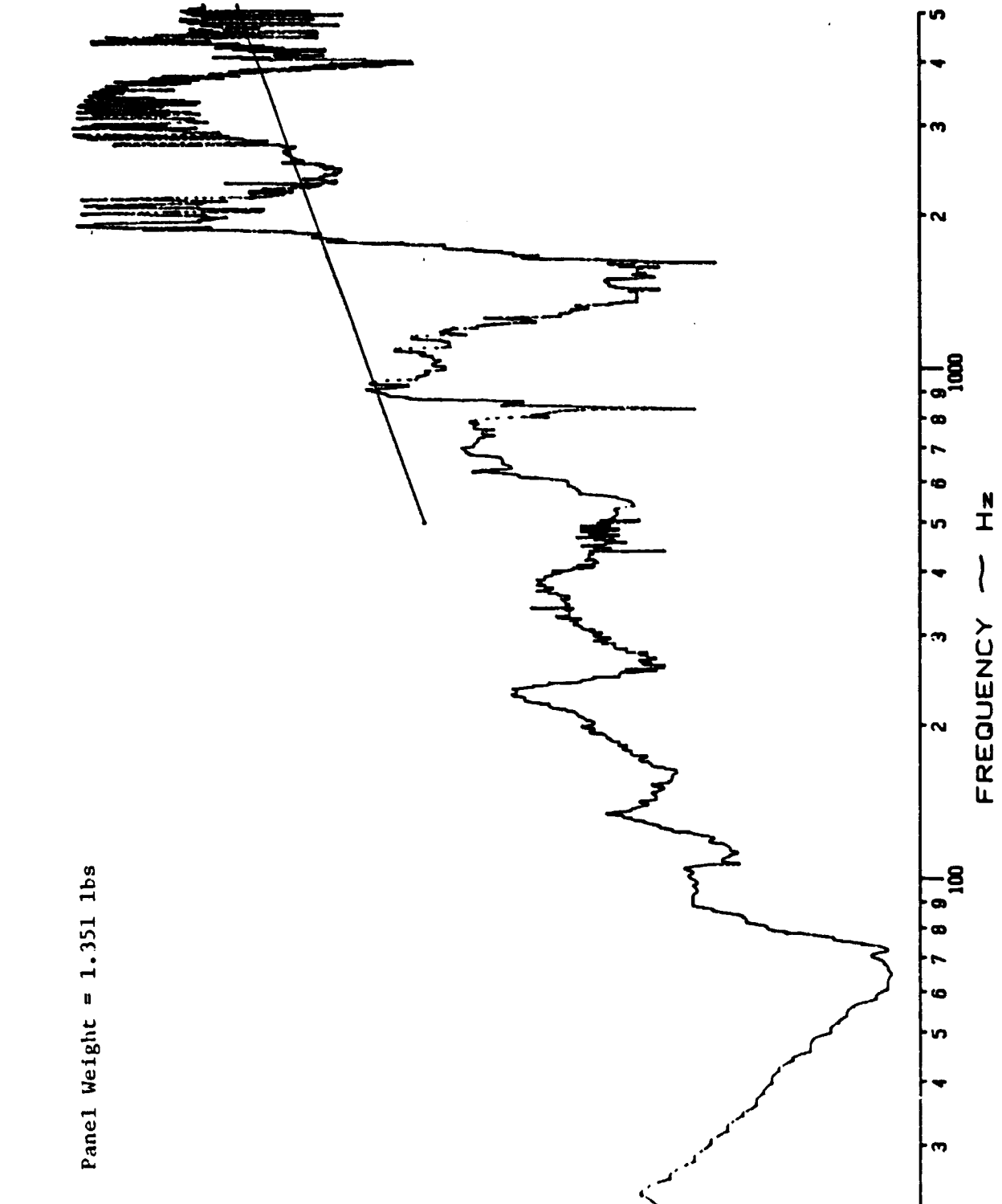

(a) Narrow Band Analysis

Figure B.8: Noise Reduction Characteristics of a Multilayered Panel with Sound Absorption Material of Density 0.091 Slugs/ft^3 when Attached to 0.025 Inch Aluminum Panel

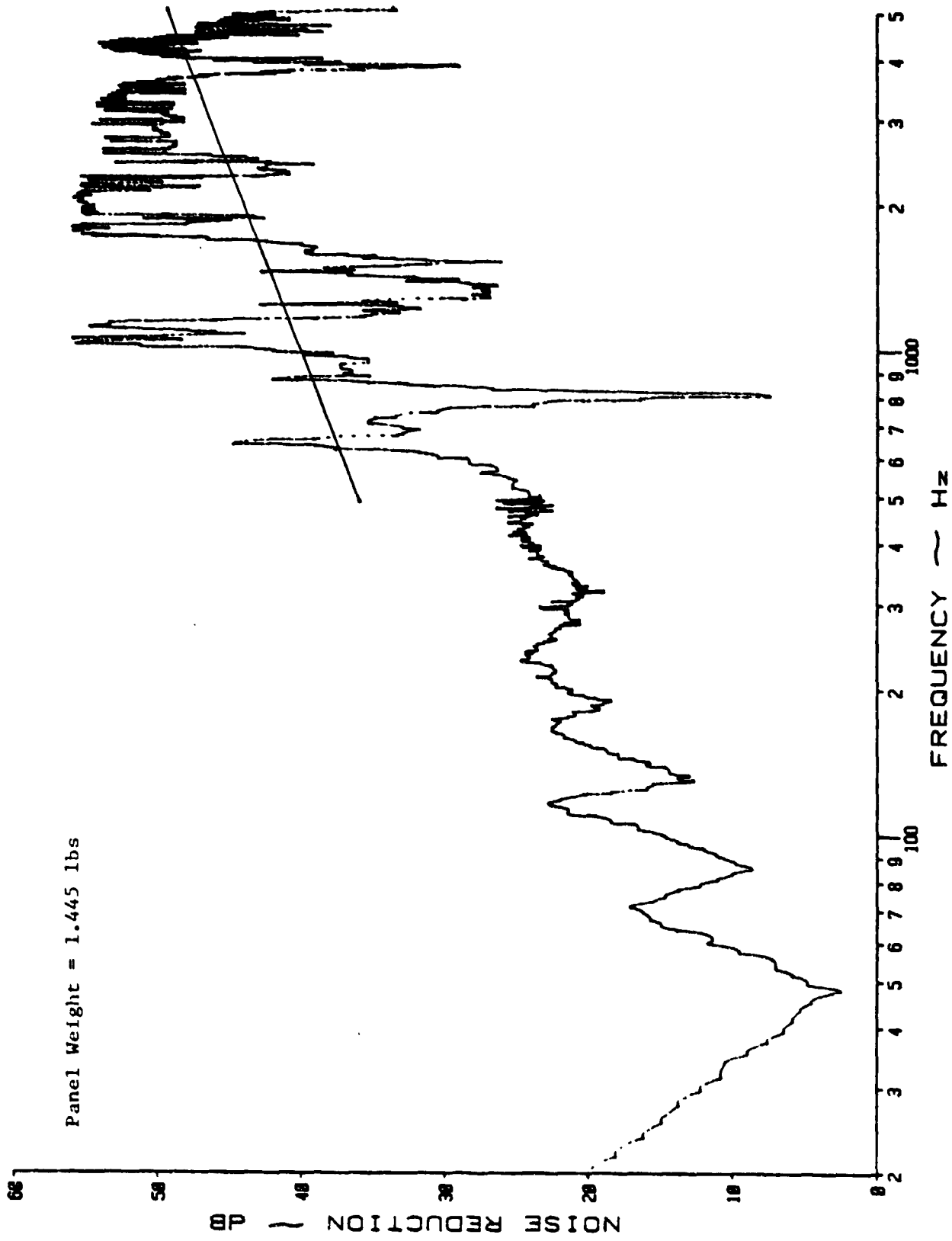

(a) Narrow Band Analysis

Figure B.9: Noise Reduction Characteristics of a Multilayered Panel with Sound Absorption Material of Density 0.114 Slugs/ft^3 when Attached to 0.025 Inch Aluminum Panel

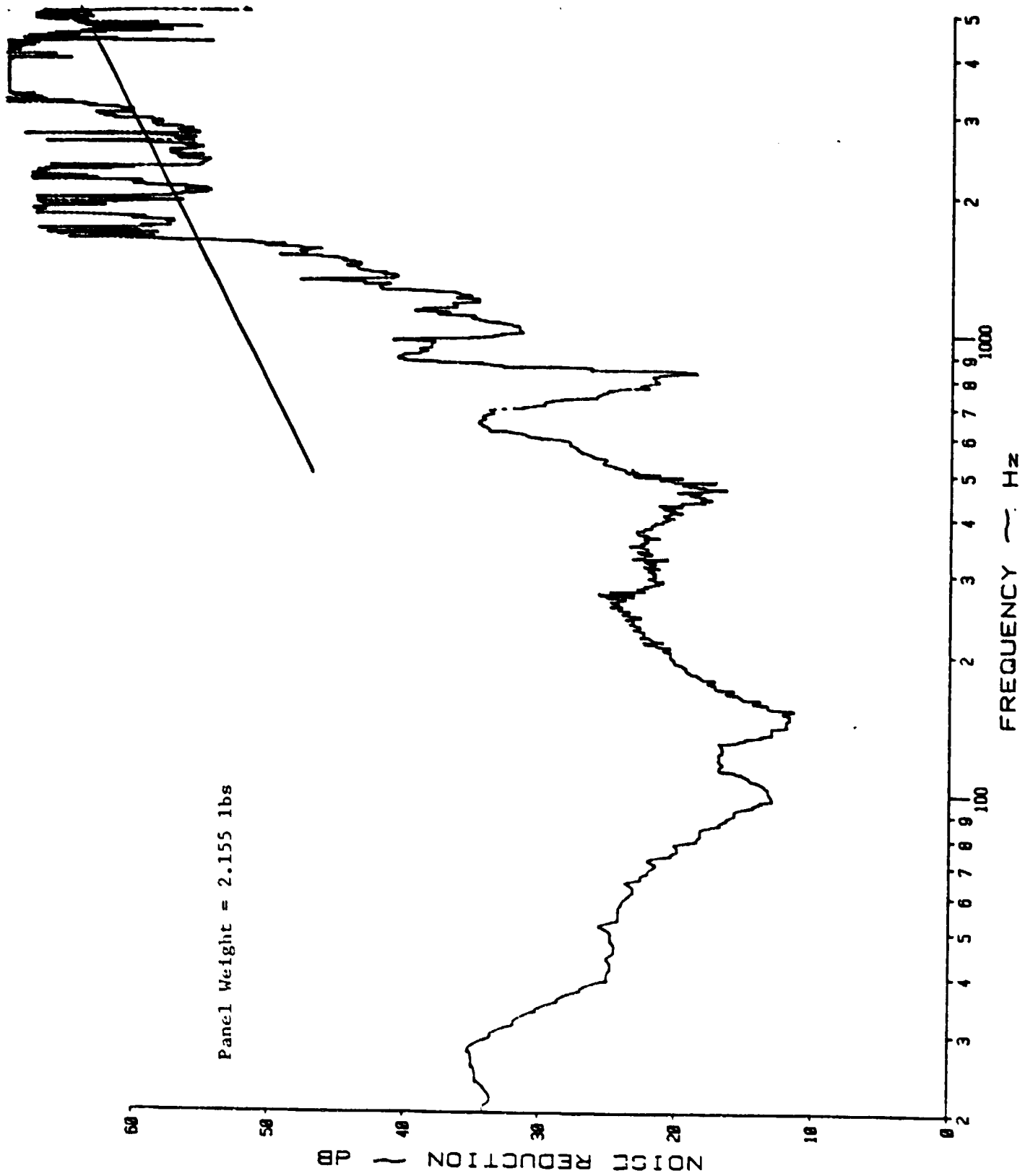

(a) Narrow Band Analysis

Figure B.10: Noise Reduction Characteristics of a Multilayered Panel with Sound Absorption Material of Density 0.082 Slugs/ft^3 when Sandwiched between 0.025 Inch Aluminim Panels

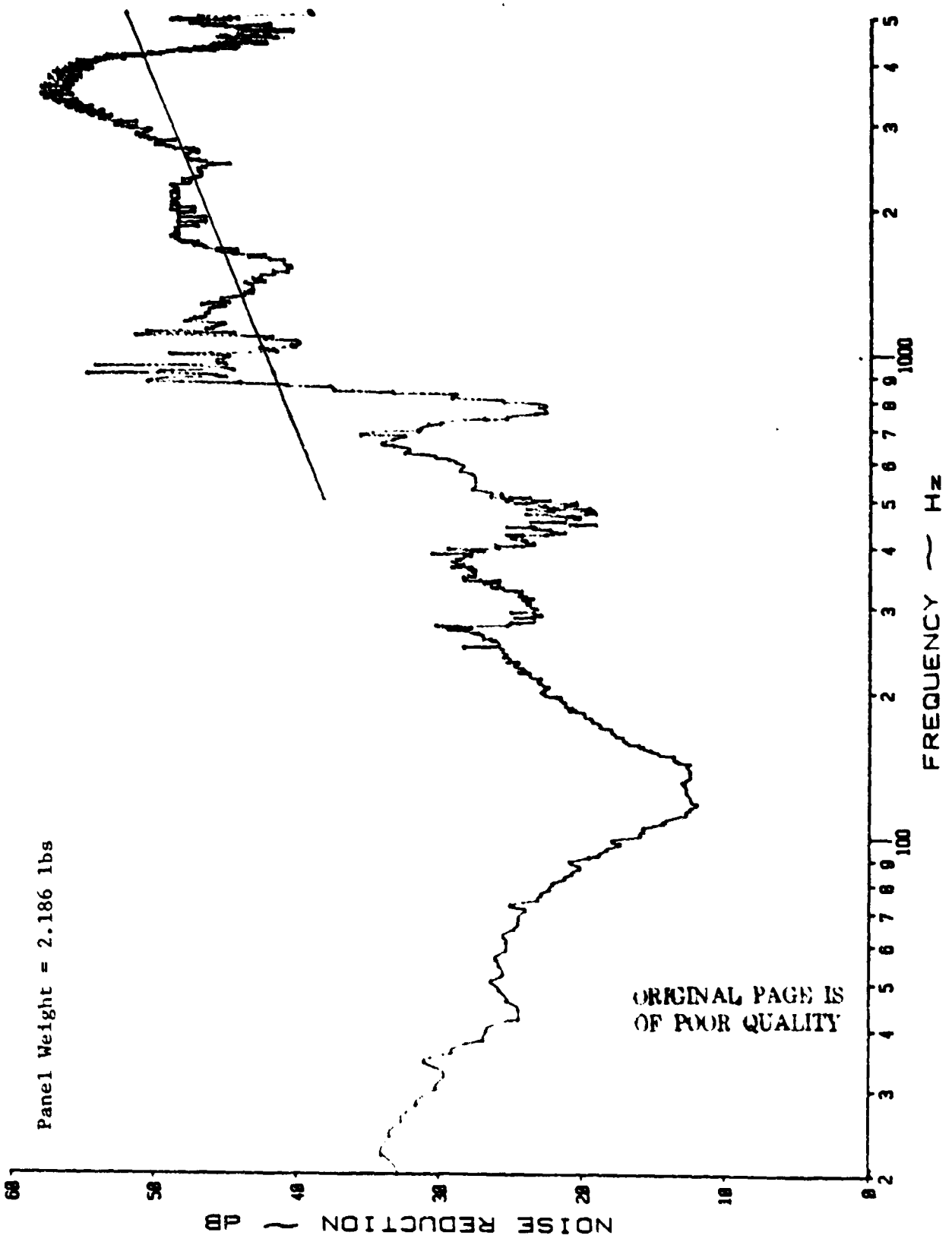

(a) Narrow Band Analysis

Figure B.11: Noise Reduction Characteristics of a Multilayered Panel with Sound Absorption Material of Density 0.091 Slugs/ft^3 when Sandwiched between 0.025 Inch Aluminum Panels

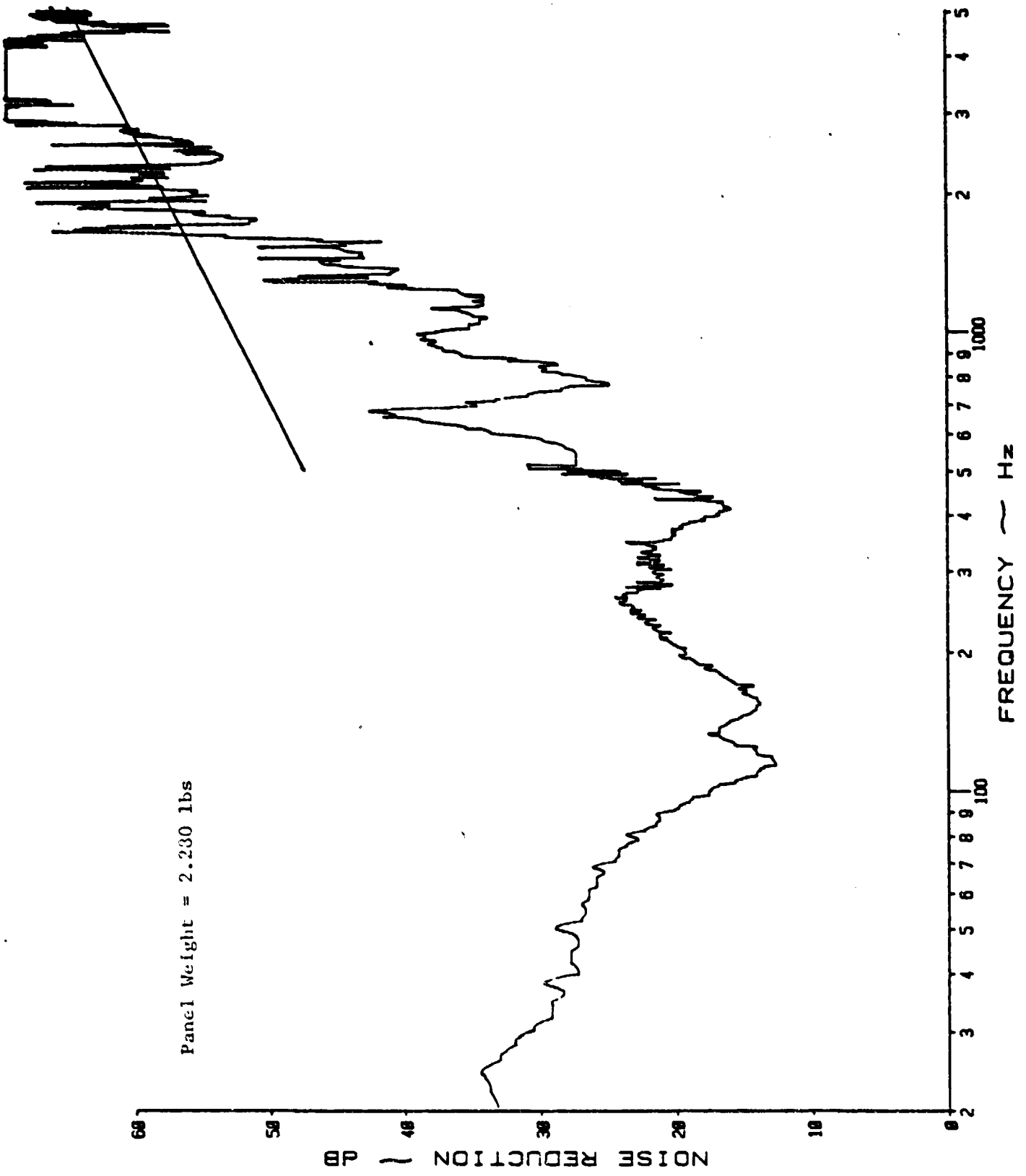

(a) Narrow Band Analysis

Figure B.12: Noise Reduction Characteristics of a Multilayered Panel with Sound Absorption Material of Density 0.114 Slugs/ft^3 when Sandwiched between 0.025 Inch Aluminum Panels

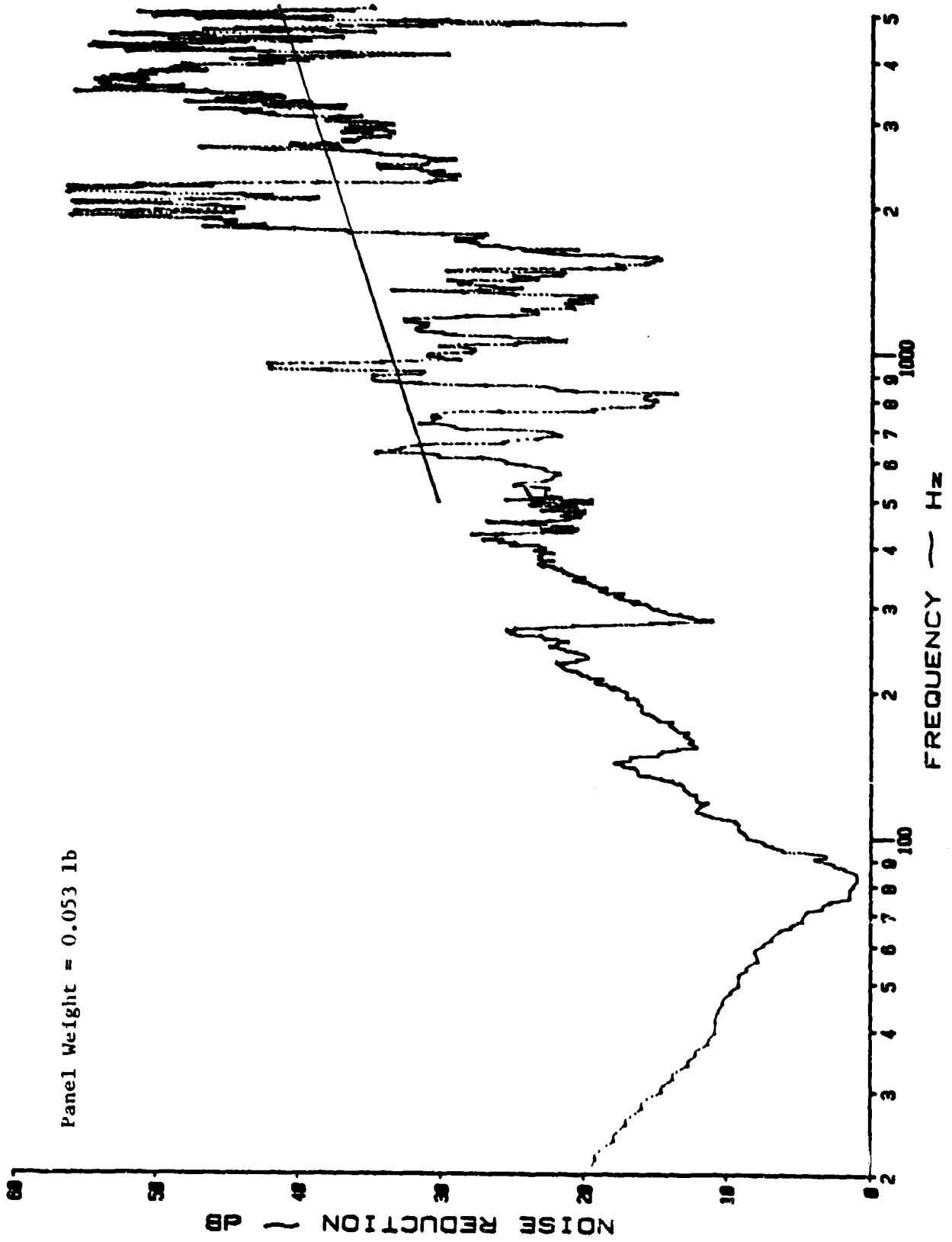

(a) Narrow Band Analysis

Figure B.13: Noise Reduction Characteristics of a Multilayered Panel with 0.25 Inch Thick Soft Polyurethene Foam Attached to 0.025 Inch Aluminum Panel

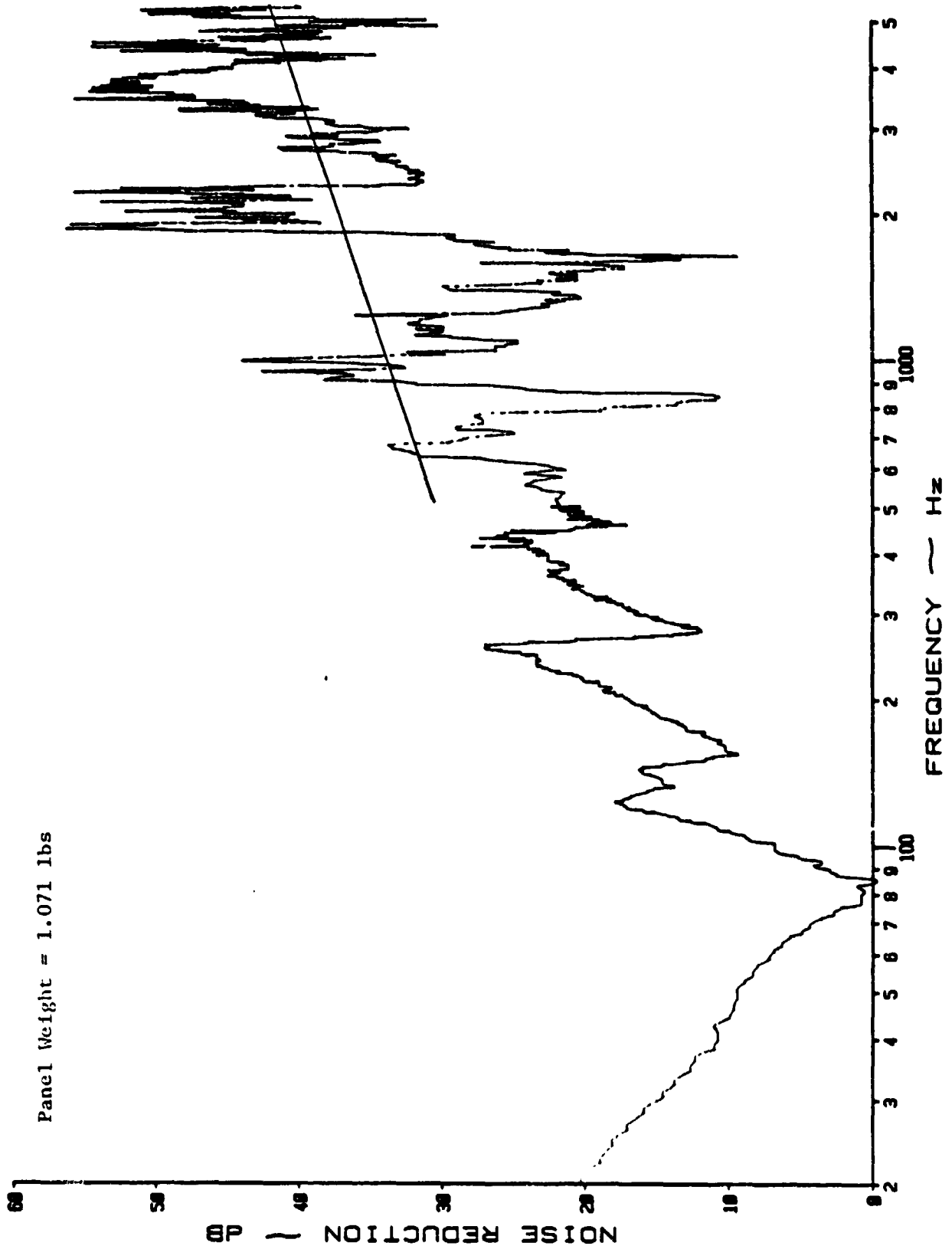

(a) Narrow Band Analysis

Figure B.14: Noise Reduction Characteristics of a Multilayered Panel with 0.5 Inch Thick Soft Polyurethene Foam Attached to 0.025 Inch Aluminum Panel

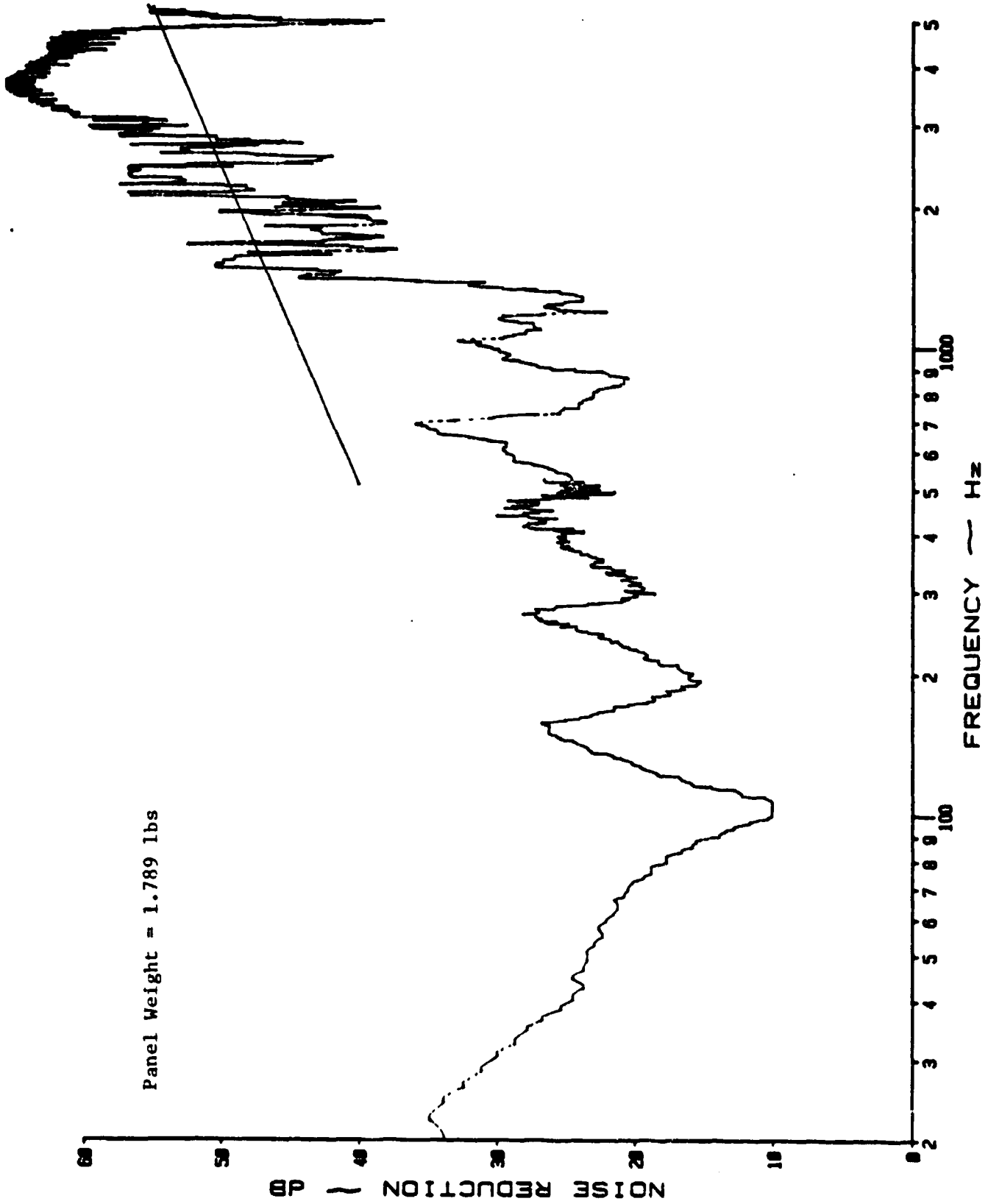

(a) Narrow Band Analysis

Figure B.15: Noise Reduction Characteristics of a Multilayered Panel with 0.25 Inch Thick Foam Sandwiched between Two 0.025 Inch Aluminum Panels

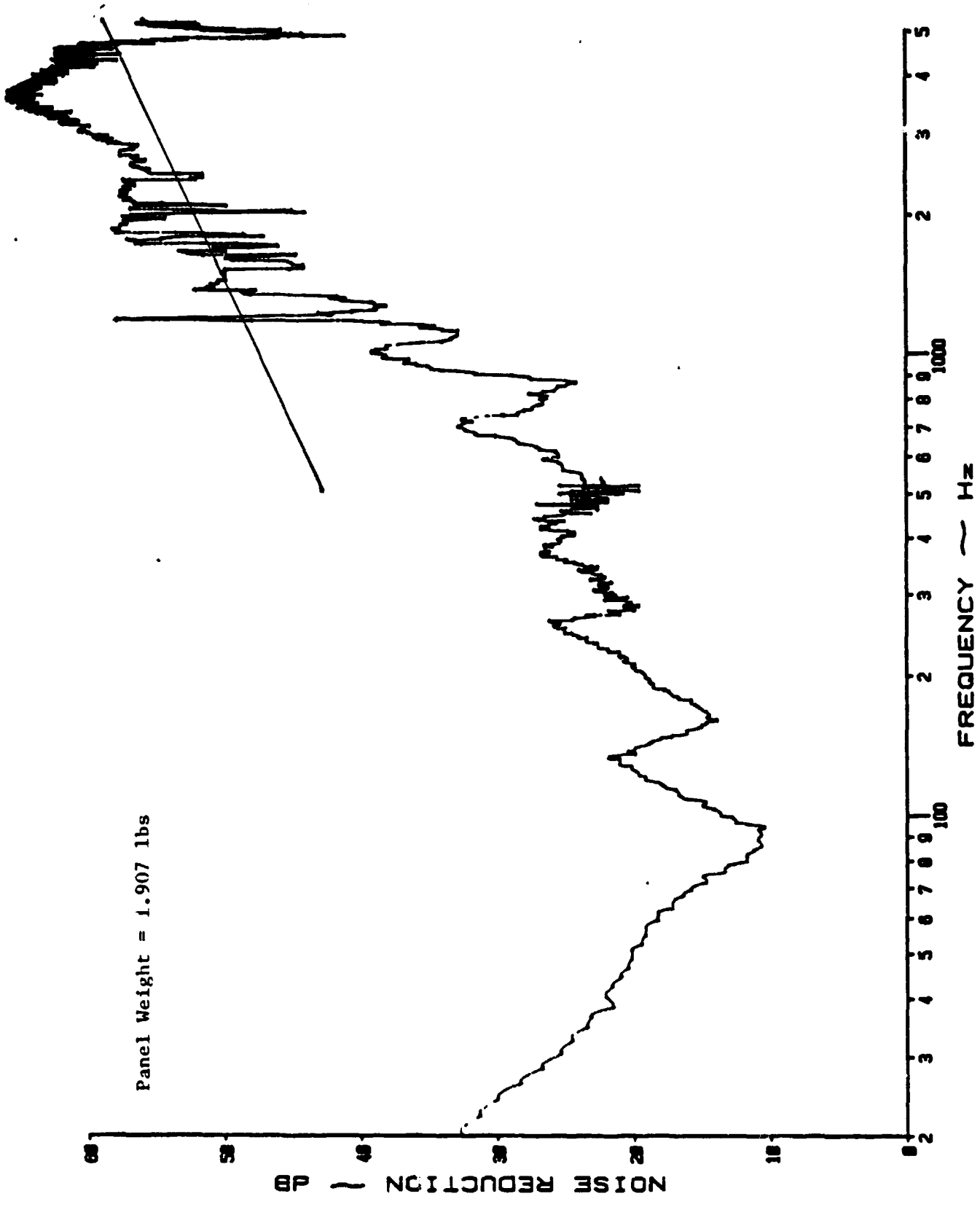

(a) Narrow Band Analysis

Figure B.16: Noise Reduction Characteristics of a Multilayered Panel with 0.5 Inch Thick Foam Sandwiched between Two 0.025 Inch Aluminum Panels

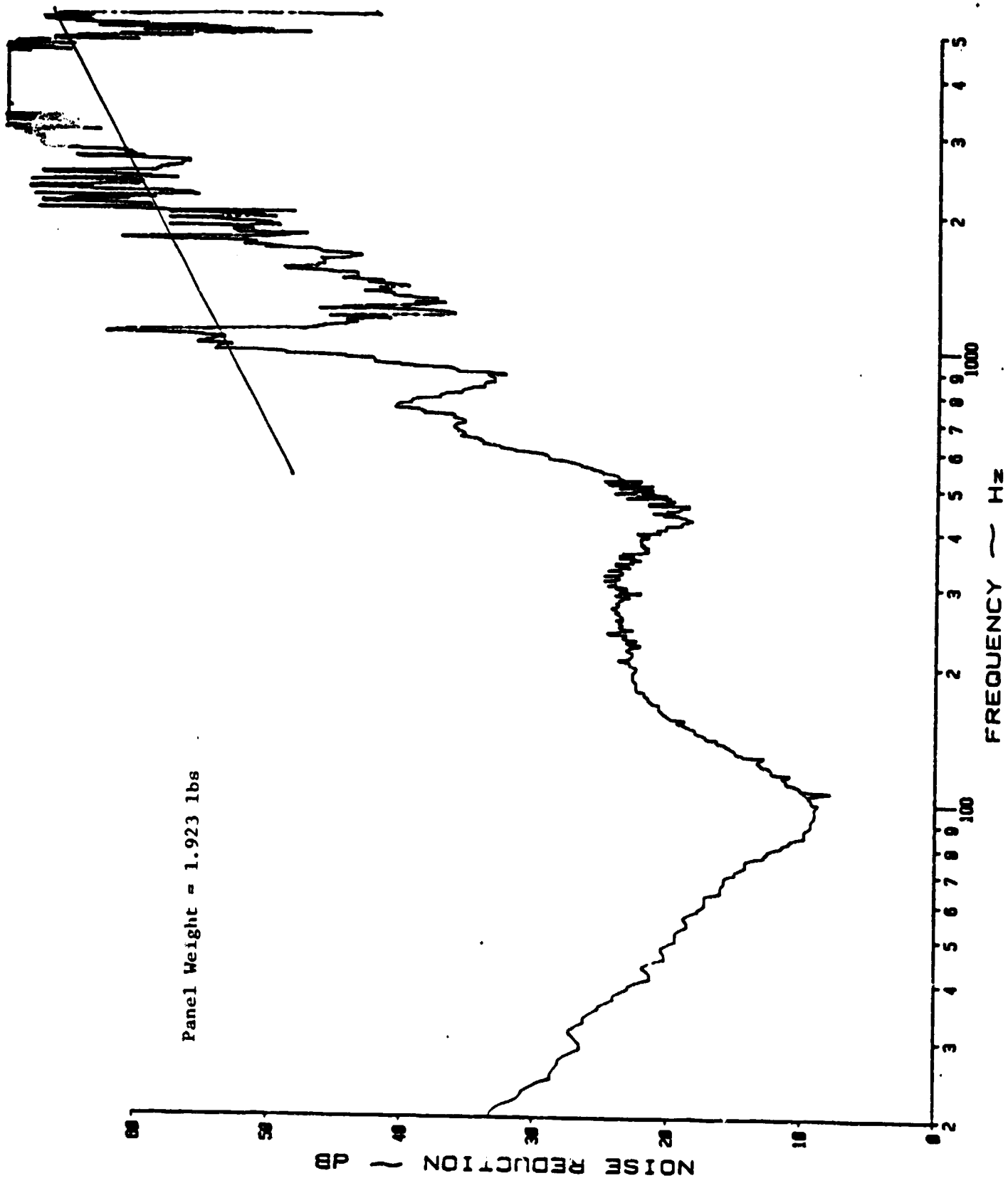

(a) Narrow Band Analysis

Figure B.17: Noise Reduction Characteristics of Fiberglass (1 Inch Thick and 3.5 lb/ft Density) Sandwiched between Two 0.020 Inch Aluminum Panels

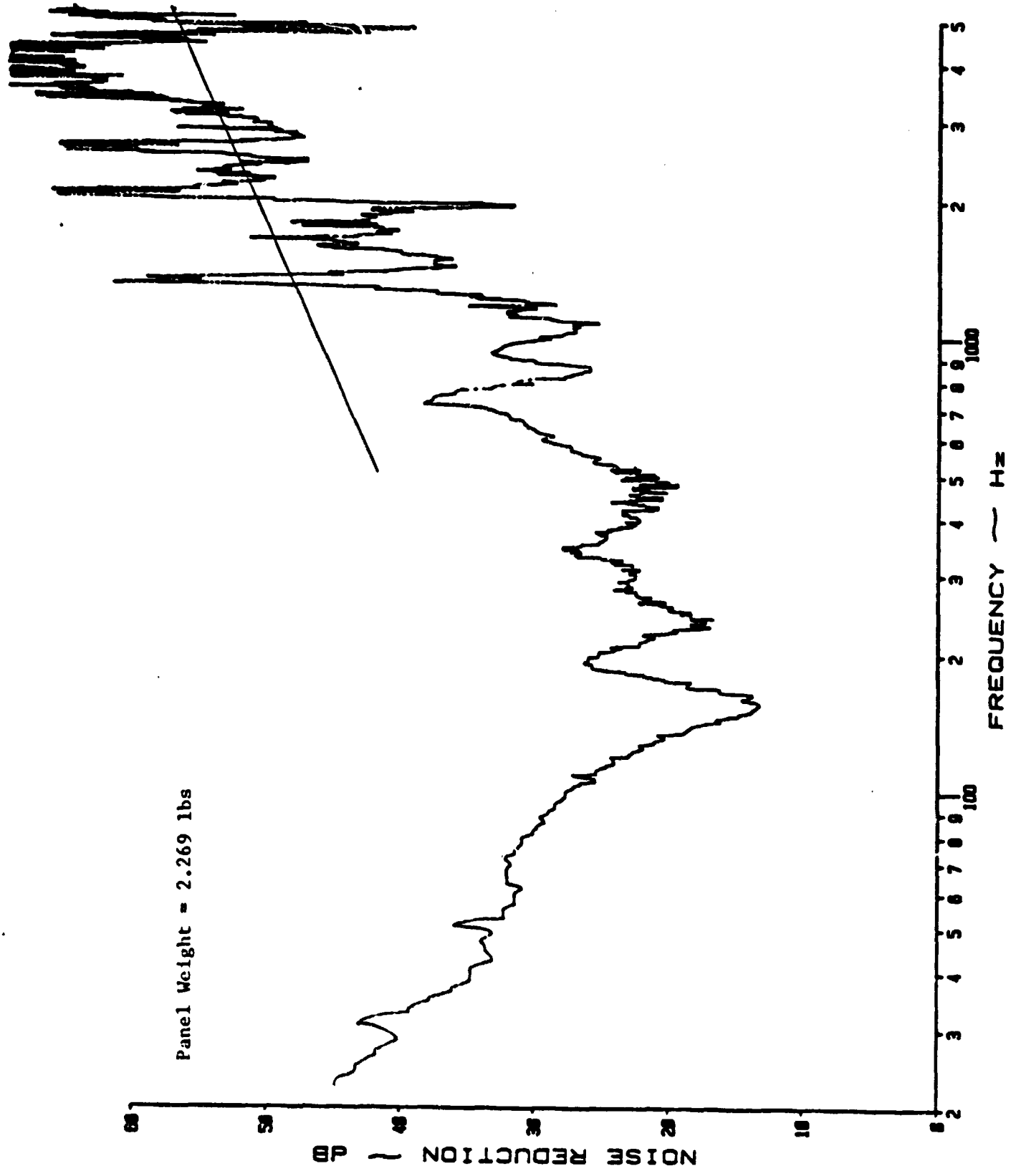

(a) Narrow Band Analysis

Figure B.18: Noise Reduction Characteristics of a Multilayered Panel Built of 0.025 Inch Aluminum Panel, 1/4 Inch P.V.C.-Based Foam of Density 0.2253 Slugs/ft^3, 1 Inch Thick Sound Absorption Material of Density 0.082 Slugs/ft^3 and 0.16 Inch Aluminum Panel

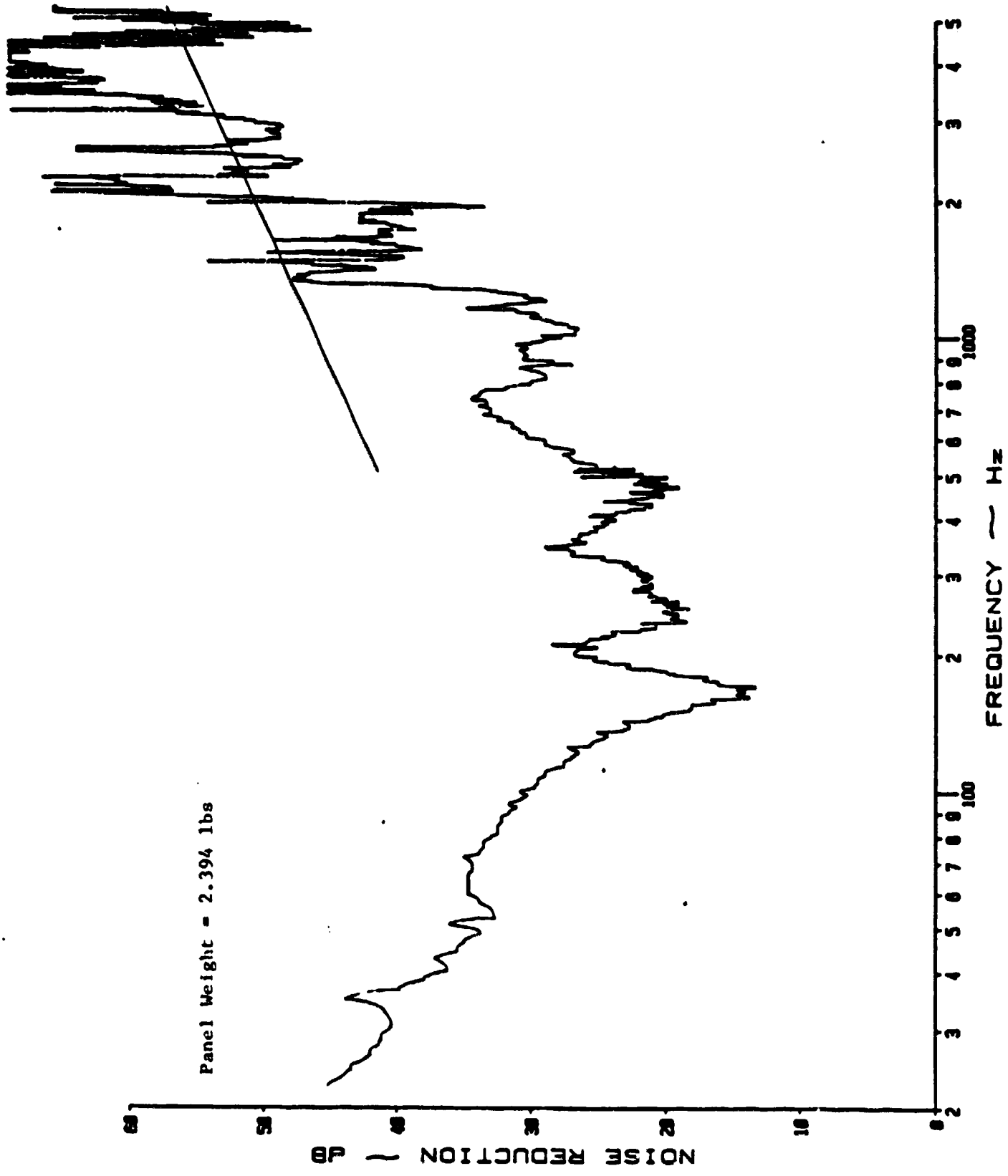

(a) Narrow Band Analysis

Figure B.19: Noise Reduction Characteristics of a Multilayered Panel Built of 0.025 Inch Aluminum Panel, 1/4 Inch P.V.C.-Based Foam of Density 0.2253 Slugs/ft^3, 1 Inch Thick Sound Absorption Material of Density 0.114 Slugs/ft^3 and 0.016 Inch Aluminum Panel

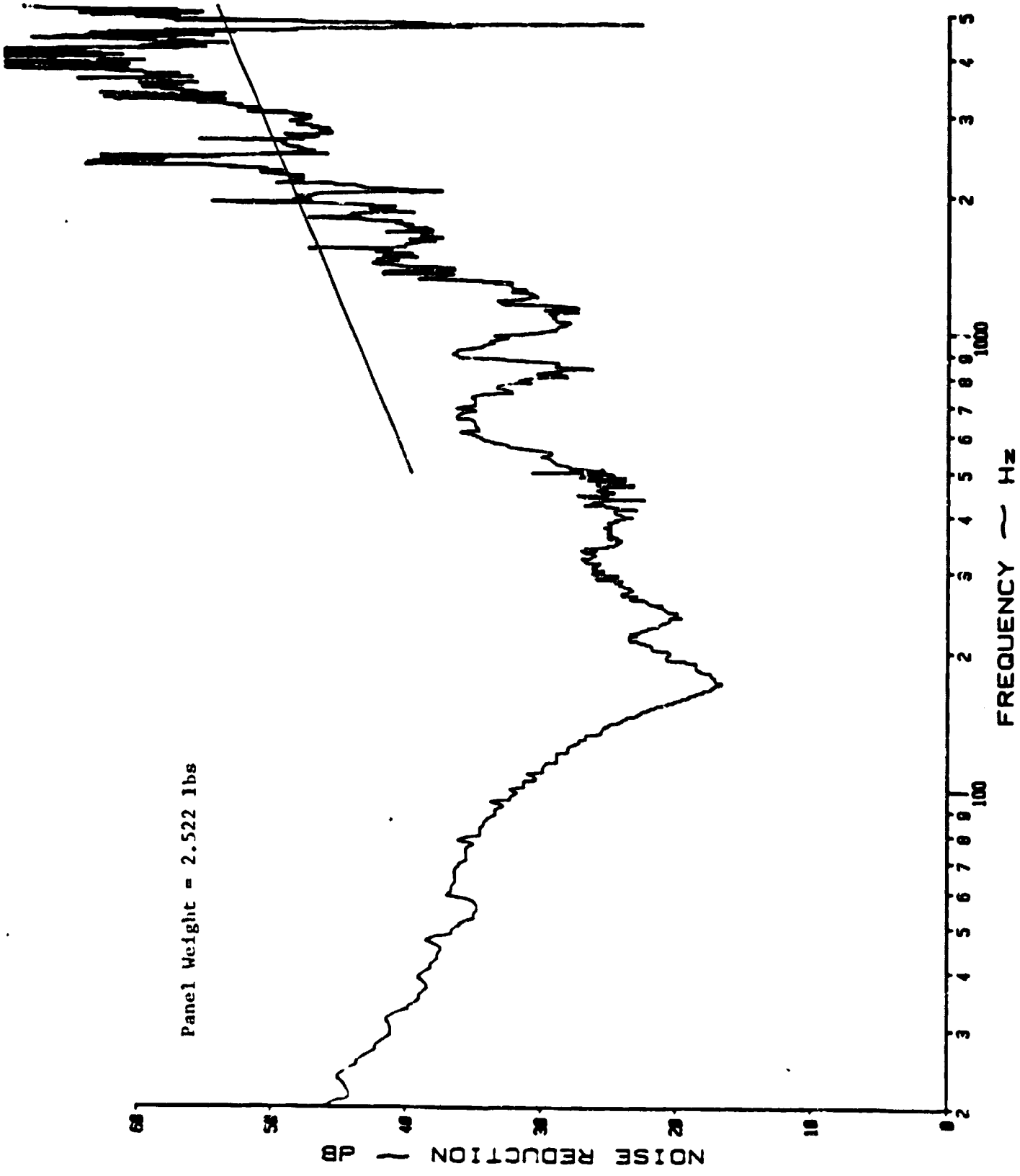

(a) Narrow Band Analysis

Figure B.20: Noise Reduction Characteristics of a Multilayered Panel Built of 0.025 Inch Aluminum Panel, 1/4 Inch P.V.C.-Based Foam of Density 0.3594 Slugs/ft^3, 1 Inch Thick Sound Absorption Material of Density 0.082 Slugs/ft^3 and 0.016 Inch Aluminum Panel

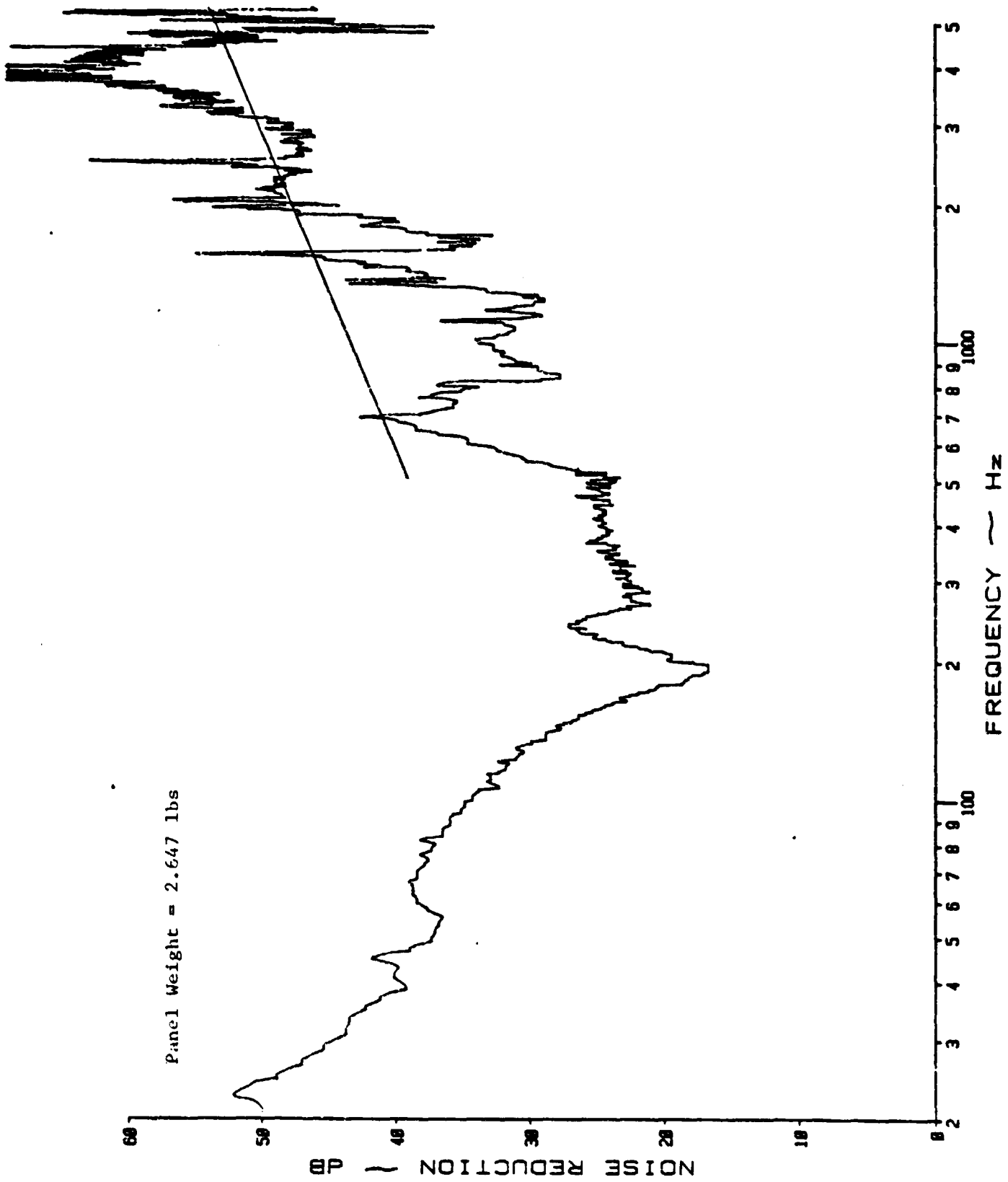

(a) Narrow Band Analysis

Figure 3.21: Noise Reduction Characteristics of a Multilayered Panel Built of 0.025 Inch Aluminum Panel, 1/4 Inch P.V.C.-Based Foam of Density 0.2253 Slugs/ft^3 and 0.016 Inch Aluminum Panel

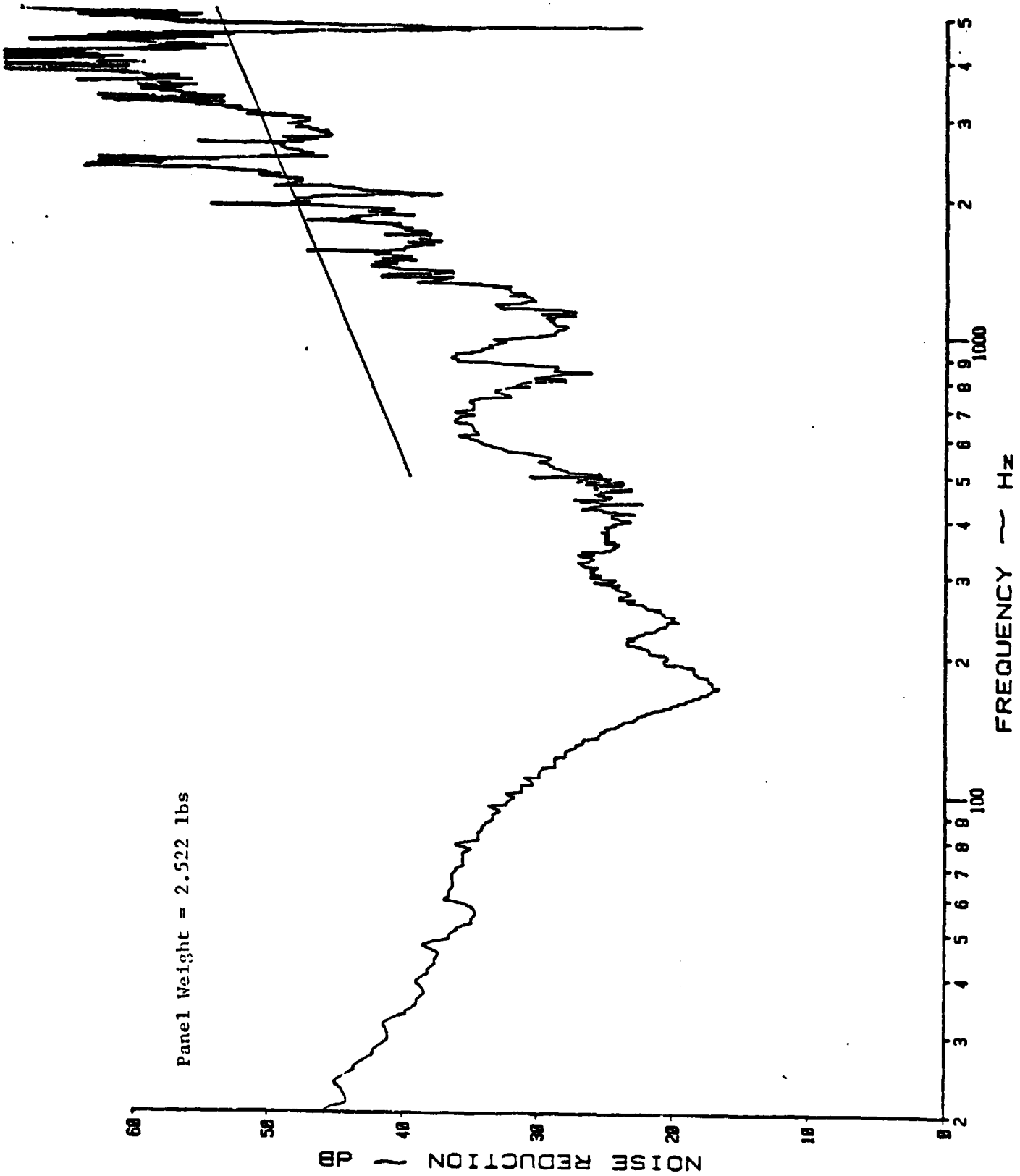

(a) Narrow Band Analysis

Figure B.22: Noise Reduction Characteristics of a Multilayered Panel, Built of 0.025 Inch Aluminum Panel, 1/4 Inch Rigid Foam of Density 0.03594 Slugs/ft^3, 1 Inch Thick Sound Absorption Material of Density 0.082 Slugs/ft^3 and 0.016 Inch Aluminum Panel

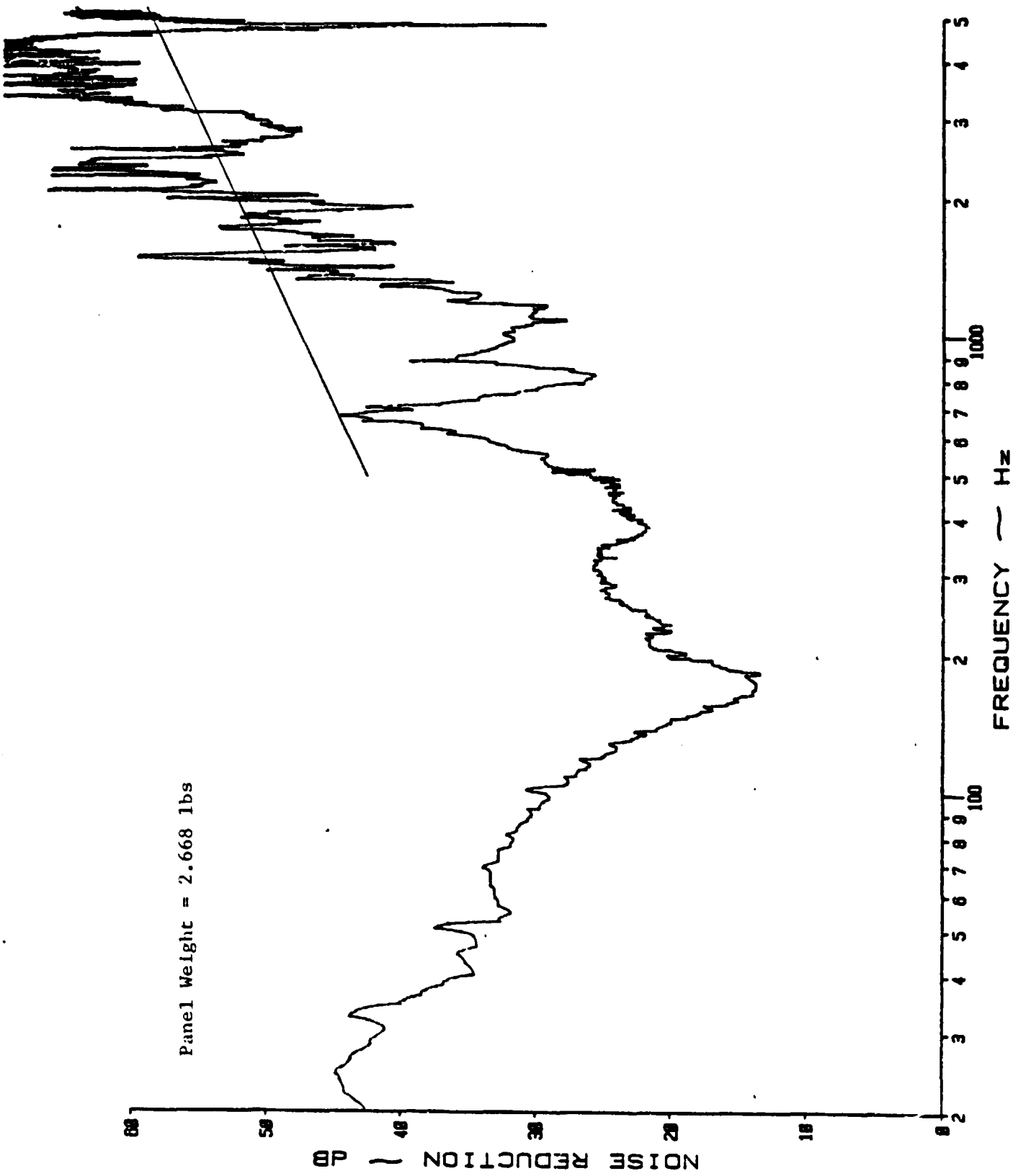

(a) Narrow Band Analysis

Figure B.23: Noise Reduction Characteristics of a Multilayered Panel Built of 0.025 Inch Aluminum Panel, 1/4 Inch Rigid Foam of Density 0.3594 Slugs/ft^3, 1 Inch Thick Sound Absorption Material of Density 0.082 Slugs/ft^3 and 0.020 Inch Aluminum Panel

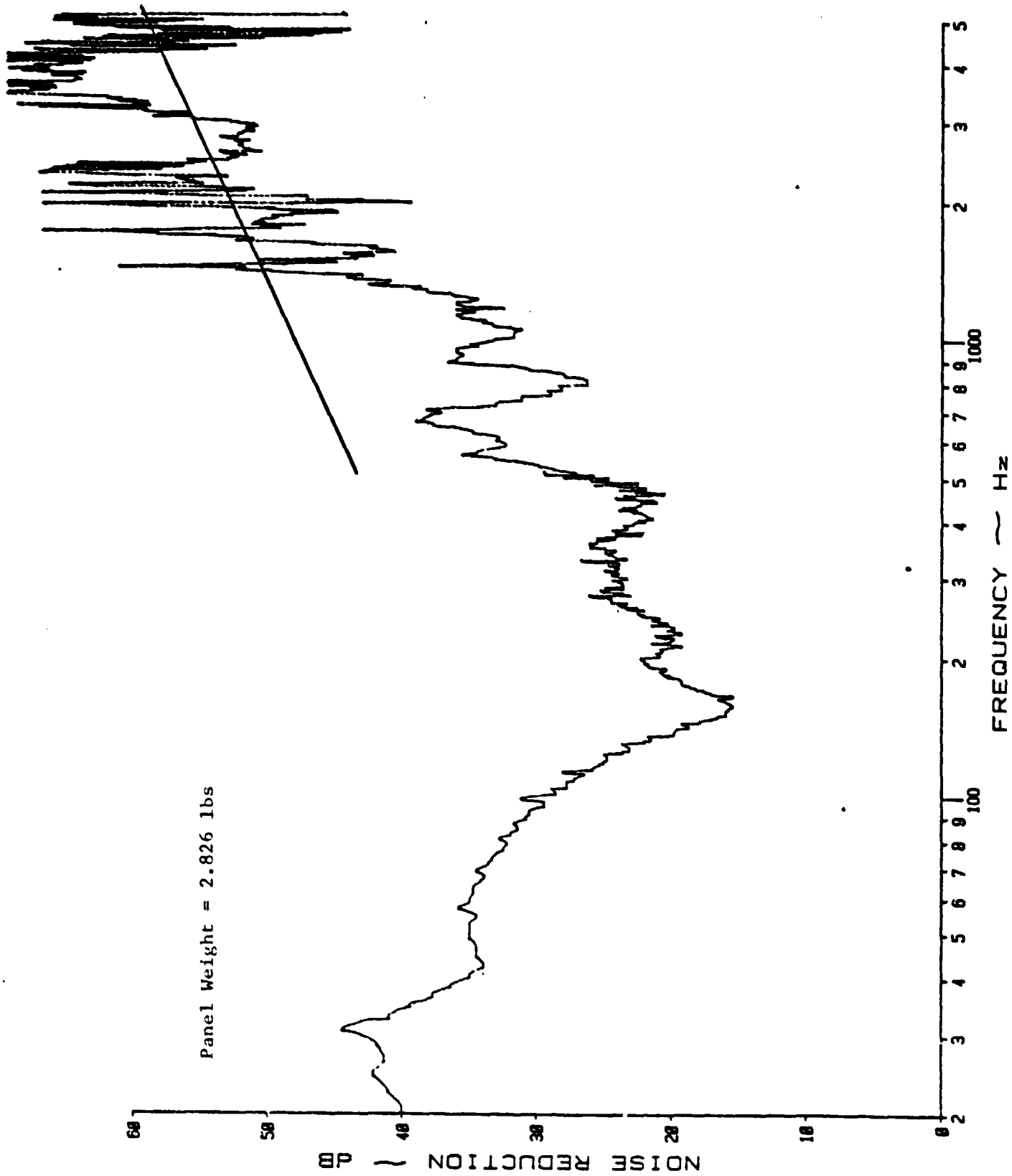

(a) Narrow Band Analysis

Figure B.24: Noise Reduction Characteristics of a Multilayered Panel Built of 0.025 Inch Aluminum Panel, 1/4 Inch Rigid Foam of Density 0.3594 Slugs/ft^3, 1 Inch Thick Sound Absorption Material of Density 0.082 Slugs/ft^3 and 0.025 Inch Aluminum Panel

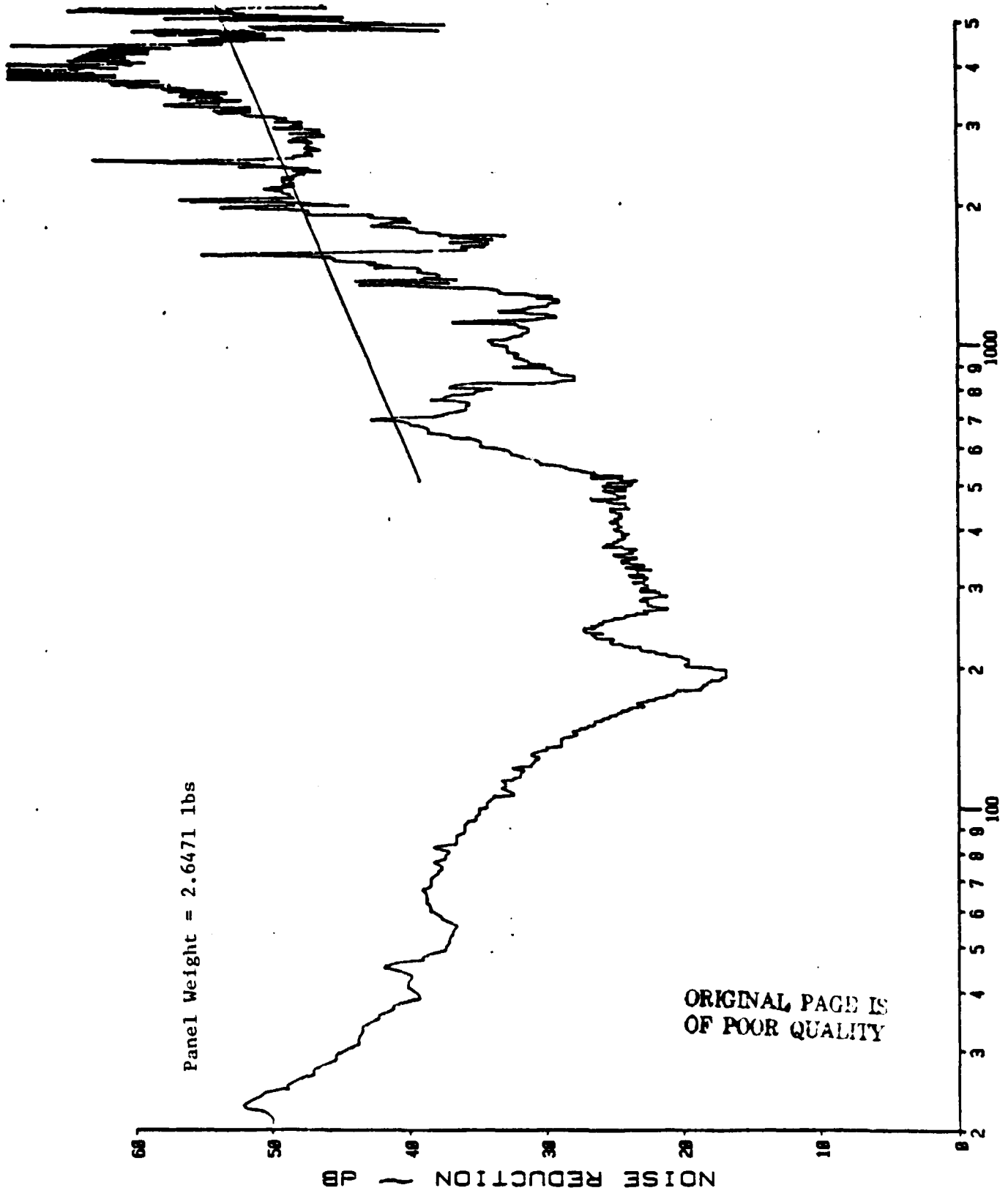

(a) Narrow Band Analysis

Figure B.25: Noise Reduction Characteristics of a Multilayered Panel Built of 0.025 Inch Aluminum Panel, 1/4 Inch Rigid Foam of Density 0.3594 Slugs/ft^3, 1 Inch Thick Sound Absorption Material of Density 0.114 Slugs/ft^3 and 0.016 Inch Aluminum Panel

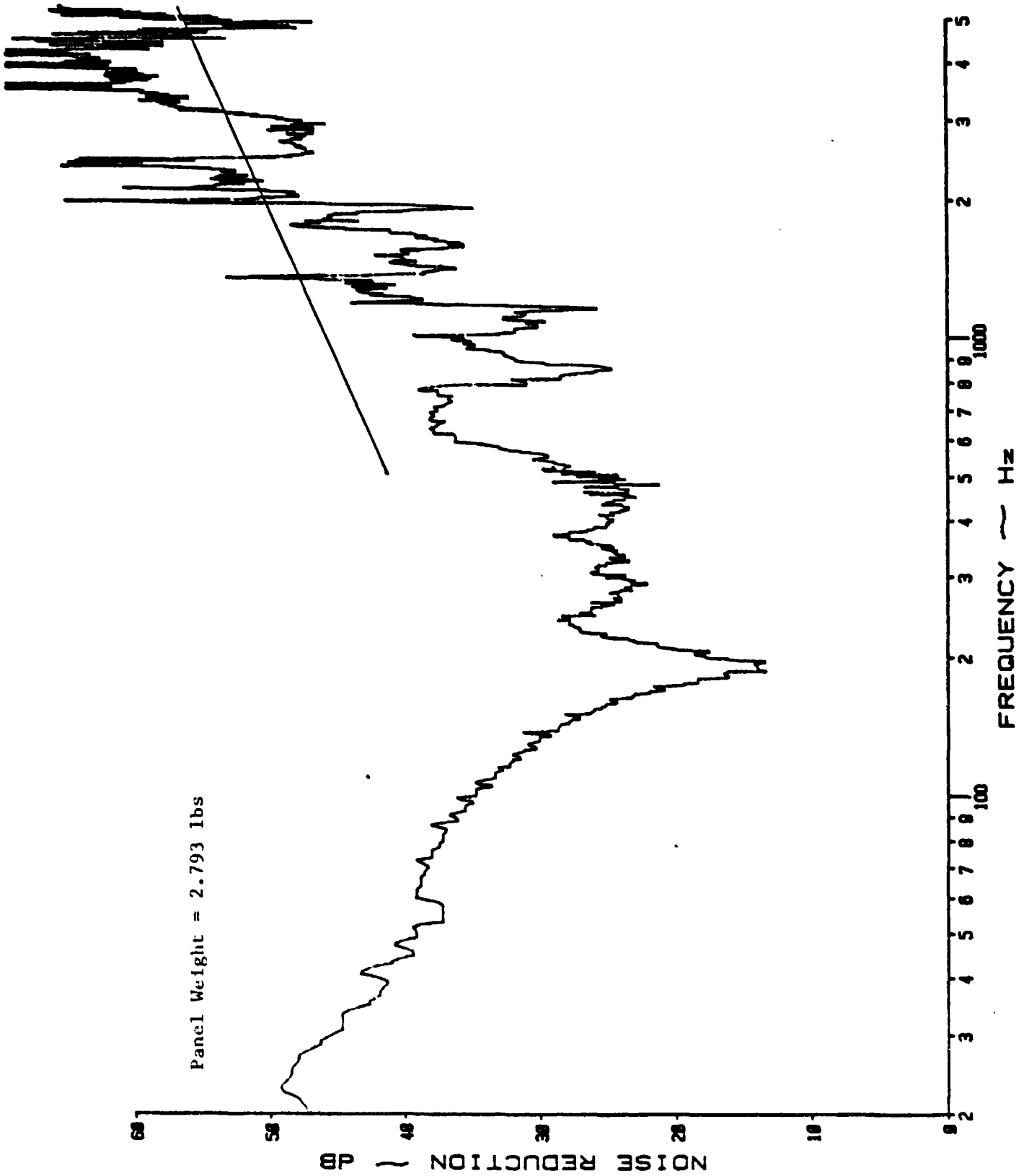

(a) Narrow Band Analysis

Figure B.26: Noise Reduction Characteristics of a Multilayered Panel Built of 0.025 Inch Aluminum Panel, 1/4 Inch Rigid Foam of Density 0.3594 Slugs/ft^3, 1 Inch Thick Sound Absorption Material of Density 0.114 Slugs/ft^3 and 0.020 Inch Aluminum Panel

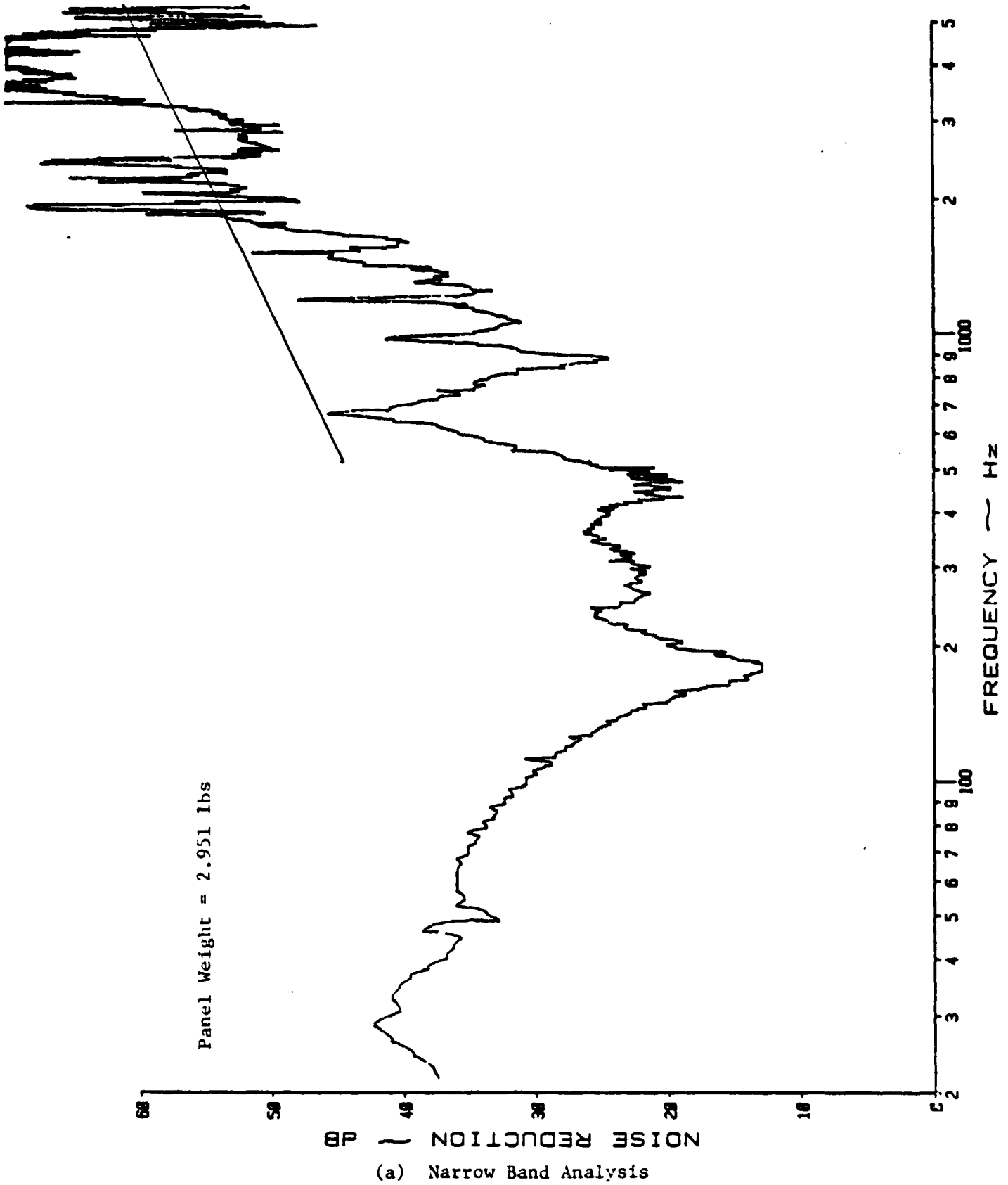

(a) Narrow Band Analysis

Figure B.27: Noise Reduction Characteristics of a Multilayered Panel Built of 0.025 Inch Aluminum Panel, 1/4 Inch Rigid Foam of Density 0.3594 Slugs/ft^3, 1 Inch Thick Sound Absorption Material of Density 0.114 Slugs/ft^3 and 0.025 Inch Aluminum Panel

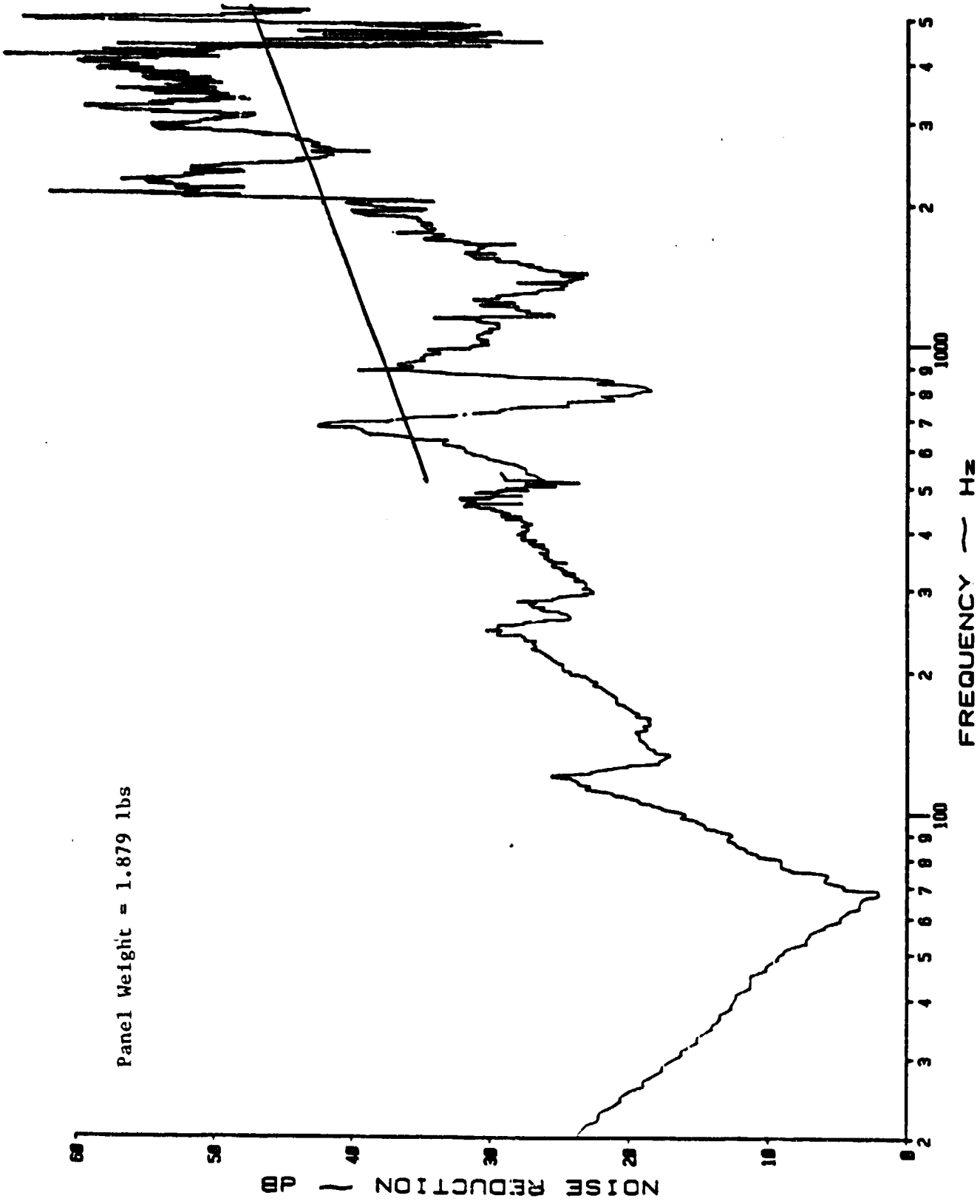

(a) Narrow Band Analysis

Figure B.28: Noise Reduction Characteristics of a Multilayered Panel Built of 0.025 Inch Aluminum Panel + Rigid P.V.C. Foam + 1/16 Inch Airspace + 0.025 Inch Aluminum Panel

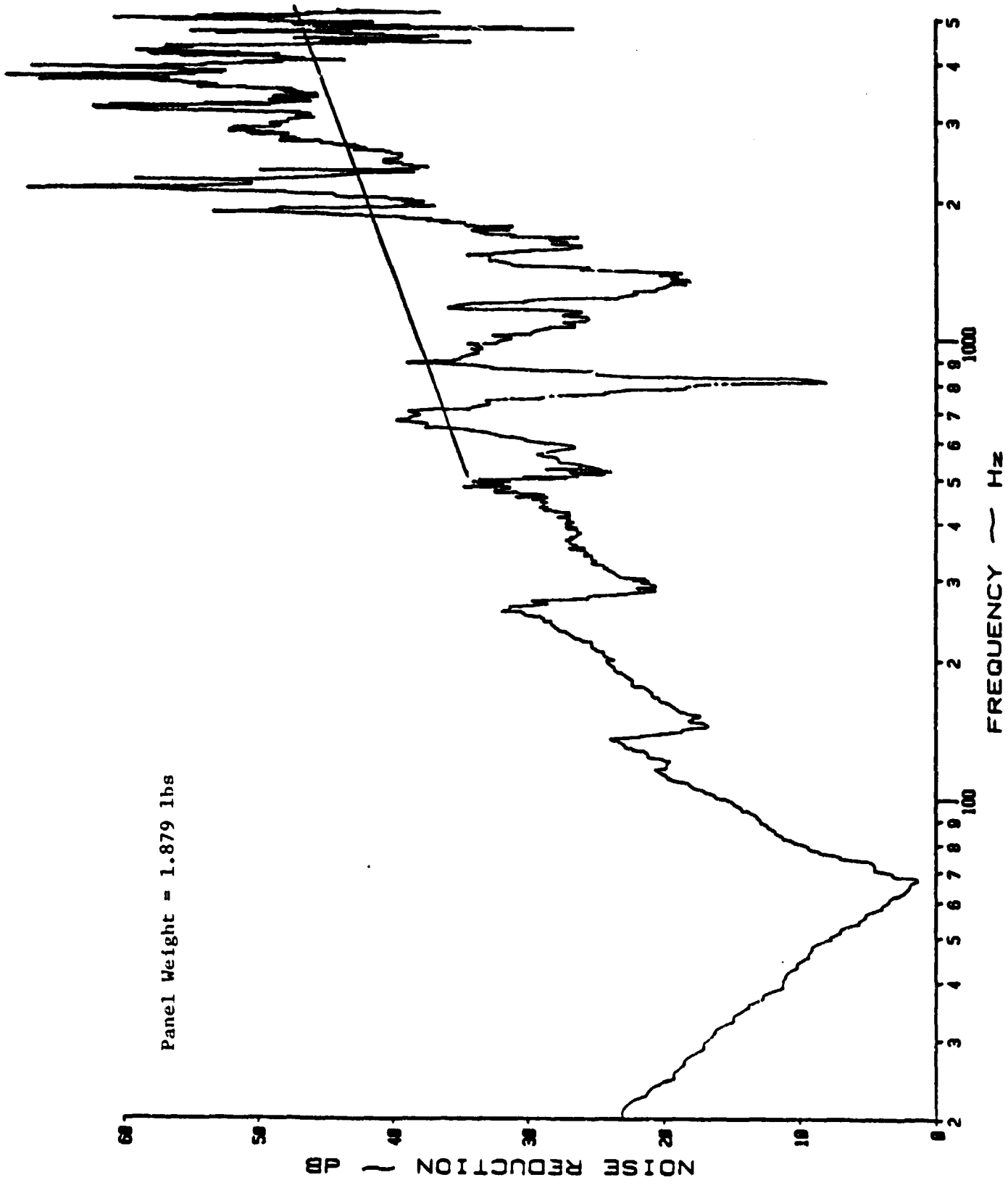

(a) Narrow Band Analysis

Figure B.29: Noise Reduction Characteristics of a Multilayered Panel Built of 0.025 Inch Aluminum Panel + Rigid P.V.C. Foam + 3/16 Inch Airspace + 0.025 Inch Aluminum Panel

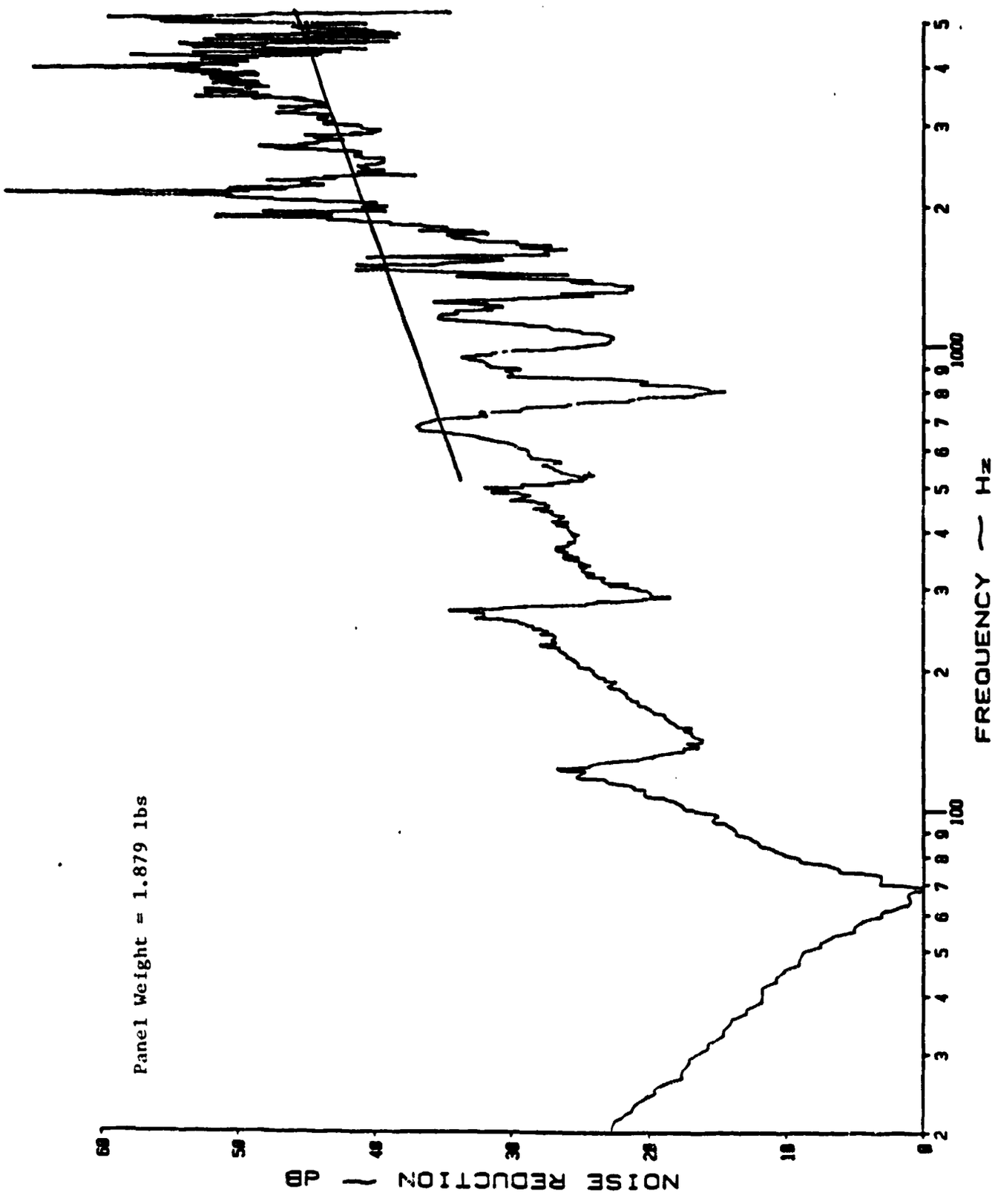

(a) Narrow Band Analysis

Figure B.30: Noise Reduction Characteristics of a Multilayered Panel Built of 0.025 Inch Aluminum Panel + Rigid P.V.C. Foam + 3/8 Inch Airspace + 0.025 Inch Aluminum Panel

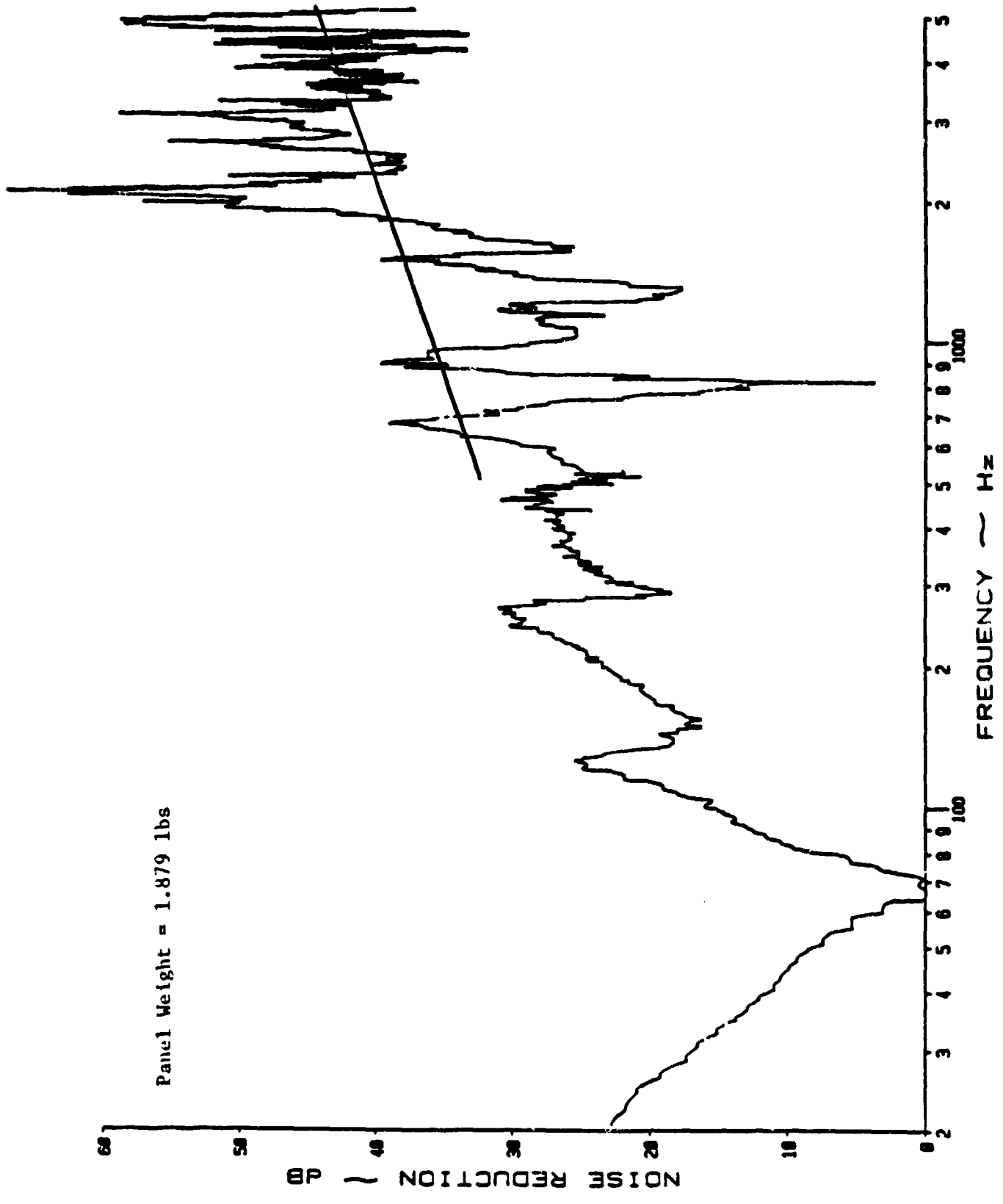

(a) Narrow Band Analysis

Figure B.31: Noise Reduction Characteristics of a Multilayered Panel Built of 0.025 Inch Aluminum Panel + Rigid P.V.C. Foam + 3/4 Inch Airspace + 0.025 Inch Aluminum Panel

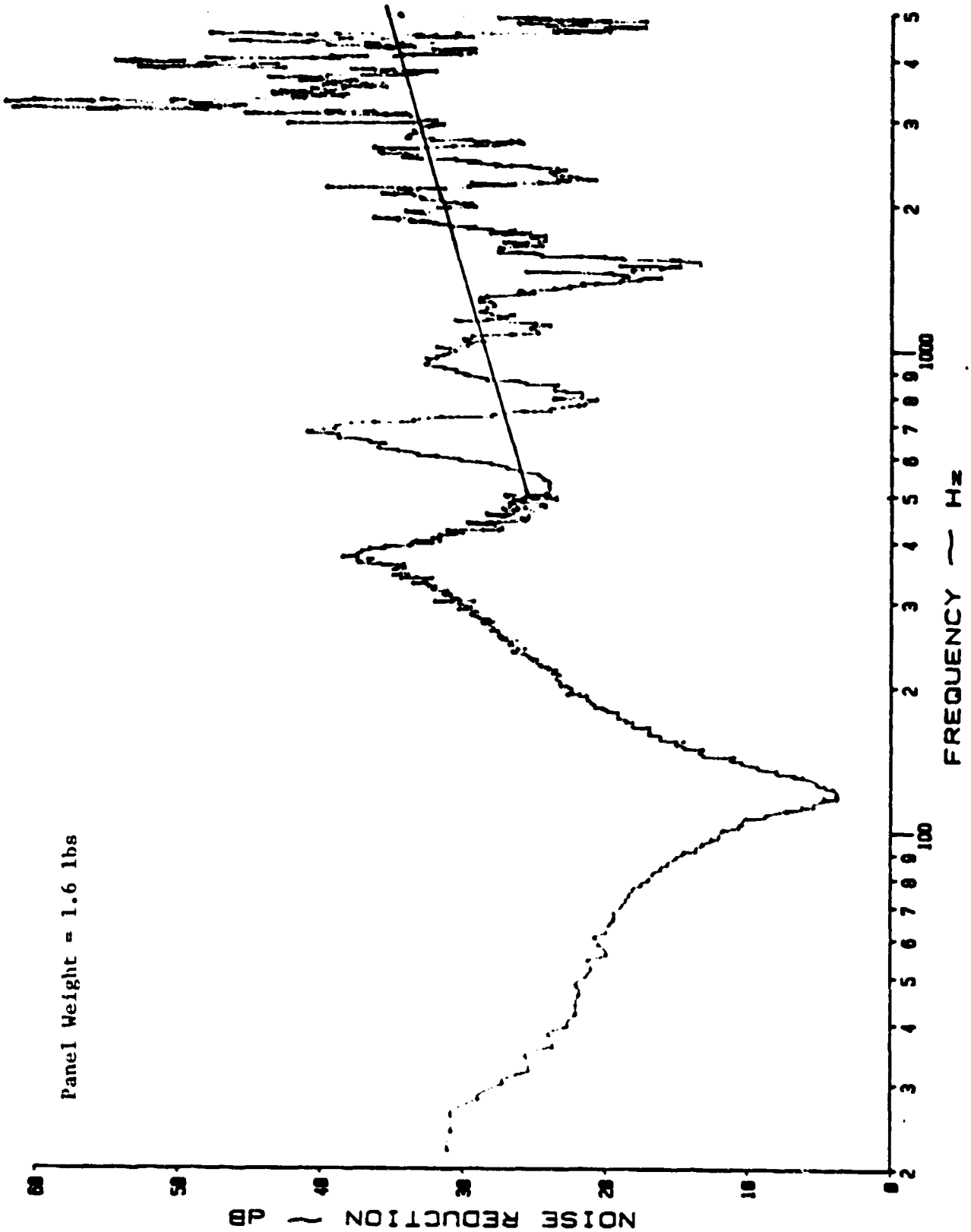

(a) Narrow Band Analysis

Figure B.32: Noise Reduction Characteristics of Honeycomb Panel with Aluminum Core (1/8 Inch Thick) and Fiberglass Facings

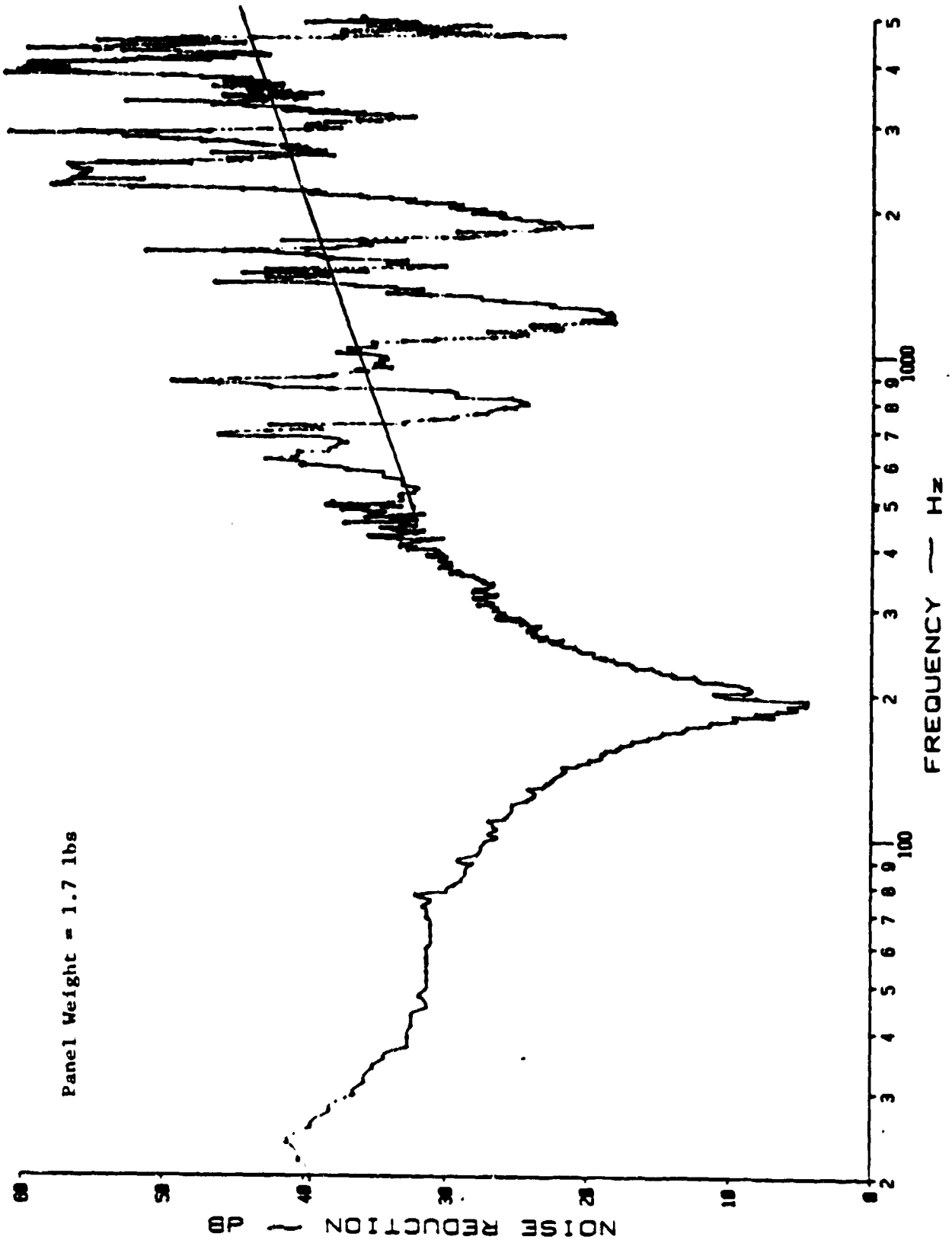

(a) Narrow Band Analysis

Figure B.33: Noise Reduction Characteristics of Honeycomb Panel with Aluminum Core (1/4 Inch Thick) and Fiberglass Facings

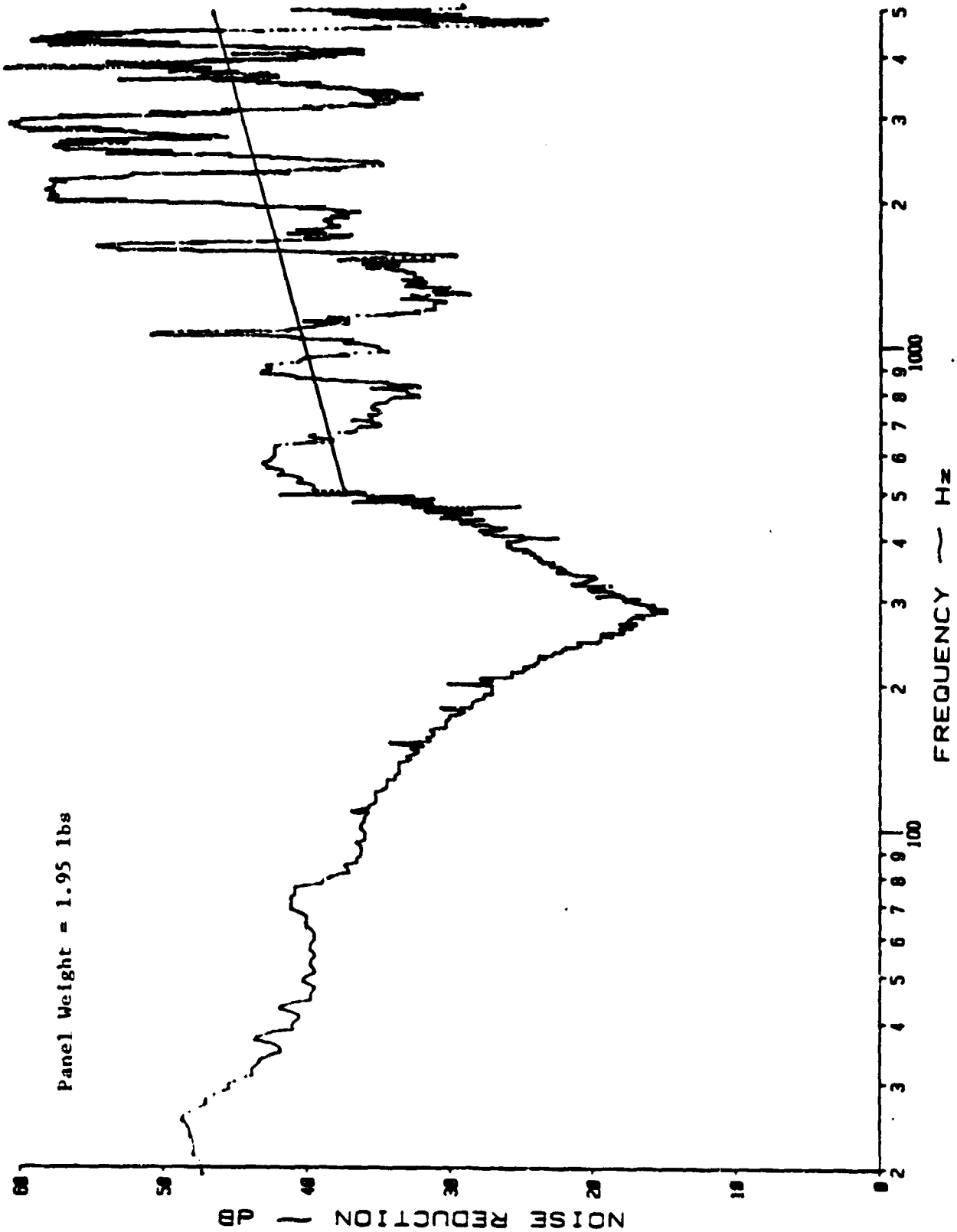

(a) Narrow Band Analysis

Figure B.34: Noise Reduction Characteristics of Honeycomb Panel with Aluminum Core (1/2 Inch Thick) and Fiberglass Facings

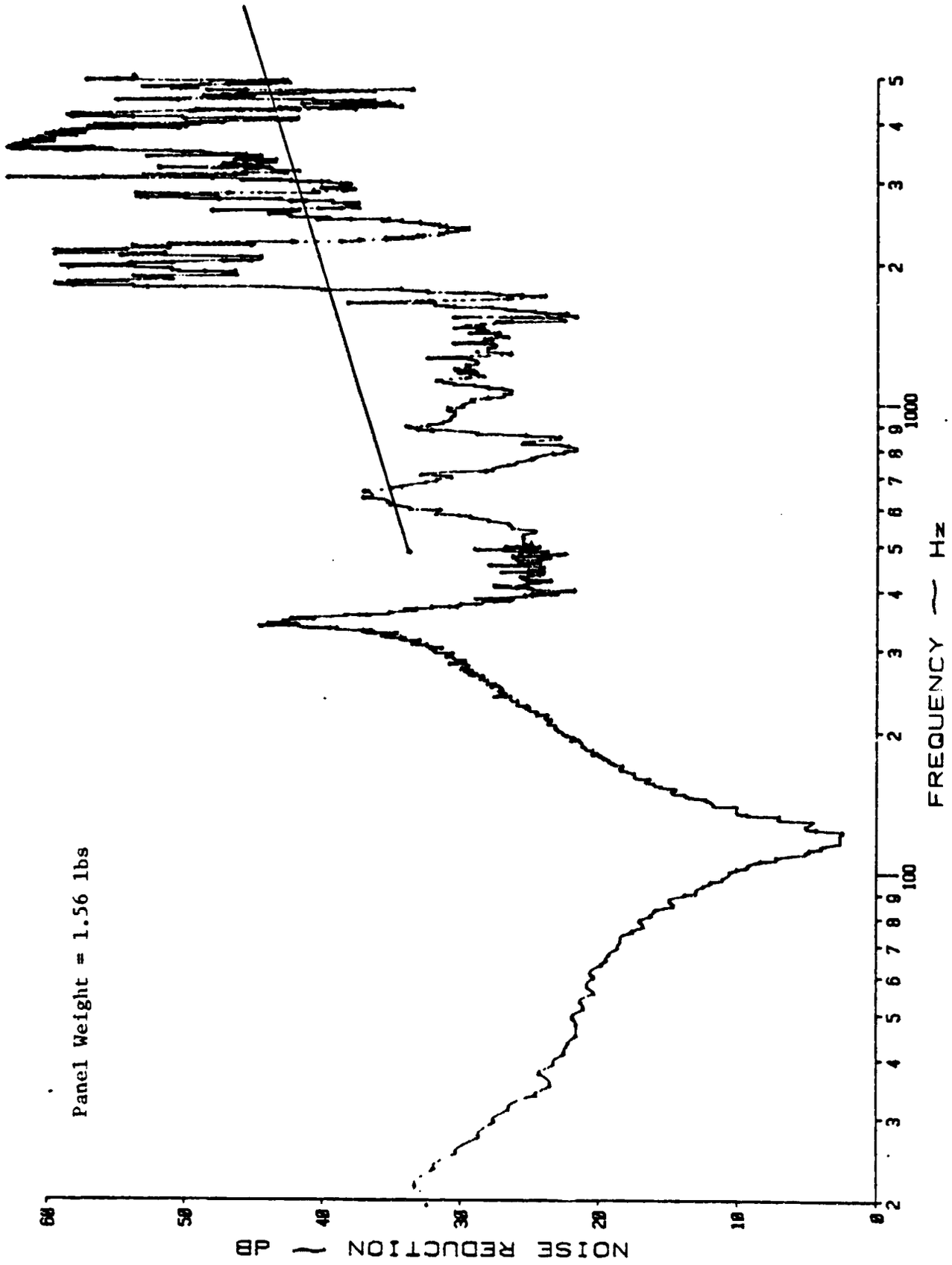

(a) Narrow Band Analysis

Figure B.35: Noise Reduction Characteristics of Honeycomb Panel with Nomex Core (1/8 Inch Thick) and Fiberglass Facings

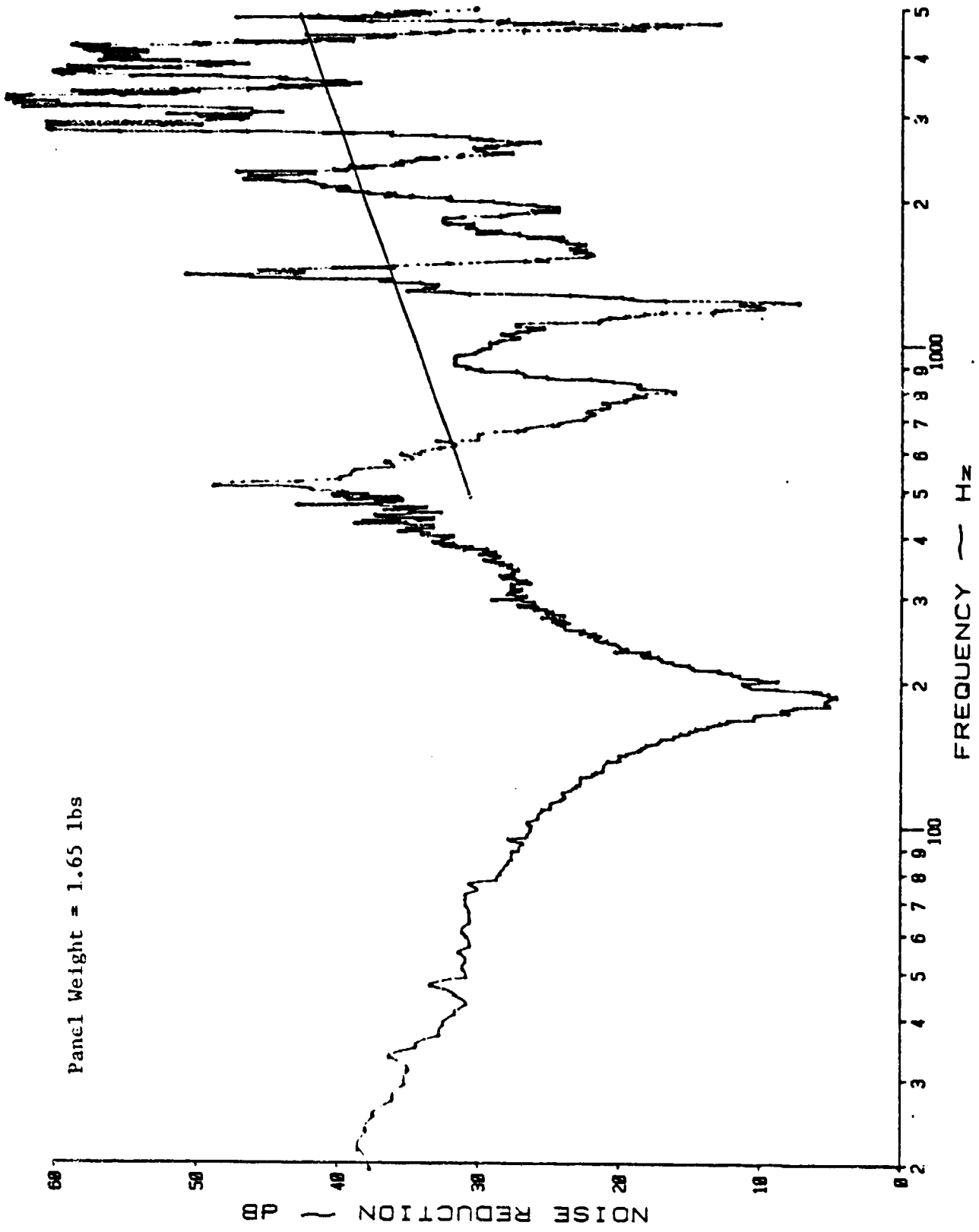

(a) Narrow Band Analysis

Figure B.36: Noise Reduction Characteristics of Honeycomb Panel with Nomex Core (1/4 Inch Thick) and Fiberglass Facings

APPENDIX C

CALCULATION OF COMPLEX IMPEDANCE AND PROPAGATION CONSTANT OF POROUS MATERIAL

Reference 8 presents a method to calculate the complex impedance and propagation constant of porous material, given its material properties. In general, both the impedance and propatation constants are complex and are functions of the frequency. The method given in Reference 8 depends upon whether the material is semirigid or porous.

C.1 CALCULATION OF CHARACTERISTIC IMPEDANCE AND PROPAGATION CONSTANT OF SEMIRIGID MATERIALS BASED ON EMPIRICAL DATA (REFERENCE 8)

Values of the characteristic impedance Z_0 and propagation constant b may be presented as universal functions of the dimensionless parameter $\rho f/R_1$ where ρ is the gas density, f is the frequency, and R_1 is the flow resistivity. A summary of the principal results valid for semirigid materials is given in Table C.1.

Table C.1 Empirical Power Law Approximations for the Complex Characteristic Impedance Z_0 and Complex Propagation Constant b of Semirigid Materials

Characteristic Impedance	Propagation Constant
$Z_0 = R + jX$	$b = \alpha + j(2\pi/\lambda_M) = \alpha + j\beta$
$R = \rho c[1 + 0.0571(\rho f/R_1)^{-0.754}]$	$\alpha = (\omega/c)[0.189(\rho f/R_1)^{-0.595}]$
$X = -\rho c[0.0870(\rho f/R_1)^{-0.732}]$	$\beta = (\omega/c)[1 + 0.0978(\rho f/R_1)^{-0.700}]$
	$0.01 \leq \rho f/R_1 \leq 1$

C.2 CALCULATION OF CHARACTERISTIC IMPEDANCE AND PROPAGATION CONSTANT OF SOFT FIBROUS MATERIAL

Reference 8 gives the following method (pages 245-269) to calculate the characteristic impedance and propagation constant, given the flow resistivity, fiber diameter, porosity, and gas density in the material.

1. Calculate the resistivity R_1 of the material.

   The relationship between the flow resistivity vs bulk density showing the parametric dependence on the fiber diameter is given in Figure 10.4 of Reference 8.

2. Calculate the structures factor s of the material.

   The approximate relation between porosity P and the structures factor s for homogeneous materials of fibers and granules with interconnecting pores and few blind alleys is given in Figure 10.5 of Reference 8.

3. Calculate effective gas compressibility K.

   The effective gas compressibility is a function of frequency and in general is complex. However, the phase angle is small and can be neglected. The magnitude of K is obtained from Figure 10.6 of Reference 8, given frequency f and resistivity R_1.

4. Calculate effective gas density ρ'.

$$\rho' = \frac{\rho s}{f_1} \left(f_2 - j \frac{R_2}{\rho s \omega}\right) \tag{C.1}$$

where:

$$f_1 = 1 + \left(\frac{R_2}{\rho_m \omega}\right)^2 \tag{C.2}$$

$$f_2 = 1 + (P + \frac{\rho_m}{\rho s})(\frac{R_2}{\rho_m \omega})^2 \qquad (C.3)$$

ρ_m = bulk density of the porous material, kg/m^3

ρ = density of the gas in the material, kg/m^3

P = porosity dimensionless

s = structures factor

ω = frequency radians/sec (= $2\pi f$)

R_2 = approximately 1.2 times the flow resistivity, R_1.

5. Calculate propagation constant, b.

$$b = j\omega\sqrt{\frac{P\rho'}{K}} \qquad (C.4)$$

Also:

$$b = \alpha + j\,\frac{2\pi}{\lambda_m} \qquad (C.5)$$

where:

α = attenuation constant, nepers/m (to convert nepers into decibels, multiply nepers by 8.69)

λ_m = wavelength in material

6. Calculate characteristic impedance Z.

$$Z = -j\,\frac{Kb}{\omega P} \qquad (C.6)$$

and $Z = R + jX$

where:

R = real part of Z in MKS Rayls

X = Imaginary part of Z in MKS Rayls.

APPENDIX D

LISTING OF COMPUTER PROGRAMS

This appendix gives the listing of programs used in the prediction methods and in data reduction. Most of the programs are in the Applesoft language and written on Apple II plus microcomputer.

D.1 LISTING OF SDOF NOISE REDUCTION

This program calculates the noise reduction values at specified frequencies, given mass per unit area (kg/m^2), the resonance frequency (Hz), and the damping ratio (ζ). This program is in Applesoft language.

```
10  REM  CALCULATION OF NOISE RED
UCTION BASED ON SINGLE DEGRE
E OF FREEDOM EQUATION
12  READ M1
13  READ F1
15 PI = 3.1415962
16 W1 = 2 * PI * F1
17  READ ZI
18 M = M1
20  READ F
25  IF F = 0 THEN  GOTO 70
30 W = 2 * PI * F
40 NR = 10 *  LOG ((1 + 2 * M * Z
I * F1 / 408) ^ 2 + (M * (W ^
2 - W1 ^ 2) / W / 408) ^ 2) /
 LOG (10)
50  PRINT F,NR
60  GOTO 20
70  END
1000  DATA      3.9573
1005  DATA  180.1.0.0
1010  DATA  20,40,60,80,100,125,1
50,175,200,225,250,300,400,5
00,600,700,800,900,1000,2000
,3000,4000,5000
1020  DATA  0
```

D.2 LISTING OF DAMPING RATIO CALCULATION

Given the values of damped resonance frequency (Hz), noise reduction at the damped resonance frequency, and the mass per unit area of the panel (kg/m^2), this program calculates the damping ratio. This program is written in Applesoft language.

```
10  REM  CALCULATION ZI GIVEN NR
AT DAMPED NATURAL FREQUENCY
15  PI = 3.1415962
20  PRINT " DAMPED NATURAL FREQ":
 READ FD
21  PRINT FD
30  WD = 2 * PI * FD
40  PRINT "NR AT DAMPED NATURAL F
REQ": READ NR
41  PRINT NR
50  PRINT "MASS PER UNIT AREA (KG
/M2)": READ M
51  PRINT M
60  W1 = WD
70  A = 10 ^ (NR / 20) - 1
80  ZI = A * 406 / (2 * A * W1)
90  PRINT "ZIAPPROX";ZI
100 W1 = WD /  SQR (1 - ZI ^ 2)
105  PRINT "W1 APRROX";W1 / (2 *
PI)
110 A1 = 10 ^ (NR / 10)
120 B1 = (M * (W1 ^ 2 - WD ^ 2) /
(WD * 406)) ^ 2
130 C1 =  SQR (A1 - B1) - 1
140 ZI = C1 * 406 / (2 * A * W1)
150 TEMP = W1
160 W1 = WD /  SQR (1 - ZI ^ 2)
170  IF  ABS (W1 - TEMP) < 1 GOTO
200
180  GOTO 120
200  PRINT "F1= ";W1 / (2 * PI)
210  PRINT "ZI= ";ZI
220  END
1000  DATA  160,5,6.1264
```

D.3 LISTING OF NOISE REDUCTION OF SANDWICH PANELS WITH SHEAR-RESISTANT CORE

Given the panel size (inch), the number of layers, the density (kg/m^3), thickness (inch), and Young's Modulus (N/m^2) of the individual layers and the mass per unit area of the panel (kg/m^2), this program calculates the fundamental flexural resonance frequency, first dilatational resonance frequency, and the noise reduction values at the specified frequencies. This program is written in Applesoft language.

```
10  REM  NOISE REDUCTION OF SANDW
ICH PANELS WITH SHEAR RESIST
ANT CORE
20 PI = 3.1415962
30  PRINT " NOISE REDUCTION OF MU
LTI LAYERED PANELS"
40  PRINT "PANEL SIZE?(INCH)"
50  READ X:X = X * .0254
60  PRINT "# OF LAYERS": READ N
70  PRINT "MASS PER UNIT AREA IN
KG/M^2": READ RO
80  FOR I = 1 TO N
90  PRINT "DENSITY(KG/M3),THICKNE
SS(INCH), YOUNG'S MODULUS (K
G/M2) OF LAYER #";I;"?"
100  READ DE(I),TH(I),E(I)
110  PRINT DE(I),TH(I),E(I)
120 TH(I) = TH(I) * .0254
130  NEXT I
140 Z(0) = 0
150  FOR I = 1 TO N
160 Z(I) = 0
170  FOR K = 1 TO I
180 Z(I) = Z(I) + TH(K)
190  NEXT K
200  NEXT I
210 B = 0:C = 0:A = 0
220 R2 = 0
230  FOR I = 1 TO N
240 C1 = E(I) / (1 - .3 ^ 2)
250 A = A + C1 * (Z(I) - Z(I - 1)
)
260 B = B + C1 / 2 * (Z(I) ^ 2 -
Z(I - 1) ^ 2)
270 C = C + C1 / 3 * (Z(I) ^ 3 -
Z(I - 1) ^ 3)
```

```
280 R2 = R2 + DE(I) * TH(I)
290  NEXT I
300 D = (A * C - B ^ 2) / A
310  REM  PI/A^2=15.0292702
320 F = 15.0292702 *  SQR (D / RO
)
330  PRINT "RES FREQUENCY=";F
340  PRINT "H CAL";R2,"H MEASURED
";RO
350 WN = 2 * PI * F
360 KP = WN ^ 2 * RO
370 XI = .1
380 RZ = 2 * XI * WN * RO
390  READ FR
400  IF FR = 0 THEN  GOTO 470
410 ZA = (406 + RZ) ^ 2 / 406 ^ 2

420 OM = 2 * PI * FR
430 ZB = (OM * RO - KP / OM) ^ 2 /
406 ^ 2
440 NR = 10 *  LOG (ZA + ZB) /  LOG
(10)
450  PRINT FR; TAB( 18);NR
460  GOTO 390
470 FD =  SQR (4 * E(2) / (TH(2) *
(2 * DE(1) * TH(1) + DE(2) *
TH(2) / 3))) / (2 * PI)
480  PRINT "FD=";FD
490  END
500  DATA  18
510  DATA  3
520  DATA  3.6246
530  DATA   2700,.016,7.24E10
540  DATA  67.3,.5,6.25E8
550  DATA    2700,.016,7.24E10
560  DATA  10,20,30,40,50,60,70,8
0,90,100,120,140,160,180,200
,220,240,260,280
570  DATA  300,320,340,350,360,38
0,400,450,500,600,700,800,90
0,1000,2000,3000,4000,5000
580  DATA  0
590  REM  CALCULATION FUNDAMENTAL
 RESONANCE FREQUENCY OF SIMP
LY SUPPORTED PLATE
600  FOR I = 1 TO 3 STEP 2
610 D(I) = E(I) * TH(I) ^ 3 / (12
 * (1 - .3 ^ 2))
620 M(I) = DE(I) * TH(I)
630 OMN(I) = 2 * PI ^ 2 / X ^ 2 *
 SQR (D(I) / M(I))
640  NEXT I
650  RETURN
```

D.4 LISTING OF NOISE REDUCTION OF SANDWICH PANELS WITH NON-SHEAR-RESISTANT CORE

D.4.1 Fortran IV Time Sharing Program

This program calculates the first flexural resonance frequencies of the skins and the noise reduction values at various frequencies, given panel size (inch), density (kg/m^3), and Young's Modulus (N/m^2) of the skin and bulk density (kg/m^3), density of air in the core (kg/m^3), resistivity (MKS rayls). porosity, structures factor, and thickness (inch) of the core.

```
10C NOISE REDUCTION OF PANEL WITH NON-SHEAR RESISTANT CORE
20 PI=3.1415962
30  DIMENSION DE(3),YM(3),TH(3),X(15),Y(15)
35 DIMENSION M(3),OMN(3),Q(3)
37  REAL KMOD
40 COMPLEX CV,B,Z2,AKL,EKL,ENKL
45 COMPLEX C2,C3,C4,C5,C6,C7,C8,C9,C10,C11
50 PRINT,"PANEL WIDTH IN INCHES?"
60 READ, SIDE
70 SIDE=SIDE*.0254
80 DO 1 I=1,3,2
85 K=I
87 IF( I.EQ. 3) K=2
90 PRINT,"DENSITY IN KG/M**3,YOUNGS MODULUS IN KG/M**2,THICKNESS IN INCHES?"
100 READ, DE(I),YM(I),TH(I)
110 PRINT, DE(I),YM(I),TH(I)
120 1  CONTINUE
130 PRINT,"BULK DENSITY,DENSITY OF GAS IN THE CORE,RESISTIVITY IN MKS UNITS"
140 READ ,DE(2),DG,R1
150PRINT,DE(2),DG,R1
160 PRINT,"POROSITY,STRUCTURES FACTOR,THICKNESS IN INCHES"
170 READ ,P,S,TH(2)
180PRINT,P,S,TH(2)
190 DO 2I=1,3
200 2 TH(I)=TH(I)*.0254
210C  CALCULATION OF IMPEDANCE
220C CALCULATION OF EFFECTIVE COMPRESSIBILITY
230 X(1)=.001
240X(2)=.002
250X(3)=.005
260 X(4)=.01
270X(5)=.02
280X(6)=.05
290X(7)=.1
300 X(8)=.2
```

```
310 X(9)=.5
320 X(10)=1.
330Y(1)=1.02E5
340Y(2)=1.03E5
350Y(3)=1.05E5
360Y(4)=1.075E5
370Y(5)=1.11E5
380Y(6)=1.165E5
390Y(7)=1.21E5
395 Y(8)=1.26E5
400Y(9)=1.32E5
410 Y(10)=1.35E5
420 DO 3 I=1,10
430 X(I)=ALOG10(X(I))
440  3 CONTINUE
490 I1=20
492 ICOUNT=0
492  PRINT,"FREQUENCY     NOISE REDUCTION"
494 I1=20
496 I2=500
498 I3=20
500  15 DO 4 I=I1,I2,I3
510 F=I*1.
520 OMEGA=2*PI*F
530 TEMP=ALOG10(F/R1)
540 IF((F/R1) .LT. 0.001) GO TO5
550 DO 6II=1,9
560 IF (TEMP.GE.X(II) .AND. TEMP.LT.X(II+1)) GOTO7
570 6  CONTINUE
580 PRINT,"K EXCEEDS THE LIMITS"
590 GOTO 1000
600 7 KMOD= (Y(II+1)-Y(II))/(X(II+1)-X(II))*(TEMP-X(II))+Y(II)
610 GOTO 8
620  5  KMOD=1.01E5
630 8  CONTINUE
640 F1=1+(1.2*R1/(DE(2)*OMEGA))**2
650 F2=1+(P+DE(2)/(DG*S))*(1.2*R1/(DE(2)*OMEGA))**2
660 A1=P*DG*S*F2/(F1*KMOD)
670 B1=-P*R1*1.2/(F1*OMEGA*KMOD)
680 CV=CMPLX(A1,B1)
690 B=CMPLX(0,OMEGA)*CSQRT(CV)
700 Z2=CMPLX(0.,(-KMOD/OMEGA/P))*B
702 ALPHA=REAL(B)*8.69
703 ALAMDA= 2.*PI/(AIMAG(B))
710 AKL=TH(2)*B
720 EKL=CEXP(AKL)
730ENKL=CEXP(-AKL)
740C  CALCULATION OF Q(1) AND Q(2)
750 DO 11 L=1,3,2
760 K=L
770 IF (L.EQ.3) K=2
780 M(K)=DE(L)* TH(L)
```

```
790  DSTIFF=YM(L)*TH(K)**3/(12.*.91)
800 OMN(K)=2*PI**2/SIDE**2*SQRT(DSTIFF/M(K))
805 OMN(K)=2.*PI*90.
810 Q(K)= M(K)*(OMN(K)**2-OMEGA**2)/(OMEGA*400.)
820 11 CONTINUE
825 Q(2)=0.
830  C2=(0.,1.)*(400.*Z(1)/Z2)
835  C3=1.-C2
840  C4=(0.,-1.)*Q(2)+Z2/400.
850  C5=1.+C4
860  C6=C3*C5*EKL
870 C7=1.+C2
880  C8= (0.,-1)*Q(2)-Z2/400.
890  C9=1.+C8
900  C10=C7*C9*ENKL
910  C11=0.5*(C6+C10)
920  ANR=10.*ALOG10(ABS(C11)**2)
930 WRITE (6,501) INT(F),ANR
955 501 FORMAT(5X,I4,10X,F6.2)
940 4  CONTINUE
950 ICOUNT=ICOUNT+1
960 IF(ICOUNT .NE. 1) GOTO 12
970 I1=550
980 I2=1000
990 I3=50
1000 GOTO15
1060 12 CONTINUE
1062 IF(ICOUNT .NE. 2) GOTO 1000
1064 I1=1500
1066 I2=5000
1067 I3=500
1068 GOTO 15
1070 1000 CONTINUE
1080 STOP
1090 END
```

D.4.2 Low Frequency Approximation in Applesoft Language

Given the same inputs as in D.4.1, this program calculates the noise reduction values up to 300 Hz.

```
5  DEF  FN LG(X) =  LOG (X) /  LOG
(10)
8  DIM XR(15),YR(15)
10  REM  NOISE REDUCTION OF SANDW
ICH PANELS WITH NON SHEAR RE
SISTANT CORE
20 PI = 3.1415962
30  PRINT " NOISE REDUCTION OF MU
LTI LAYERED PANELS"
40  PRINT "PANEL SIZE?(INCH)"
50  READ X:X = X * .0254
60  REM  NON SHEAR RESISTANT CORE

70  FOR K = 1 TO 3 STEP 2
80  IF K = 3 THEN I = 2: GOTO 100

90 I = K
100  PRINT "DENSITY(KG/M3),THICKN
ESS(INCH), YOUNG'S MODULUS (
KG/M2) OF FACE";I;"?"
110  READ DE(K),TH(K),E(K)
120  PRINT DE(K),TH(K),E(K)
130  NEXT K
140  PRINT " CORE MATERIAL PROPER
TIES"
150  PRINT "DENSITY (KG/M3),THICK
NESS(INCH), RESISTIVITY (MKS
 RAYLS/M)"
160  READ DE(2),TH(2),R
170  PRINT DE(2),TH(2),R
180  PRINT "POROSITY,SRUCTURES FA
CTOR,DENSITY OF GAS IN THE M
ATERIAL":
190  READ P,S,DF
200  PRINT P,S,DF
205  GOSUB 1000
210  FOR I = 1 TO 3
220 TH(I) = TH(I) * .0254
230  NEXT I
240  GOSUB 530
270  REM  CONTINUE
280  READ F
290  IF F = 0 THEN  GOTO 450
300 W = 2 * PI * F
310  GOSUB 600
335  FOR I = 1 TO 2
340  IF I = 2 THEN K = 3: GOTO 36
0
350 K = I
360 M(I) = DE(K) * TH(K)
```

```
370 Q(I) = M(I) * (OMN(K) ^ 2 - W
  ^ 2) / (406 * W)
380  NEXT I
382 KL =  SQR (A ^ 2 + BI ^ 2) *
TH(2)
385 CKL =  COS (KL):SKL =  SIN (K
L)
390 Z2 =  SQR (R2 ^ 2 + X2 ^ 2)
400 RE = CKL + Q(1) * 406 * (R2 -
Q(2) * X2) * SKL / Z2 ^ 2 -
X2 * SKL / 406
410 IM =  - (Q(1) + Q(2)) * CKL -
Q(1) * 406 * (X2 + Q(2) * R2
) * SKL / Z2 ^ 2 + R2 * SKL /
406
420 NR = 10 *  LOG (RE ^ 2 + IM ^
2) /  LOG (10)
430  PRINT F,NR
440  GOTO 270
450  END
460  DATA  18
470  DATA  2700,.025,7.24E10
480  DATA   2700,.025,7.24E10
490  DATA  9.6,1.0,4.1E4
500  DATA  .99,1...073665
502  DATA  .001..002,.005,.01,.02
,.05..1..2..5,1
506  DATA  1.02E5,1.03E5,1.05E5,1
.075E5,1.11E5,1.165E5,1.21E5
,1.26E5,1.32E5,1.35E5
510  DATA  20,30,40,50,60,70,80,9
0,100,110,120,130,140,150,16
0,170,180,190,200
520  DATA 210,220,230,240,250,260
,270,280,290,300,0
530  REM  CALCULATION FUNDAMENTAL
 RESONANCE FREQUENCY OF SIMP
LY SUPPORTED PLATE
540  FOR I = 1 TO 3 STEP 2
550 D(I) = E(I) * TH(I) ^ 3 / (12
 * (1 - .3 ^ 2))
560 M(I) = DE(I) * TH(I)
570 OMN(I) = 2 * PI ^ 2 / X ^ 2 *
 SQR (D(I) / M(I))
580  NEXT I
590  RETURN
600  REM  CALCULATION OF IMPEDANC
E AND PROPAGATION CONSTANT
610 C1 =  EM LG(F / R)
615  IF F / R < .001 THEN K = 1.0
165: GOTO 670
```

```
620  FOR I = 1 TO 10
630  IF (T1 >  = XR(I) AND T1 < X
R(I + 1)) THEN  GOTO 660
640  NEXT I
650  PRINT "K EXCEEDS THE LIMITS"
: STOP
660 K = (YR(I + 1) - YR(I)) / (XR
(I + 1) - XR(I)) * (T1 - XR(
I)) + YR(I)
670 F1 = 1 + (1.2 * R / DE(2) / W
) ^ 2
680 F2 = 1 + (P + DE(2) / DF / S)
 * (1.2 * R / DE(2) / W) ^ 2

690 RD = DF * S * F2 / F1:XD =  -
1.2 * R / (F1 * W)
700 RD = RD * P / K:XD = XD * P /
K
710 SR =  SQR (RD ^ 2 + XD ^ 2):O
 =  ATN (XD / RD)
720 RSR =  SQR (SR):O2 = O / 2
730 A =  - RSR *  SIN (O2) * W:BI
 = RSR *  COS (O2) * W
740 R2 = RSR *  COS (O2) * K / P:
X2 = RSR *  SIN (O2) * K / P

770  RETURN
1000  REM  CALCULATION OF MOD K
1010  FOR I = 1 TO 10
1020  READ XR(I):XR(I) =  FN LG(X
R(I))
1030  NEXT I
1040  FOR I = 1 TO 10
1050  READ YR(I)
1060  NEXT I
1070  RETURN
```

D.5 LISTING OF DUAL PANE WINDOW

Given the pane size (inch), Density (kg/m^3), thickness (inch), and Young's Modulus (N/m^2) of the panes and the spacing (inch), this program calculates the funcamental resonance frequencies of the panes and the first pane-air-pane resonance frequency and the noise reduction values at the specified frequency values. This program is in the Applesoft language.

```
10  REM  CALCULATION OF NOISE RED
UCTION OF DUAL PANE WINDOW
20 PI = 3.1415962
30  PRINT "PANEL SIZE?(INCH)"
40  READ X:X = X * .0254
50  FOR K = 1 TO 3 STEP 2
60  IF K = 3 THEN I = 2: GOTO 80
70 I = K
80  PRINT "DENSITY(KG/M3),THICKNE
SS(INCH),YOUNG'S MODULUS (KG
/M2) OF PANE";I;"?"
90  READ DE(K),TH(K),E(K)
100  PRINT DE(K),TH(K),E(K)
110  NEXT K
120  PRINT " SPACING BETWEEN PANE
S (INCH)"
130  READ TH(2)
140  PRINT TH(2)
150  FOR I = 1 TO 3
160 TH(I) = TH(I) * .0254
170  NEXT I
180  GOSUB 380
190  GOSUB 470
200  PRINT "FREQUENCY"; TAB( 20);
"NR (DB)"
210  REM  CONTINUE
220  READ F
230  IF F = 0 THEN  GOTO 370
240 W = 2 * PI * F
250 KL = W / 343 * TH(2):SKL =  SIN
(KL):CKL =  COS (KL)
260  FOR I = 1 TO 2
270  IF I = 2 THEN K = 3: GOTO 29
0
280 K = I
290 M(I) = DE(K) * TH(K)
300 Q(I) = M(I) * (OMN(K) ^ 2 - W
 ^ 2) / (406 * W)
310  NEXT I
320 RE = CKL + Q(1) * SKL
330 IM = CKL * (( - Q(1) - Q(2)) +
(1 - Q(1) * Q(2)) *  TAN (KL
))
340 NR = 10 *  LOG (RE ^ 2 + IM ^
2) /  LOG (10)
350  PRINT F,NR
360  GOTO 210
370  END
```

```
380  REM  CALCULATION FUNDAMENTAL
 RESONANCE FREQUENCY OF SIMP
LY SUPPORTED PLATE
390  FOR I = 1 TO 3 STEP 2
400 D(I) = E(I) * TH(I) ^ 3 / (12
 * (1 - .3 ^ 2))
410 M(I) = DE(I) * TH(I)
420 OMN(I) = 2 * PI ^ 2 / X ^ 2 *
 SQR (D(I) / M(I))
430 OMN(I) = OMN(I) * 16 / 9
440  PRINT "FUNDA RESO FREQ OF PA
NE= ";OMN(I) / (2 * PI)
450  NEXT I
460  RETURN
470 F1 = 1 / (2 * PI) *  SQR (406
 * 343 / (M(1) * TH(2)) + OM
N(1) ^ 2)
480 Q(1) = M(1) * (OMN(1) ^ 2 - (
2 * PI * F1) ^ 2) / (406 * 2
 * PI * F1)
490 XZ =  - 2 / Q(1)
500 T =  TAN (2 * PI * F1 * TH(2)
 / 343)
510  IF  ABS (XZ - T) < .01 THEN
 GOTO 530
520 F1 = F1 + 2: GOTO 480
530  PRINT "FIRST PANE-AIR-PANE
          RESO FREQ= ";F1:F
 = F1: RETURN
540  DATA      13
550  DATA  1180,.125,3.1E9
560  DATA   1180,.125,3.1E9
570  DATA   4
580  DATA  10,20,30,40,50,60,70,8
0,90,100,110,120,130,140,150
,160,170,180,190,200,0
```

D.6 LISTING OF HELMHOLTZ RESONATOR

This program was developed to study the effects of the various parameters of the type of Helmholtz resonator tested at the KU-FRL acoustic test facility. Given the spacing (inch), width (inch),

resonator length (inch), number of tubes, alpha (defined in Chapter 3), and the resonance frequency (Hz), this program calculates the resonator tube diameter and the increase in noise reduction due to the Helmholtz resonator. It also allows the effects of the variation of different parameters to be studied. This program is in Applesoft language.

```
5 PI = 3.1415962
10  INPUT "SPACING (INCH)";W
20  INPUT "CAVITY WIDTH (IN)?";D2

30  INPUT "NECK LENGTH (IN.)?";T
35 T = .0254 * T
40  INPUT "NUMBER OF TUBES?";N
44  PRINT " DO YOU WANT TO CALCUL
ATE ALPHA?"
46  PRINT "1=YES": INPUT AL
48  IF AL = 1 THEN  GOTO 2000
50  INPUT "ALPHA?";PHA
60  INPUT "RESONANCE FREQUENCY (H
Z)?";FO
70  INPUT "FREQUENCY RANGE AND DE
LTA FREQUENCY";F1,F2,DF
75  CALL  - 922
80  PRINT "FREQUENCY"; TAB( 17);"
LTL"
100 RHO = 1.225
110 C = 340.28
115  GOSUB 500
130 M = (6.28 * FO / C) ^ 2 * V
140 A2 = (2 * M * T + .64 * M ^ 2
 / N):A3 = (M * T) ^ 2
150 AO = (A2 +  SQR (A2 ^ 2 - 4 *
A3)) / 2
160 RS = AO * AL * RHO * C / S1
180 AO = AO / .0254 ^ 2
190 D =  SQR (AO / (.785 * N))
230  FOR F = F1 TO F2 STEP DF
240 LTL = 10 *  LOG (1 + ((AL + .
25) / (AL ^ 2 + (B * (F / FO
 - FO / F)) ^ 2))) /  LOG (1
0)
```

```
290  PRINT F; TAB( 15);LTL
300  NEXT F
310  PRINT "RESONATOR REACTANCE (
BETA)= ";B;" (DIMENSIONLESS)
"
315  PRINT "TOTAL APERTURE AREA=
";AO;" IN^2"
320  PRINT "FLOW RESISTANCE IN RE
SO TUBES (RS) = ";RS;" MKS R
AYLS"
325  PRINT "FOR THE RESO FREQ ";F
O;"HZ, HOLE DIA NEEDED= ";D;
" IN"
330  PRINT "DO YOU WANT TO CHANGE
 ANY PARAMETER?1=YES": INPUT
Q1
340  IF Q1 <  > 1 THEN  GOTO 445
350  PRINT "WHICH PARAMETR DO YOU
 WANT TO CHANGE?"
351  PRINT "D=SPACING; W=WIDTH;N=
TUBE LENGTH;A=ALPHA;T=# OF T
UBES": INPUT WS
360  PRINT "CHANGED VALUE?": INPUT
NV
365  IF WS = "D" THEN W = NV
370  IF WS = "W" THEN T2 = NV
380  IF WS = "N" THEN T = NV * .0
254
390  IF WS = "A" THEN PHA = NV
400  IF WS = "T" THEN N = NV
410  PRINT "DEPTH=";W; TAB( 20);"
WIDTH=";T2
420  PRINT "NO OF TUBES=";N; TAB(
20);"NECK =";T / .0254
430  PRINT "ALPHA=";PHA
440  GOTO 75
445  GOSUB 1000
450  END
500  REM  CALCULATION OF A,B
510 S1 = (15 - 2 * T2) ^ 2 * .025
4 ^ 2
530 V = (225 - (15 - 2 * T2) ^ 2)
 * W * .0254 ^ 3
540 B = S1 * C / (6.28 * FO * V)
550 AL = B * PHA
560  RETURN
1000  REM  CALCULATION REN FREQ G
IVEN OTHER PARAMETERS
```

```
1005  PRINT "DO YOU WANT TO CHANG
E HOLE DIA?1=YES": INPUT IH
1008  IF IH <  > 1 GOTO 1090
1010  PRINT "DIA OF THE APERTURE"
: INPUT D
1020 D = D * .0254
1030 AO = PI * D ^ 2 * N / 4
1040 TH1 = T + .8 *  SQR (AO / N)

1050 FO = C / (2 * PI) *  SQR (AO
 / (V * TH1))
1060  PRINT "RESO FREQ=";FO
1080  GOTO 1005
1090  RETURN
1110 FO = C / (2 * PI) *  SQR (AO
 / V * TH1)
2000  REM  CALCULATION OF ALPHA G
IVEN TL AT FO
2010  PRINT "RESO FREQ AND TL AT
RESO FREQ?": INPUT FO,TL
2020 A1 = 10 ^ (TL / 20)
2030 A = 0.5 / (A1 - 1)
2040  PRINT " HOLE DIA?": INPUT D

2050 D = .0254 * D
2060 AO = PI * D ^ 2 / 4 * N
2070 RHO = 1.226
2080 C = 343
2090 S1 = (15 - 2 * T2) ^ 2 * .02
54 ^ 2
2140  PRINT "ALPHA=";A
2150 RS = AO * A * RHO * C / S1
2160  PRINT "RS=";RS;"MKS RAYS"
2170  END
```

D.7 LISTING OF HELMHOLTZ DATA REDUCTION

This program reduces the data from the real time analyzer and plots the noise reduction values in the frequency region 20-200 Hz. This program is in Applesoft language.

```
10  LOMEM: 16500
20  DIM Y(1025),NR(515),FR(501),H
Z(501)
30  DEF  FN AN(I) =  LOG (I) /  LOG
(10)
40  PRINT " DATA REDUCTION PROGRA
M FOR HELMHOLTZ RESONATORS"
50 D$ = "": REM  CTRL-D
60  PRINT "FILE NAME?": INPUT N$
65  IF  RIGHT$ (N$,3) <  > "VLF" THEN
 PRINT "FILENAME MISMATCH": GOTO
600
70  PRINT D$;"BLOAD";N$
80 IC =  PEEK (10240):AR% =  PEEK
(10241)
90  FOR I = 0 TO 1023
100 Y(I) = ( PEEK (8192 + 1024 +
I)) * 256 +  PEEK (8192 + I)

110 Y(I) = Y(I) / 100
120  NEXT I
130  FOR I = 0 TO 511
140 NR(I) = Y(I) - Y(512 + I)
150  NEXT I
160  FOR I = 1 TO 509
180 DF = 1
200  IF NR(I) > NR(I - 1) + DF THEN
 GOTO 230
210  IF NR(I) < NR(I - 1) - DF THEN
 GOTO 250
220  GOTO 270
230  IF NR(I + 1) > NR(I - 1) + 2
 * DF THEN NR(I) = NR(I - 1)
 + (NR(I + 2) - NR(I - 1)) /
3: GOTO 270
240 NR(I) = (NR(I - 1) + NR(I + 1
)) / 2: GOTO 270
250  IF NR(I + 1) < NR(I - 1) - 2
 * DF THEN NR(I) = NR(I - 1)
 - (NR(I - 1) - NR(I + 2)) /
3: GOTO 270
260 NR(I) = (NR(I - 1) + NR(I + 1
)) / 2
270  NEXT I
290  IF IC <  > 3 GOTO 600
300 B = .4:L1 = 50:L2 = 500
330  FOR I = L1 TO L2
340 FR(I) = B * I
350  NEXT I
```

```
360  GOSUB 2000
370 C1 = 20:C2 = 200
371  GOSUB 3000
520  PRINT "ENTER 1 TO PLOT AGAIN
": INPUT IX
530  IF IX = 1 THEN  GOTO 360
560  GOSUB 6000
570  PRINT "ENT 1 FOR REDUCING ON
E MORE TEST": INPUT IL
580  IF IL = 1 THEN  GOTO 60
590  PRINT "DONE"
600  END
2000  PRINT "ENTER 1 TO PLOT": INPUT
PT
2010  IF PT <  > 1 THEN  GOTO 218
0
2020  PRINT "SWITCH ON PLOTTER.PE
N LIFT OFF": STOP
2030 IP = 1
2050  POKE  - 15103,0: POKE  - 15
104,( INT (255 / 7))
2060 N$ = "20HZ-0DB": GOSUB 4000
2070  STOP : POKE  - 15103,255: POKE
 - 15104,( INT (255))
2080 N$ = "200HZ-60DB": GOSUB 400
0
2120  STOP :IP = IP + 1
2130  IF IP = 3 THEN  GOTO 2150
2140  GOTO 2050
2150  PRINT "IS THE ADJUSTMENT OK
?1=YES:2=NO": INPUT IA
2160  IF IA = 2 THEN  GOTO 2030
2170  POKE  - 15103,0: POKE  - 15
104,0
2180  RETURN
3000  PRINT "ENTER 1 TO SCREEN PL
OT": INPUT SP
3010  IF SP = 1 THEN  HGR : HCOLOR=
1: HPLOT 0,0
3020  IF PT <  > 1 AND SP <  > 1 THEN
 GOTO 3210
3030  FOR I = L1% TO L2% STEP 2
3040 X% = ( INT ((FR(I) - C1) * 2
55 / (C2 - C1)))
3070 W = NR(I) + 10
3080 W% = ( INT (W * 255 / 70))
3090  IF X% < 0 THEN X% = 0
3100  IF X% > 255 THEN X% = 255
3110  IF W% < 0 THEN W% = 0
```

```
3120  IF W% > 255 THEN W% = 255
3130  POKE  - 15103,X%: POKE  - 1
5104,W%
3140  PRINT FR(I),NR(I): FOR K =
0 TO 200: NEXT K
3150 W% = 150 -  INT (W% * 150 /
255):X% = X% + 1
3160  IF W% < 0 THEN W% = 0
3170  IF W% > 150 THEN W% = 150
3180  HPLOT  TO X%,W%
3190  NEXT I
3200  GOTO 3240
3210  FOR I = L1% TO L2%
3220  PRINT FR(I),NR(I)
3230  NEXT I
3240  TEXT
3250  RETURN
4000  PRINT "ADJUST";N$;"POINT": RETURN
5000  FOR K = 0 TO 40: NEXT K: RETURN

6000  PRINT "ENT 1 FOR DRAWING AX
ES": INPUT IY
6010  IF IY <  > 1 THEN  GOTO 621
0
6015 F% =  INT (255 / 7)
6020  PRINT "PEN UP": STOP : POKE
 - 15103,0: POKE  - 15104,F%

6030  PRINT "PEN DOWN": STOP
6040 X = 20
6050 X1 = X:X% =  INT ((X1 - C1) *
255 / (C2 - C1))
6060  GOSUB 5000
6070  IF X% > 255 THEN X% = 255
6080  IF X% < 0 THEN X% = 0
6090  POKE  - 15103,X%: GOSUB 500
0
6100  POKE  - 15104,(F% + 2): GOSUB
5000: POKE  - 15104,F%: GOSUB
5000
6130  IF X < 200 THEN X = X + 20:
 GOTO 6050
6140  POKE  - 15103,0: POKE  - 15
104,F%
6150  FOR I = 1 TO 6
6160  GOSUB 5000
6170 X% =  INT (255 * I / 7): POKE
 - 15104,X%
```

```
6180  GOSUB 5000
6190  POKE  - 15103,2: GOSUB 5000
: POKE  - 15103,0: GOSUB 500
0
6200  NEXT I
6210  POKE  - 15104,F%: RETURN
```

```
620  FOR I = 1 TO 10
630  IF (T1 >  = XR(I) AND T1 < X
R(I + 1)) THEN  GOTO 660
640  NEXT I
650  PRINT "K EXCEEDS THE LIMITS"
: STOP
660 K = (YR(I + 1) - YR(I)) / (XR
(I + 1) - XR(I)) * (T1 - XR(
I)) + YR(I)
670 F1 = 1 + (1.2 * R / DE(2) / W
) ^ 2
680 F2 = 1 + (P + DE(2) / DF / S)
 * (1.2 * R / DE(2) / W) ^ 2

690 RD = DF * S * F2 / F1:XD =  -
1.2 * R / (F1 * W)
700 RD = RD * P / K:XD = XD * P /
K
710 SR =  SQR (RD ^ 2 + XD ^ 2):O
 =  ATN (XD / RD)
720 RSR =  SQR (SR):O2 = O / 2
730 A =  - RSR *  SIN (O2) * W:BI
 = RSR *  COS (O2) * W
740 R2 = RSR *  COS (O2) * K / P:
X2 = RSR *  SIN (O2) * K / P

770  RETURN
1000  REM  CALCULATION OF MOD K
1010  FOR I = 1 TO 10
1020  READ XR(I):XR(I) =  FN LG(X
R(I))
1030  NEXT I
1040  FOR I = 1 TO 10
1050  READ YR(I)
1060  NEXT I
1070  RETURN
```

D.5 LISTING OF DUAL PANE WINDOW

Given the pane size (inch), Density (kg/m^3), thickness (inch), and Young's Modulus (N/m^2) of the panes and the spacing (inch), this program calculates the funcamental resonance frequencies of the panes and the first pane-air-pane resonance frequency and the noise reduction values at the specified frequency values. This program is in the Applesoft language.

```
10  REM  CALCULATION OF NOISE RED
UCTION OF DUAL PANE WINDOW
20 PI = 3.1415962
30  PRINT "PANEL SIZE?(INCH)"
40  READ X:X = X * .0254
50  FOR K = 1 TO 3 STEP 2
60  IF K = 3 THEN I = 2: GOTO 80
70 I = K
80  PRINT "DENSITY(KG/M3),THICKNE
SS(INCH),YOUNG'S MODULUS (KG
/M2) OF PANE";I;"?"
90  READ DE(K),TH(K),E(K)
100  PRINT DE(K),TH(K),E(K)
110  NEXT K
120  PRINT " SPACING BETWEEN PANE
S (INCH)"
130  READ TH(2)
140  PRINT TH(2)
150  FOR I = 1 TO 3
160 TH(I) = TH(I) * .0254
170  NEXT I
180  GOSUB 380
190  GOSUB 470
200  PRINT "FREQUENCY"; TAB( 20);
"NR (DB)"
210  REM  CONTINUE
220  READ F
230  IF F = 0 THEN  GOTO 370
240 W = 2 * PI * F
250 KL = W / 343 * TH(2):SKL =  SIN
(KL):CKL =  COS (KL)
260  FOR I = 1 TO 2
270  IF I = 2 THEN K = 3: GOTO 29
0
280 K = I
290 M(I) = DE(K) * TH(K)
300 Q(I) = M(I) * (OMN(K) ^ 2 - W
 ^ 2) / (406 * W)
310  NEXT I
320 RE = CKL + Q(1) * SKL
330 IM = CKL * ( - Q(1) - Q(2)) +
(1 - Q(1) * Q(2)) *  TAN (KL
))
340 NR = 10 *  LOG (RE ^ 2 + IM ^
2) /  LOG (10)
350  PRINT F,NR
360  GOTO 210
370  END
```

```
380  REM  CALCULATION FUNDAMENTAL
 RESONANCE FREQUENCY OF SIMP
LY SUPPORTED PLATE
390  FOR I = 1 TO 3 STEP 2
400 D(I) = E(I) * TH(I) ^ 3 / (12
 * (1 - .3 ^ 2))
410 M(I) = DE(I) * TH(I)
420 OMN(I) = 2 * PI ^ 2 / X ^ 2 *
 SQR (D(I) / M(I))
430 OMN(I) = OMN(I) * 16 / 9
440  PRINT "FUNDA RESO FREQ OF PA
NE= ";OMN(I) / (2 * PI)
450  NEXT I
460  RETURN
470 F1 = 1 / (2 * PI) *  SQR (406
 * 345 / (M(1) * TH(2)) + OM
N(1) ^ 2)
480 Q(1) = M(1) * (OMN(1) ^ 2 - (
2 * PI * F1) ^ 2) / (406 * 2
 * PI * F1)
490 XZ =  - 2 / Q(1)
500 T =  TAN (2 * PI * F1 * TH(2)
 / 345)
510  IF  ABS (XZ - T) < .01 THEN
 GOTO 550
520 F1 = F1 + 2: GOTO 480
550  PRINT "FIRST PANE-AIR-PANE
           RESO FREQ= ";F1:F
 = F1: RETURN
540  DATA     13
550  DATA  1180,.125,3.1E9
560  DATA   1180,.125,3.1E9
570  DATA   4
580  DATA  10,20,30,40,50,60,70,8
0,90,100,110,120,130,140,150
,160,170,180,190,200,0
```

D.6 LISTING OF HELMHOLTZ RESONATOR

This program was developed to study the effects of the various parameters of the type of Helmholtz resonator tested at the KU-FRL acoustic test facility. Given the spacing (inch), width (inch),

resonator length (inch), number of tubes, alpha (defined in Chapter 3), and the resonance frequency (Hz), this program calculates the resonator tube diameter and the increase in noise reduction due to the Helmholtz resonator. It also allows the effects of the variation of different parameters to be studied. This program is in Applesoft language.

```
5 PI = 3.1415962
10  INPUT "SPACING (INCH)";W
20  INPUT "CAVITY WIDTH (IN)?";D2

30  INPUT "NECK LENGTH (IN.)?";T
35 T = .0254 * T
40  INPUT "NUMBER OF TUBES?";N
44  PRINT " DO YOU WANT TO CALCUL
ATE ALPHA?"
46  PRINT "1=YES": INPUT AL
48  IF AL = 1 THEN  GOTO 2000
50  INPUT "ALPHA?";PHA
60  INPUT "RESONANCE FREQUENCY (H
Z)?";FO
70  INPUT "FREQUENCY RANGE AND DE
LTA FREQUENCY";F1,F2,DF
75  CALL  - 922
80  PRINT "FREQUENCY"; TAB( 17);"
LTL"
100 RHO = 1.225
110 C = 340.28
115  GOSUB 500
130 M = (6.28 * FO / C) ^ 2 * V
140 A2 = (2 * M * T + .64 * M ^ 2
 / N):A3 = (M * T) ^ 2
150 A0 = (A2 +  SQR (A2 ^ 2 - 4 *
A3)) / 2
160 RS = A0 * AL * RHO * C / S1
180 A0 = A0 / .0254 ^ 2
190 D =  SQR (A0 / (.785 * N))
230  FOR F = F1 TO F2 STEP DF
240 LTL = 10 *  LOG (1 + ((AL + .
25) / (AL ^ 2 + (B * (F / FO
 - FO / F)) ^ 2))) /  LOG (1
0)
```

```
290  PRINT F; TAB( 15);LTL
300  NEXT F
310  PRINT "RESONATOR REACTANCE (
BETA)= ";B;" (DIMENSIONLESS)
"
315  PRINT "TOTAL APERTURE AREA=
";AO;" IN^2"
320  PRINT "FLOW RESISTANCE IN RE
SO TUBES (RS) = ";RS;" MKS R
AYLS"
325  PRINT "FOR THE RESO FREQ ";F
O;"HZ, HOLE DIA NEEDED= ";D;
" IN"
330  PRINT "DO YOU WANT TO CHANGE
 ANY PARAMETER?1=YES": INPUT
Q1
340  IF Q1 <  > 1 THEN  GOTO 445
350  PRINT "WHICH PARAMETR DO YOU
 WANT TO CHANGE?"
351  PRINT "D=SPACING; W=WIDTH;N=
TUBE LENGTH;A=ALPHA;T=# OF T
UBES": INPUT WS
360  PRINT "CHANGED VALUE?": INPUT
NV
365  IF WS = "D" THEN W = NV
370  IF WS = "W" THEN T2 = NV
380  IF WS = "N" THEN T = NV * .0
254
390  IF WS = "A" THEN PHA = NV
400  IF WS = "T" THEN N = NV
410  PRINT "DEPTH=";W; TAB( 20);"
WIDTH=";T2
420  PRINT "NO OF TUBES=";N; TAB(
20);"NECK =";T / .0254
430  PRINT "ALPHA=";PHA
440  GOTO 75
445  GOSUB 1000
450  END
500  REM  CALCULATION OF A,B
510 S1 = (15 - 2 * T2) ^ 2 * .025
4 ^ 2
520 V = (225 - (15 - 2 * T2) ^ 2)
 * W * .0254 ^ 3
540 B = S1 * C / (6.28 * FO * V)
550 AL = B * PHA
560  RETURN
1000  REM  CALCULATION REM FREQ G
IVEN OTHER PARAMETERS
```

```
1005  PRINT "DO YOU WANT TO CHANG
E HOLE DIA?1=YES": INPUT IH
1008  IF IH <  > 1 GOTO 1090
1010  PRINT "DIA OF THE APERTURE"
: INPUT D
1020 D = D * .0254
1030 AO = PI * D ^ 2 * N / 4
1040 TH1 = T + .6 *  SQR (AO / N)

1050 FO = C / (2 * PI) *  SQR (AO
 / (V * TH1))
1060  PRINT "RESO FREQ=";FO
1080  GOTO 1005
1090  RETURN
1110 FO = C / (2 * PI) *  SQR (AO
 / V * TH1)
2000  REM  CALCULATION OF ALPHA G
IVEN TL AT FO
2010  PRINT "RESO FREQ AND TL AT
RESO FREQ?": INPUT FO,TL
2020 A1 = 10 ^ (TL / 20)
2030 A = 0.5 / (A1 - 1)
2040  PRINT " HOLE DIA?": INPUT D

2050 D = .0254 * D
2060 AO = PI * D ^ 2 / 4 * N
2070 RHO = 1.226
2080 C = 343
2090 S1 = (15 - 2 * T2) ^ 2 * .02
54 ^ 2
2140  PRINT "ALPHA=";A
2150 RS = AO * A * RHO * C / S1
2160  PRINT "RS=";RS;"MKS RAYS"
2170  END
```

D.7 LISTING OF HELMHOLTZ DATA REDUCTION

This program reduces the data from the real time analyzer and plots the noise reduction values in the frequency region 20-200 Hz. This program is in Applesoft language.

```
10  LOMEM: 16500
20  DIM Y(1025),NR(515),FR(501),H
Z(501)
30  DEF  FN AN(I) =  LOG (I) /  LOG
(10)
40  PRINT " DATA REDUCTION PROGRA
M FOR HELMHOLTZ RESONATORS"
50 D$ = "": REM  CTRL-D
60  PRINT "FILE NAME?": INPUT N$
65  IF  RIGHT$ (N$,3) <  > "VLF" THEN
 PRINT "FILENAME MISMATCH": GOTO
600
70  PRINT D$;"BLOAD";N$
80 IC =  PEEK (10240):AR% =  PEEK
(10241)
90  FOR I = 0 TO 1023
100 Y(I) = ( PEEK (8192 + 1024 +
I)) * 256 +  PEEK (8192 + I)

110 Y(I) = Y(I) / 100
120  NEXT I
130  FOR I = 0 TO 511
140 NR(I) = Y(I) - Y(512 + I)
150  NEXT I
160  FOR I = 1 TO 509
180 DF = 1
200  IF NR(I) > NR(I - 1) + DF THEN
 GOTO 230
210  IF NR(I) < NR(I - 1) - DF THEN
 GOTO 250
220  GOTO 270
230  IF NR(I + 1) > NR(I - 1) + 2
 * DF THEN NR(I) = NR(I - 1)
 + (NR(I + 2) - NR(I - 1)) /
3: GOTO 270
240 NR(I) = (NR(I - 1) + NR(I + 1
)) / 2: GOTO 270
250  IF NR(I + 1) < NR(I - 1) - 2
 * DF THEN NR(I) = NR(I - 1)
 - (NR(I - 1) - NR(I + 2)) /
3: GOTO 270
260 NR(I) = (NR(I - 1) + NR(I + 1
)) / 2
270  NEXT I
290  IF IC <  > 3 GOTO 600
300 B = .4:L1% = 50:L2% = 500
330  FOR I = L1% TO L2%
340 FR(I) = B * I
350  NEXT I
```

```
360  GOSUB 2000
370 C1 = 20:C2 = 200
371  GOSUB 3000
520  PRINT "ENTER 1 TO PLOT AGAIN
": INPUT IX
530  IF IX = 1 THEN  GOTO 360
560  GOSUB 6000
570  PRINT "ENT 1 FOR REDUCING ON
E MORE TEST": INPUT IL
580  IF IL = 1 THEN  GOTO 60
590  PRINT "DONE"
600  END
2000  PRINT "ENTER 1 TO PLOT": INPUT
PT
2010  IF PT <  > 1 THEN  GOTO 218
0
2020  PRINT "SWITCH ON PLOTTER.PE
N LIFT OFF": STOP
2030 IP = 1
2050  POKE  - 15103,0: POKE  - 15
104,( INT (255 / 7))
2060 N$ = "20HZ-0DB": GOSUB 4000
2070  STOP : POKE  - 15103,255: POKE
 - 15104,( INT (255))
2080 N$ = "200HZ-60DB": GOSUB 400
0
2120  STOP :IP = IP + 1
2130  IF IP = 3 THEN  GOTO 2150
2140  GOTO 2050
2150  PRINT "IS THE ADJUSTMENT OK
?1=YES:2=NO": INPUT IA
2160  IF IA = 2 THEN  GOTO 2030
2170  POKE  - 15103,0: POKE  - 15
104,0
2180  RETURN
3000  PRINT "ENTER 1 TO SCREEN PL
OT": INPUT SP
3010  IF SP = 1 THEN  HGR : HCOLOR=
1: HPLOT 0,0
3020  IF PT <  > 1 AND SP <  > 1 THEN
 GOTO 3210
3030  FOR I = L1% TO L2% STEP 2
3040 X% = ( INT ((FR(I) - C1) * 2
55 / (C2 - C1)))
3070 W = NR(I) + 10
3080 W% = ( INT (W * 255 / 70))
3090  IF X% < 0 THEN X% = 0
3100  IF X% > 255 THEN X% = 255
3110  IF W% < 0 THEN W% = 0
```

```
3120  IF W% > 255 THEN W% = 255
3130  POKE  - 15103,X%: POKE  - 1
5104,W%
3140  PRINT FR(I),NR(I): FOR K =
0 TO 200: NEXT K
3150 W% = 150 -  INT (W% * 150 /
255):X% = X% + 1
3160  IF W% < 0 THEN W% = 0
3170  IF W% > 150 THEN W% = 150
3180  HPLOT  TO X%,W%
3190  NEXT I
3200  GOTO 3240
3210  FOR I = L1% TO L2%
3220  PRINT FR(I),NR(I)
3230  NEXT I
3240  TEXT
3250  RETURN
4000  PRINT "ADJUST";N$;"POINT": RETURN
5000  FOR K = 0 TO 40: NEXT K: RETURN

6000  PRINT "ENT 1 FOR DRAWING AX
ES": INPUT IY
6010  IF IY <  > 1 THEN  GOTO 621
0
6015 F% =  INT (255 / 7)
6020  PRINT "PEN UP": STOP : POKE
 - 15103,0: POKE  - 15104,F%

6030  PRINT "PEN DOWN": STOP
6040 X = 20
6050 X1 = X:X% =  INT ((X1 - C1) *
255 / (C2 - C1))
6060  GOSUB 5000
6070  IF X% > 255 THEN X% = 255
6080  IF X% < 0 THEN X% = 0
6090  POKE  - 15103,X%: GOSUB 500
0
6100  POKE  - 15104,(F% + 2): GOSUB
5000: POKE  - 15104,F%: GOSUB
5000
6130  IF X < 200 THEN X = X + 20:
 GOTO 6050
6140  POKE  - 15103,0: POKE  - 15
104,F%
6150  FOR I = 1 TO 6
6160  GOSUB 5000
6170 X% =  INT (255 * I / 7): POKE
 - 15104,X%
```

```
6180  GOSUB 5000
6190  POKE  - 15103,2: GOSUB 5000
: POKE  - 15103,0: GOSUB 500
0
6200  NEXT I
6210  POKE  - 15104,F%: RETURN
```